BETA FREQUENCY NEURONAL NETWORK ACTIVITY IN THE PRIMARY MOTOR CORTEX

Naoki Yamawaki

Doctor of Philosophy

Aston University

January 2009

Aston University

BETA FREQUENCY NEURONAL NETWORK ACTIVITY IN THE PRIMARY MOTOR CORTEX.

Naoki Yamawaki

Doctor of Philosophy

2009

In Parkinson's disease (PD), the activity of several nuclei of the basal ganglia (BG) including the subthalamic nucleus (STN) and globus pallidus show enhanced synchronous neuronal oscillatory activity at beta frequency which is correlated with symptoms of bradykinesia. In PD and animal models of the disease, synchronous beta frequency oscillatory activity of the primary motor cortex (M1) also appears enhanced. In this study I investigated the mechanisms of neuronal network oscillatory activity in rat M1 using pharmacological manipulations and electrical stimulation protocols, employing the *in vitro* brain slice technique in rat and magnetoencephalography (MEG) in man.

Co-application of kainic acid and carbachol generated *in vitro* beta oscillatory activity in all layers in M1. Analyses indicated that oscillations originated from deep layers and indicated significant involvement of $GABA_A$ receptors and gap junctions. A modulatory role of $GABA_B$, NMDA, and dopamine receptors was also evident.

Intracellular recordings from fast-spiking (FS) GABAergic inhibitory cells revealed phase-locked action potentials (APs) on every beta cycle. Glutamatergic excitatory regular-spiking (RS) and intrinsically-bursting (IB) cells both received phase locked inhibitory postsynaptic potentials, but did not fire APs on every cycle, suggesting the dynamic involvement of different pools of neurones in the overall population oscillations. Stimulation evoked activity at high frequency (HFS; 125Hz) evoked gamma oscillations and reduced ongoing beta activity. 20Hz stimulation promoted theta or gamma oscillations whilst 4Hz stimulation enhanced beta power at theta frequency.

I also investigated the modulation of pathological slow wave (theta and beta) oscillatory activity using magnetoenchephalography. Abnormal activity was suppressed by sub-sedative doses of $GABA_A$ receptor modulator zolpidem and the observed desynchronising effect correlated well with improved sensorimotor function.

These studies indicate a fundamental role for inhibitory neuronal networks in the patterning beta activity and suggest that cortical HFS in PD re-patterns abnormally enhanced M1 network activity by modulating the activity of FS cells. Furthermore, pathological oscillation may be common to many neuropathologies and may be an important future therapeutic target.

Key words: Oscillations, interneurones, inhibitory postsynaptic potentials magnetoencephalography, zolpidem.

ACKNOWLEDGEMENTS

CONTENTS

LIST OF FIGURES AND TABLES

ABBREVIATIONS

6-OHDA – 6-hydroxydopamine
AMPA – Alpha-amino-3-hydroxy-5-methyl-4-isoxazolepropionic acid
AP – Action potential
AHP – Afterhyperpolarisation
BG – Basal ganglia
CBX – Carbenoxolone
CCh – Carbachol (carbamylcholine)
CCK – Cholecystokinin
CNQX – 6-cyano-7-nitroquinoxaline-2,3-dione
CT – Computer tomography
DA – Dopamine
DBS – Deep brain stimulation
DFT – Discrete Fourier Transform
DHPG – Dihydroxyphenylglycine
DLPFC – Dorsolateral prefrontal cortex
EEG – Electroencephalography
EP – Entopeduncular nucleus
EPSP – Excitatory postsynaptic potential
ERD – Event-related desynchronisation
ERS – Event-related synchronisation
FFT – Fast Fourier Transform
FS – Fast spiking
GABA – Gamma-aminobutyric acid
GPe – Globus pallidus externa
GPi – Globus pallidus interna
HFS – High frequency stimulation
IB – Intrinsically bursting
ING – Interneuronal network gamma
IPSP – Inhibitory postsynaptic potential
KA – Kainic acid
LFP – Local field potential
LTS – Low-threshold spiking
LS – Late spiking
mGluR – Metabotropic glutamate receptor
M1 – Primary motor cortex
MEG – Magnetoencephalography
MRI – Magnetic resonance image
MRS – Proton magnetic resonance spectroscopy
MPEP – 2-methyl-6-(phenylethynyl)pyridine
MPTP – 1-methyl-4-phenyl-1, 2, 3, 6-tetrahydropyridine
NMDA – N-methyl-D-asparate
PD – Parkinson's disease
PENT – Pentobarbitol
PET – Positron emission tomography
PING – Pyramidal-interneuronal network gamma
PTX – Picrotoxin
PV – Parvalbumin
rTMS – Repetitive transcranial magnetic stimulation
RS – Regular spiking

11

RSNP	–	Regular spiking non-pyramidal cell
SAM	–	Synthetic aperture magnetometry
S1	–	Primary somatosensory cortex
SNr	–	Substantia nigra pars reticulata
SNc	–	Substantia nigra pas compacta
SOM	–	Somatostatin
SPECT	–	Single-photon emission computed tomography
STN	–	Subthalamic nucleus
TTX	–	Tetrodotoxin
VIP	–	Vasoactive intestinal polypeptide
ZOL	–	Zolpidem

CHAPTER 1:

INTRODUCTION

1.1 PARKINSON'S DISEASE

1.1.1 Overview

Parkinson's disease (PD) is a disorder of voluntary movement, which is characterised by a resting tremor (rhythmical and alternating movement), rigidity (resistance to a passive movement), akinesia (difficulty in initiating movement) and bradykinesia (slowness in executing movements). The prevalence of PD is approximately 0.3% of the world population; PD affects more than 1% of those older than 60 years and up to 4% of those older than 80 years (Schapira, 2008). Thus, PD is the second most common neurodegenerative disorder after Alzheimer's disease (Sinha et al., 2005; Schapira, 2008). Initial symptoms usually occur between 50-60 years of age and the disease gradually progresses (Calne and Sandler, 1970; Lee and Liu, 2008). The description of PD symptoms was formally introduced in 1817 by Dr. James Parkinson in the monograph "Essay on the shaking palsy". The pathophysiology of this disease was later discovered to involve disruption of neuronal communication within the subcortical structures known collectively as basal ganglia.

1.1.2 The basal ganglia

The basal ganglia (BG) comprises a collection of nuclei which process motor-related information delivered from the cortex. The BG is located in the forebrain and midbrain, and consists of seven different nuclei (figure 1.1). The putamen and the caudate nuclei, which are collectively called the striatum (in rodents), are the main access point for cortical inputs (Wise and Jones, 1977; Donoghue et al., 1979; Donoghue and Herkenham 1986). Retrograde tracing studies of rat cortex have revealed that all cortical regions project to the striatum (McGeorge and Faull, 1989), and the origin of these corticostriatal projections were found to lie principally in cortical layer Va (i.e. the superficial part of layer V, see section 1.2.2), though small portions are derived from the layer III region (McGeorge and Faull, 1989). These cortical inputs are topographically organised within the striatum. For example, neurones from rostral sensorimotor cortex (where head area is represented) project to the central/ventral area of striatum. In contrast, neurones from caudal

sensorimotor cortex (where limbs are represented) selectively project to the dorsolateral striatum (McGeorge and Faull, 1989; Ebrahimi et al., 1992).

GABAergic

Glutamatergic

Dopaminergic

Basal ganglia
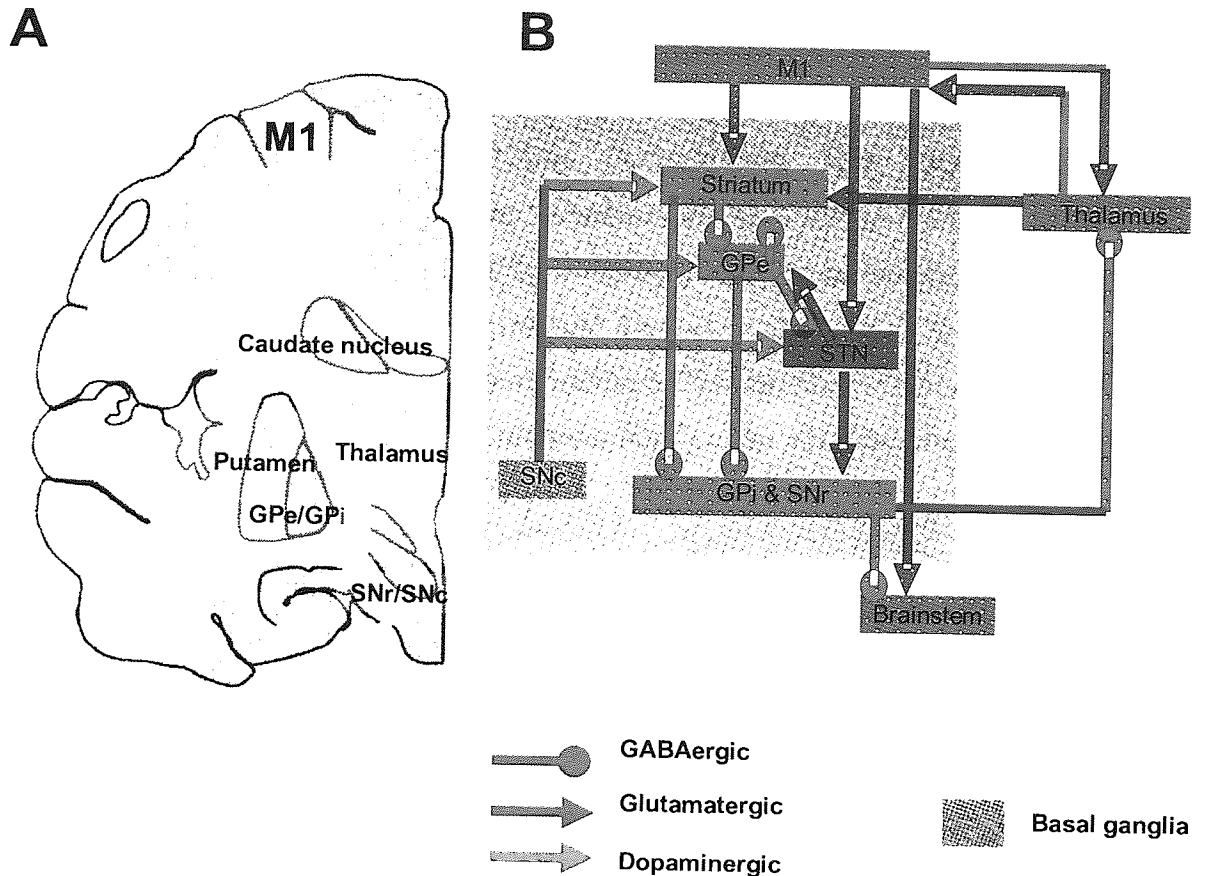
Figure 1.1 – Location and synaptic connectivity of BG nuclei. (A) Coronal section of the right hemisphere of human brain showing the relative location of M1, BG nuclei and thalamus. (B) The schematic representation of (A) with known synaptic organisation. Note that M1 sends descending projections towards thalamus, STN, striatum, and brainstem. Red arrows indicate inhibitory projections while green arrows indicate excitatory projections and pink arrows indicate dopaminergic projections.

95% of striatal neurones are GABAergic projection neurones known as medium spiny neurones (MSNs, Albin et al., 1989). Labelling and immunohistochemical studies have shown that these MSNs make rich synaptic contacts with GABA-containing cells of the globus pallidus[1] (GP), entopeduncular nucleus[2] (EP) and substantia nigra pars reticulata (SNr) in rat (Fink-Jensen and Mikkelsen, 1989; Smith and Bolam, 1989, 1991; Gandia and Giménez-Amaya, 1991; von Krosigk et al.,1992). One study involving juxtacellular labelling of striatal neurones reported that 36.4% of striatal neurones project to GP, 26% to GP and SNr and 37.6% to GP, EP and SNr (Wu et

---

[1] in primate, the structure functionally homologous to rat globus pallidus (GP) is globus pallidus externa (GPe)

[2] in primate, the structure functionally homologous to rat entopeduncular nucleus (EP) is called globus pallidus interna (GPi).

15

al., 2000). The EP and SNr are the output stations of BG, and because of this, connectivity between striatum and EP/SNr neurones are termed "the direct pathway" (referring to direct innervation of output nuclei by the input station). In contrast, striatal connections to GP are termed "the indirect" pathway. In rat, axons of GP neurones terminate in the subthalamic nucleus (STN), EP, and SNr (Bolam and Smith, 1992; Kita and Kitai, 1994). Furthermore, light microscopic study of intracellularly labelled cells from rat revealed that STN neurones send their axons to GP, EP, and SNr (Kita et al., 1983), indicating reciprocal connections between GP and STN which is the only glutamatergic excitatory nucleus in the BG. Importantly, recent anatomical studies of primates indicated the existence of yet another pathway termed "hyper-direct", in which projections from cortex directly form synapses in STN (Nambu et al., 2002).

The EP projects to various subcortical nuclei including pedunculopontine nucleus (PPN), superior colliculus, and thalamus (Galvan and Wichmann, 2008). Biotin labelling studies of EP axons have revealed that there are two populations of EP neurones, those that only project to vetrolateral (VL) and ventromedial (VM) thalamus, where motor-related information is processed and those that projected to both VL and VM thalamus and other structures (Kha et al., 2000). There is also a report that has shown the EP projects to SNr (Bolam and Smith, 1992). Similarly, neurones of the SNr project to VL and VM region of thalamus, although there are subsets which project elsewhere (Kha et al., 2000). The VL thalamus provides synaptic input to frontal regions of cortex, including motor cortex, where it modulates the subsequent cortical output from cortex to BG (Jones and Leavitt 1974; Herkenham 1980; Jones 1983).

Perhaps, the most critical nucleus of BG, at least in terms of pathophysiology of PD (see section 1.1.3), is the substantia nigra pars compacta (SNc). It is dopaminergic in nature, and neurones from this nucleus principally project to striatum, where they have various functions including modulation of corticostriatal inputs. Fluorescent histochemical analysis of rat nigrostriatal fibres indicate that its axon collaterals also extend to GP (Lindvall and Björklund, 1979), suggesting dopamine modulation of non-striatal neuronal activity. Furthermore, Gauthier et al. (1999) studied axonal arborisation of single nigrostriatal neurones of rat via anterograde labelling. They

found two distinct projection subsystems; one that arborises abundantly with striatum, but less with extrastriatal component of BG and one that predominantly arborises with extrastriatal component of BG (i.e. GP, STN, and EP).

1.1.3 PD Aetiology and pathophysiology

PD has been linked with genetic mutation and environmental factors. Six genes, namely α-synuclein, parkin, UCH-L1, PINK1, DJ-1 and LRRK2/dardarin, have been identified so far whose mutations have been suggested to have direct implications for development of PD (Lee and Liu, 2008). Such mutations may be clinically characterised by an early onset of PD symptoms (usually before 40 years old, Lee and Liu, 2008). Environmental factors, including rural living, exposure to pesticides, herbicides, and organic solvents, have also been reported to have impact, according to a number of case control studies, though none has been clearly identified as a direct causal agent (Ghione et al., 2007). Currently, the majority of the PD cases (approximately 90%) are classified as idiopathic[3] and ageing is the only proven risk factor (Weintraub et al., 2008).

It is well documented that the prime cause of PD is a loss of the dopaminergic nigrostriatal pathway (Bernheimer et al., 1973; Gerlach et al., 1996; Wilson et al., 1996). This leads to a reduction in a number of dendritic spines found on MSNs in striatum (Ingham et al., 1989). As striatal dendritic spines receive inputs from corticostriatal neurones as well as nigrostriatal neurones, this significantly compromises corticostriatal communication. Interestingly, initial motor symptoms of PD only appear after substantial loss of nigrostriatal nerve terminals (greater than 70%, Bernheimer et al., 1973) and SNc cell bodies (approximately 60%, Lee and Liu, 2008), indicating the great deal of redundancy in the dopaminergic system. Indeed, in 6-hydroxydopamine (6-OHDA)[4] lesioned rats, the dopamine receptors (in particular, D1-like type) become supersensitive to agonist, significantly facilitating locomotion at small doses of dopamine administration in vivo (Breese et al., 1987). These results

---

[3] PD with no clear aetiology
[4] 6-OHDA is a neurotoxin, which selectively kills dopaminergic and noradrenergic neurones. Thus, it is often used in conjunction with inhibitors of noradrenaline uptake.

may partially explain the functional flexibility of cortico-BG circuitry towards loss of dopaminergic projections.

From an electrophysiological point of view, the rate of the activity in the BG nuclei is considerably altered in absence of dopamine. In fact, studies of 1-methyl-4-phenyl-1, 2, 3, 6-tetrahydropyridine (MPTP)[5]-treated primates and PD patients have revealed an increase in mean firing rate of neurones in the STN and GPi (Filion and Tremblay, 1991; Bergman et al., 1994; Hutchison et al., 1997; Raz et al., 2000). In contrast, GPe activity appears to be significantly reduced during the dopamine-depleted state (Miller and DeLong, 1988; Filon and Tremblay, 1991; Raz et al., 2000). From these observations, DeLong (1990) has suggested that striatopallidal neuronal activity is disinhibited in PD, reducing GABAergic influence of GPe to STN and as a consequence, STN activity is over-excited, increasing activity of the output nuclei (i.e. GPi and SNr). This causes excessive inhibition of their target sites particularly in thalamus, reducing activity in thalamocortical motor loop, leading to symptoms of akinesia and bradykinesia.

However, DeLong's hypothesis alone is insufficient to fully explain a number of experimental observations related to PD. For instance, lesion of the thalamus is expected to worsen PD symptoms but it appears not to be the case (Page et al., 1993; Marsden and Obeso, 1994). Also, the model predicts that hyperkinesia[6] is associated with reduced firing rate of output nuclei, although GPi activity seen in such conditions is similar to that in PD in some patients (Hutchison et al., 2003). Furthermore, anatomical studies of GPe-STN-GPi connectivity have revealed that the GPe represents the sensorimotor region projects to the dorsolateral region of the STN but the STN input to GPi originates from ventromedial region, leaving the circuit open (Parent and Hazrati,1995).

Therefore, numerous investigators have focused upon the change in spatiotemporal firing pattern of BG neurones rather than change in firing rate (see Brown et al., 2003 for review). Regular, irregular and oscillatory (or rhythmic bursting) modes of

---

[5] MPTP is a neurotoxin that is selectively transported into dopaminergic neurones and is metabolised to MPP+. This metabolite inhibits mitochondrial complex I enzyme thereby blocking electron transport chain. Consequently cellular content of ATP is decreased and lead to neuronal degeneration (Dauer and Przedborski, 2003; Smeyne and Jackson-Lewis, 2005)
[6] abnormal increase in muscle activity

discharge have been described in normal single STN and GPi neurones *in vivo* (Magill *et al.,* 2001; Brown, 2003). These firing patterns co-exist in the normal functioning BG, and their relative intensity is thought to alternate over time and space to shape individual motor behaviours. In the resting PD state, however, oscillatory activity becomes a predominant feature (Nini *et al.,* 1995; Boraud *et al.,* 1998; Raz *et al.,* 2000). This firing pattern typically occurs at the frequency band of 4-10Hz (known as theta band) and 15-30Hz (known as beta band), and is abnormally synchronised across the GPe, STN and GPi (Bergman *et al.,* 1994; Raz *et al.,* 2000; Brown *et al.,* 2001; Magill *et al.,* 2001). Numerous studies support the hypothesis that these oscillations are a pathophysiological phenomenon. Firstly, the emergent theta activity appears to correlate with the frequency of tremor (Hutchison *et al.,* 1997; Raz *et al.,* 2000; Amtage *et al.,* 2008). Secondly, administration of levodopa (first-line treatment for PD, see section 1.4.1) reduces coherent low frequency activity (<20Hz) in GPi and STN, which was accompanied by motor improvement (Brown *et al.,* 2001; Kühn *et al.,* 2006).

Although enhanced power and synchrony of theta/beta oscillations between the BG nuclei is associated with pathology of PD, such activity has been described in normally functioning striatum of awake primates (Courtemanche *et al.,* 2003). This may indicate that synchronised activity of BG nuclei alone may not fully describe the pathophysiology of the PD brain.

1.1.4 Effect of dopamine-depletion on cortical and subcortical oscillatory activity

Oscillations at beta and gamma (30-80Hz) frequencies have also been detected in normal primary motor cortex (M1) particularly before the initiation of movement (Murthy and Fetz, 1992; Donoghue *et al.,* 1998), using local field potential[7] (LFP) recordings. This activity appears enhanced in the PD state. As previously outlined there is significant functional association between cortex and STN. Indeed,

---

[7] LFPs represent the synchronous activities of population of neurones. For detail, see method section 2.2.2

simultaneous recording of cortical electroencephalography (EEG[8]) and STN single-unit firing has shown coherent activity between STN neurones and cortical slow wave activity (SWA, ~1Hz) in the anaesthetised rat (Magill *et al.*, 2001). This correlation appears enhanced in dopamine depleted state while transection of neuronal cortico-STN connections regularised STN activity. These results highlight the large influence of cortex on STN neuronal activity via "the hyper-direct" pathway which is enhanced in PD. Recent evidence further supports this view: first, assessment of temporal pattern of LFPs revealed the effective direction of coupling from cortex to STN rather than *vice versa* (Sharott *et al.*, 2005b). Secondly, cortical spike-wave oscillations (5-9Hz) seen during non-convulsive seizure in epileptic rats generate coherent activity in STN neurones (Magill *et al.*, 2005). Thirdly, in the 6-OHDA lesioned rat, enhanced apomorphine-sensitive beta oscillatory activity in the STN is strongly correlated with that of cortex (Sharott *et al.*, 2005a). Because of the significant influence of cortex on BG activity, I will now concentrate on cortex, in particular M1, where voluntary movement is thought to be directly controlled.

---

[8] EEG is a non-invasive device which detects small electrical currents within the brain, thought to be primarily reflecting the activity of pyramidal neurones.

1.2 PRIMARY MOTOR CORTEX

1.2.1 Overview

In man, the motor cortex is located anterior to the central sulcus, occupying approximately one third of the frontal lobe surface area. It can be subdivided into the primary motor cortex (M1) and the non-primary motor cortex, consisting of pre-motor and supplementary motor areas. M1 itself is believed to be associated with voluntary movement generation as well as motor learning (Rioult-Pedotti *et al.*, 1998). Early studies involving low-intensity microstimulation on the surface of M1 revealed a somatotopic[9] arrangement of leg, arm, head, and face (Penfield and Rasmussen, 1950). This mapping was later studied through the intra-cortical electrical stimulation technique (Stoney *et al.*, 1968). Using this method, various groups described the topographic representation of sub-regions of particular body parts within the motor cortical column such that different movements (digit, wrist, elbow, or shoulder) were evoked when tracking stimulating electrodes in small steps across M1 (Asanuma and Ward, 1971; Kwan *et al.* 1978; Donoghue *et al.* 1992). However, strict, non-overlapping somatotopic representations of individual muscles is not an adequate description of function in M1 since stimulation of M1 at multiple, spatially separated locations was shown to influence similar muscle types (Donoghue *et al.* 1992). Single M1 neurones also appeared to participate in multiple hand motor actions, and neurones influencing different digits or the wrist seems to be distributed randomly (Schieber and Hibbard, 1993; Sanes and Donoghue, 2000). These data suggest that muscle representation in M1 involves the dynamic assembly of specific individual elements into a functional unit.

The non-primary motor cortex is linked with higher motor control such as movement planning, learning and refinement based upon somatosensory feedback (Tanji, 1994). Although a detailed description of this area of motor cortex is beyond the scope of this thesis, the interaction between these two motor areas is necessary to achieve highly coordinated movement.

---

[9] in relation to particular body parts

1.2.2 Neuronal organisation of M1

Cortical neurones with similar topographic relationships are aggregated into a vertical columnar structure. In M1, this vertical organisation comprises five horizontal layers, namely, plexiform (layer I), external granular layer (layer II), external pyramidal layer (layer III), internal pyramidal layer (Layer V), and fusiform (Layer VI). Layer IV appears to be absent in M1 due to a lack of granular cortex.

Layer I

The plexiform layer appears to possess no excitatory cell bodies (Chu *et al.,* 2003). Indeed, Gabbott and Somogyi (1986) have shown that approximately 95% of neurones in this layer are inhibitory. Two morphological types of inhibitory neurones termed Retzius-Cajal neurones (possessing a horizontally elongated dendritic tree) and small neurones (possessing a highly localized dendritic and axon arbour) are exclusive to this layer (Douglas and Martin, 2004). This layer receives glutamatergic input from local pyramidal axon collaterals and thalamus (Douglas and Martin, 2004). Other neurochemically-defined inputs have also been identified, most prominently, cholinergic fibres from the nuclei of the basal forebrain and similar inputs of local origin (Emson and Lindvall, 1979; Penny *et al.,* 1982; Rausell and Avendano, 1985; Bear *et al.,* 1985; Lysakowski *et al.,* 1986; Cauller and Conners, 1994; Kawaguchi and Kubota, 1997).

Layer II/III

Layer II/III receives multiple neurochemical projections including noradrenaline, 5-hydroxytryptamine (5-HT), and dopamine. Here, thalamic axons appear to occur at highest density relative to input from other layers (Douglas and Martin, 2004). A population of regular-spiking non-pyramidal cells (RSNP cell, see section 1.2.4 below for detail) and parvalbumin (PV)-positive fast spiking cells (FS cells, see section 1.2.4 below for detail) are most prominent in this layer (Kawaguchi 1995).

Layer V

The pyramidal cells found in this layer possess large cell bodies (75-100μm in primate), which are termed giant cell of Betz. Type 1 Betz cells send cortical output to striatum, superior colliculus, spinal cord, and basal pons, they have thick, tufted

apical dendrites and exhibit intrinsic burst firing (see Molnár and Cheung, 2006 for review). Type II Betz cells send their axons to the contralateral hemisphere or to the ipsilateral striatum, show slender, obliquely oriented apical dendrites and are always regular spiking (Molnár and Cheung, 2006). Those Betz cells located in deep parts of layer V (termed layer Vb) tend to possess smaller cell bodies than superficial part (layer Va). Those axon projecting to brainstem form the corticobulbar tract innervate muscles in the face, head, and neck, while axons projecting to spinal cord via the corticospinal tract innervate the limbs. Those cells found in layer Va are known to send its axons to BG nuclei, in particular, striatum (Lei *et al.*, 2004).

Anatomical studies have revealed that apical dendrite of layer V pyramidal cells receives synaptic input primarily from layer II/III pyramidal neurones (Kaneko *et al.*, 2000). Dopaminergic projections from ventral tegmental area (VTA), the rostral mesencephalic, and the nucleus linearis are also found in this layer (Descarries *et al.*, 1987; Berger *et al.*, 1991; Towers and Hestrin, 2008).

Layer VI

The major pyramidal cells found in layer VI are corticothalamic neurones, which project to, and receive input from, VL thalamus (Kaneko *et al.*, 2000). In addition, pyramidal and non-pyramidal neurones in this layer receive input from callosal neurones (Karayannis *et al.*, 2006). Unmyelinated axons containing noradrenaline, which originate from locus coeruleus form synapses with cells in layer VI (Papadopoulos *et al.*, 1987).

1.2.3 Electrophysiological characteristics of cell types in M1

Cells within M1 can be broadly classified into spiny neurones or aspiny neurones (with reference to dendritic spines). The former neuronal type consist primarily of pyramidal cells (so-called due to their pyramid-like morphology) that are thought to be glutamatergic (i.e. excitatory) in nature and a minority of inhibitory GABAergic stellate cells (so-called due to their star-like neuronal structure). Spiny neurones are known to comprise approximately 80% of total neuronal population in cortex (Gao and Zheng, 2004; Halabisky *et al.*, 2006). The remaining 20% are locally distributed

inhibitory GABA-releasing aspiny neurones, whose responsibility is to regulate cortical activity principally driven by spiny neurones (Beaulieu et al., 1992). For clarity, I refer below only to pyramidal or non-pyramidal neurones.

Pyramidal neurones

Pyramidal neurones are the major output neurones of M1. These cells occupy approximately 70% of cortical neuronal population (Sloper et al., 1979), connecting the cortex and subcortical structures such as striatum and thalamus. They also have axonal collaterals confined to the area in which they occur, providing excitatory input within the local circuitry of the cortex (Douglas and Martin, 2004). Two classes of pyramidal cells have been observed electrophysiologically in sensorimotor region of rat cortex *in vitro* (Connors et al., 1982; McCormick et al., 1985; Van Brederode and Snyder, 1992; Chen et al., 1996). Regular-spiking (RS) cells appear to be most abundant and exhibit spike frequency adaptation[10] upon depolarising current injection (figure 1.2A). Indeed, there is a high correlation between spike frequency and injected current intensity. In contrast, intrinsically bursting (IB) cells show an initial spike burst followed by low frequency, non-adapting action potentials (APs, figure 1.2B). Furthermore, the afterhyperpolarisation (AHP)[11] observed after a single spike is relatively small compared to RS cells. Interestingly, the firing property of IB cell changes dramatically when positive current is injected to the cell with slightly depolarised membrane potential, such that characteristic bursting disappears and AHPs become much shorter, allowing AP frequency to increase (figure1.2B).

---

[10] spike frequency adaptation - decrease in instantaneous discharge rate during a sustained current injection, thought to be influenced by cumulative nature of slow AHP (see footnote 11 below), and the slow-activating non-inactivating voltage-sensitive K^+ current (known as M-current) (Fuhrmann et al., 2002).

[11] AHP - two components, fast AHP (fAHP), which is mediated by BK channel (Ca^{2+}-activated fast K^+ current) and slow AHP (sAHP), which is mediated by SK channels (Ca^{2+}-activated slow K^+ current) (Connors et al., 1982; Hille, 1992)

A

RS cell

B
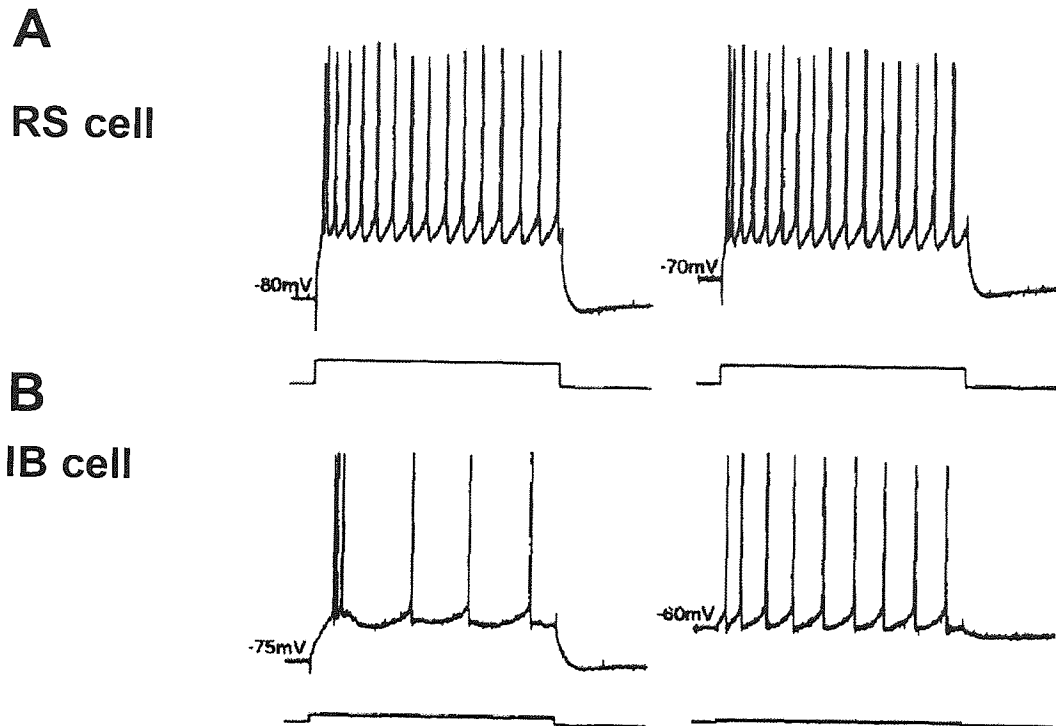
IB cell

Figure 1.2 – The different firing properties exhibited by RS cells and IB cells. Note that changing the holding potential alters the firing rate of IB cell but not RS cell. Figure modified from Chen *et al.*, 1996.

Non-pyramidal neurones

A number of properties have been examined in an attempt to establish classification of non-pyramidal cells including presence of GABA, the expression pattern of proteins involved in cell signalling, axonal target, dendritic/axonal morphology, generation of IPSPs, and AP firing pattern. However, characterisation was found to be a difficult task because of significant overlap of cell characteristics (Galarreta and Hestrin, 2002; Somogyi and Klausberger, 2005). Based upon dendritic morphology, non-pyramidal neurones can be classified into bipolar, multipolar, bitufted or stellate subtypes. In contrast, the arrangement of axonal branching divides non-pyramidal cells into at least 16 different types (see Somogyi and Klausberger, 2005 for review). Discrimination of cells by their postsynaptic target is favoured by some researchers because of their specificity for precise location along the somatodendritic axis (e.g Mann *et al.*, 2005). For example, some axons preferentially target the proximal soma and dendrite (e.g. basket cells), mid-field dendrites (e.g. bitufted, double bouquet and neurogliaform cells), or axon initial segment (e.g. chandelier cells; Douglas and Martin, 2004; Mann, *et al.*, 2005).

In sensorimotor cortex, FS cells and RSNP cells are most commonly identified electrophysiologically (table 1.1, figure 1.3A and B, Kawaguchi, 1995; Cauli *et al.*, 1997). FS cells are characterised by a repetitive discharge of APs whose duration is significantly shorter compared to that of pyramidal cells. The maximum "steady state" firing rate of a FS cell, as determined from the number of spikes at the highest current strength before depolarisation block[12], can reach 100Hz (Erisir *et al.*, 1999; Tateno *et al.*, 2004). Such fast spiking behaviour can be achieved because of the characteristic monophasic, short duration AHP. These cells preferentially form synaptic connections at perisomatic and proximal dendritic regions of neighbouring pyramidal cells and are thought to exert powerful control over large assemblies of target cells (Cobb *et al.*, 1995; Tamas *et al.*, 1997). RSNP cells seem to be most widespread aspiny neurone within the agranular frontal cortex (Kawaguchi, 1995; Cauli *et al.*, 1997). They exhibit two different types of firing behaviour depending on the intensity of the depolarising current applied. At threshold, APs are generated mainly at the early part of depolarisation. Application of stronger stimulus induces repetitive spike firing, which undergoes adaptation and may even cease before the end of the current pulse. Furthermore, injection of hyperpolarising current elicits a notable sag of membrane potential, a characteristic known to be caused by the hyperpolarisation-activated non-specific cation current (I_h)[13].

---

[12] depolarisation block is membrane potential state where no further depolarisation/AP can occur due to steady-state inactivation of fast Na^+ channels underlying the AP.

[13] I_h is a time- and voltage-dependent inward rectifier whose voltage sensitivity and activation time-constant varies with subunit composition and hence among cell types. I_h which is activated at or near resting membrane potential can affect the firing rate of spontaneously active neurones (Chan *et al.*, 2004). In contrast, if I_h is only activated at membrane potentials more negative compared to resting, it will not affect spontaneous firing events. Functionally, I_h is reported to reduce the location-dependent variability of temporal summation of synaptic inputs at the soma thereby linearising synaptic integration by reducing the decay time-constant of synaptic inputs at the dendrites relative to soma via its hyperpolarising effect during the activated state (Magee, 2000)
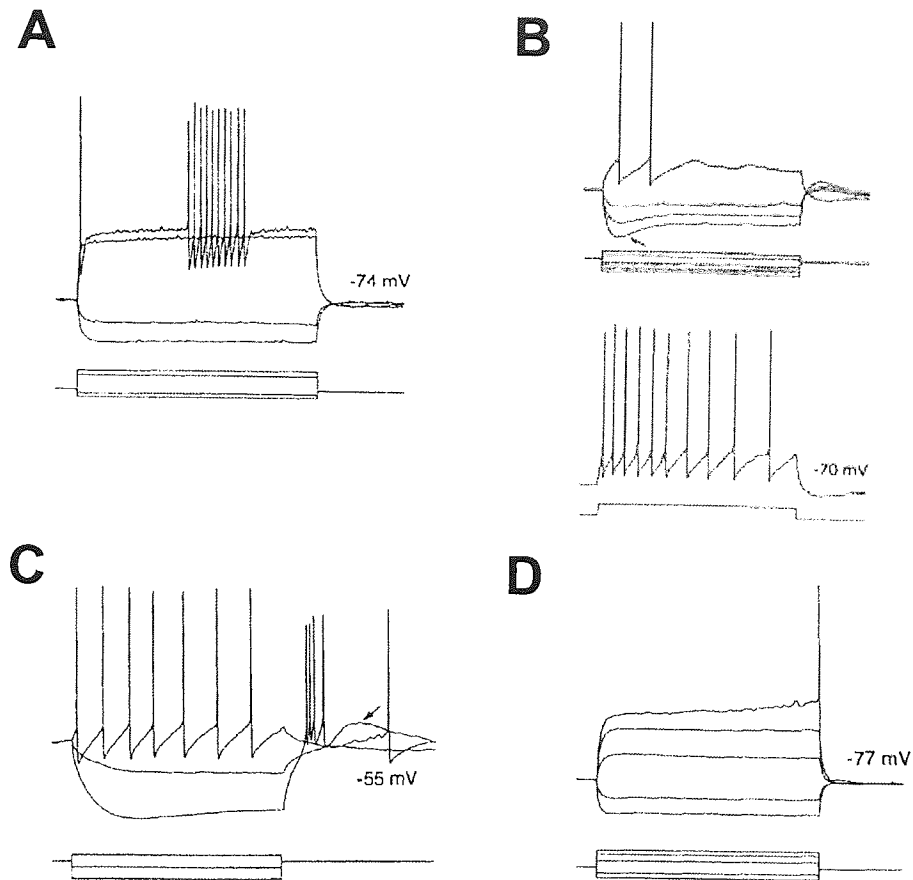
Figure 1.3 – Electrophysiological types of non-pyramidal neurones. (A) FS cell **(B)** RSNP cell. Upper figure showing I_h upon hyperpolarisation. Lower figure showing spike frequency adaptation. **(C)** LTS cell **(D)** LS cell. Figures from Kawaguchi, 1995.

The low-threshold spiking (LTS) and late-spiking (LS) cells constitute a small proportion of interneuronal population. Similar to RSNP cells, LTS cells show voltage sag during hyperpolarising current injection, and these cells are characterised by 2-4 rebound spikes[14] upon reversal from membrane hyperpolarisation (figure 1.3C). Repetitive firing with spike frequency adaptation is observed upon depolarising pulse injection from resting membrane potential (Kawaguchi 1995; Kawaguchi 1997). The current amplitude required to produce an AP is smaller, and the spike frequency adaptation is greater than observed in FS cells.

In LS cells, ramp depolarisations followed by a single AP is observed at subthreshold current (Kawaguchi, 1995; Brecht *et al.*, 2004). Stimulation by current pulse just

---

[14] rebound spikes are induced by 1) activation of low-threshold T-type Ca^{2+} currents with small depolarisations from low resting membrane potentials (-80 to 100mV) and/or 2) the de-inactivation of I_h (Hille, 1992).

above threshold causes LS cells to fire at constant rate without spike frequency adaptation (figure 1.3D).

Firing patterns	Notes	Axon morphology	Ca²⁺ binding	Synaptic

Aston University

Illustration removed for copyright restrictions

Table 1.1 – Types of non-pyramidal neurones that may exist in M1 in vitro. (Kawaguchi, 1995; Halasy et al., 1996; Kawaguchi and Kubota, 1997; Cauli et al., 1997; Chu et al., 2003; Kalinichenko et al., 2006). Relative proportion of these types in the cortex is estimated to be the order of RSNP>FS>LS>LTS.

1.2.4 Possible influence of somatosensory cortex (S1/2) on M1 activity

Movement coordination requires continuous refinement of proprioception coupled with movement execution. For example, grasping an object requires activity of digits, the wrist, forelimbs, and shoulder (M1). However, in order to achieve this, information regarding the relative position of limbs, muscle load, muscle tension and location of objects within the hand must be constantly provided in order to coordinate the multiple muscle contractions which are required. This information is provided by the somatosensory cortex (S1/2), which is located posterior to the central sulcus,

adjacent to the M1. Stimulation of S1/2 has been shown to facilitate movement in healthy subjects as well as those with motor deficits (Johansson *et al.,* 1993; Hamdy *et al.,* 1998; Kaelin-Lang *et al.,* 2002), while reduction of sensory inputs by local anaesthesia has been shown to impair motor control (Edin and Johansson, 1995).

S1/2 shares a similar topographical organisation to the M1 (Huffman and Krubitzer, 2001), and is closely associated with M1 through reciprocal connectivity. Retrograde labelling studies have shown that layer III of area 3a (corresponding to S1) sends axons to the motor cortex (Porter and Sakamoto, 1988; Porter, 1991, 1992, 1996) which appear to terminate on clusters throughout the cortical column with highest density in layer III (Porter, 1991, 1992). Similar studies revealed that projections to area 3a originate from cells located in layer II to VI of the motor cortex (Porter 1991, 1992). The existence of functional connectivity at cellular level has also been confirmed. ICMS of somatosensory cortex caused short-latency, monosynaptic EPSPs in the neurones located in layer II/III of the motor cortex (Kosar *et al.,* 1985).

Autoradiographic studies have shown dopamine innervation of the prefrontal and motor area (including the M1) and S1/2 regions, particularly in deep layers (layer V-VI, Descarries *et al.,* 1987; Berger *et al.,* 1988). This may indicate that during dopamine depletion the activity of M1 and S1 may be disrupted and may indicate that M1-S1/2 interactions have a significant role on PD pathophysiology.

Several clinical studies suggest that impaired sensory feedback contribute to the movement deficits observed in PD patients. For example, when visual information is removed, during hand movement, both the accuracy and speed of movement are compromised (Flowers, 1976; Baroni *et al.,* 1984; Abbruzzese and Berardelli, 2003), while administration of levodopa reduced the "visual cue" dependency (Baroni *et al.,* 1984). In addition, it has been shown that presenting the external or auditory cues can aid the initiation of movement (Morris *et al.,* 1996; Oliveira *et al.,* 1997; McIntosh *et al.,* 1997; Marchese *et al.,* 2000), In addition, many PD patients appear to present abnormal muscle stretch reflexes in upper and lower limbs which give rise to disturbances in proprioception regulation (Rothwell *et al.,* 1983; Berardelli *et al.,* 1983).

Taken together, the motor deficit observed in PD patients may arise from abnormal central processing within the M1, M1-BG interactions or compromised S1/2-M1 interactions.

In the following section, the functional aspects of cortex are discussed, with particular reference to oscillatory activity, which appears to play significant role during PD.

1.3 CORTICAL NETWORK ACTIVITY

1.3.1 Overview

Local networks of neurones in cortex generate patterns of electrical activity known as synchronous oscillations. This phenomenon was first described by Berger (1929), who observed an alpha (8 to 12 Hz) oscillatory rhythm from the human scalp using EEG. Further studies of cortical activity through this technique identified various other oscillatory patterns, which were thought to be dependent on behavioural state. However, it is currently recognised that particular frequencies of rhythm are not strictly confined to particular behaviours, as one state often engages oscillatory activity at several frequency bands. For example, during exploration, network oscillation at gamma (30-80Hz) and theta frequency (5-10Hz) band are co-generated in rat hippocampal region *in vivo* (Bragin *et al.,* 1995). Similarly, slow wave oscillations found in somatosensory cortex during sleep are characterised by complex activity containing ultra-slow (<1Hz), delta (1-4Hz), theta, and gamma oscillations (Steriade, 2006). Among the several oscillatory frequencies observed *in vivo*, gamma oscillations have received particular attention because of their predominance in brain-awake states, and due to their possible implication in higher-level cortical processes such as sensory binding (Singer, 1993), memory (Lisman and Idiart, 1995), and consciousness (Llinas *et al.*, 1998). Indeed, population activity at this frequency band seems to be strongly associated with sensory input (Gray and Singer, 1989).

Due to technical difficulties with physiological and pharmacological analysis of network oscillatory activity, underlying mechanisms have only begun to emerge. Advances coincided with the development of methods to generate persistent and transient synchronous network oscillations *in vitro*, which eliminated limitations such as difficulties in pharmacological dissection of physiological systems *in vivo*. The hippocampus is most commonly chosen to study this population activity because of its well-defined laminar structure. This area generates persistent (lasting hours) gamma oscillations upon cholinergic activation (Fishan *et al.,* 1998), kainate receptor activation (Fisahn, 1999) or metabotropic glutamate receptor activation (Whittington

31

et al., 1995; Pálhalmi *et al.,* 2004). In contrast transient (lasting milliseconds to seconds) gamma oscillations, can be evoked by tetanic electrical stimulation (e.g. Whittington *et al.,* 1995, 1997a, 1997b; Traub *et al.,* 1996b). It has been suggested that persistent gamma oscillations generated in hippocampus *in vitro* are analogous to those gamma oscillations concurrently occurring with theta oscillations in hippocampus *in vivo* (Traub *et al.,* 1996b; Traub *et al.,* 1999b; Whittington *et al.,* 2000), while transient gamma oscillations are thought to be associated with those gamma oscillations evoked by sensory stimulus *in vivo* (Gray and Singer, 1989, Whittington *et al.,* 1995; Traub *et al.,* 1996b, Whittington *et al.,* 1997a, 1997b; Traub *et al.,* 2004).

There appear to be two principal mechanisms by which local oscillatory activity is generated in neocortex. First of all, rhythmic firing of a subset of the neuronal population entrains the local network. Here, both synaptic and electrical communication between neurones is critical. Secondly, synchronised rhythmic network activity can be produced by intrinsic properties of individual cells, which play a role as pacemakers entraining remote but synaptically connected neuronal networks. The details of these mechanisms are described below using hippocampal gamma oscillations as a principal model, unless otherwise stated.

1.3.2 Oscillations driven by synaptic activity

Interneurone Network Gamma (ING)
Rhythmic network activity can be generated from reciprocally connected and hence mutually inhibiting GABAergic interneurones. The recurrent excitatory feedback from pyramidal cells is not required in ING, as oscillations can occur when ionotropic glutamate receptors are pharmacologically blocked, or when pyramidal cells are not firing (Whittington *et al.,* 1995; Traub *et al.,* 1996b). The tonic excitation of interneurones through the activation of metabotropic receptors (glutamate or cholinergic/muscarinic acetylcholine) is however essential for initiating this mechanism (Whittington *et al.,* 1995; Traub *et al.,* 1996b). The frequency of oscillation generated in ING is dependent on several factors, including excitatory driving current, GABA$_A$ decay time constant ($T_{GABA(A)}$), and amplitude of unitary hyperpolarising GABA$_A$ receptor-mediated conductance ($g_{GABA(A)}$). In a simulation

32

model (96 interneurone all-to-all connected network), the relationship between mean excitatory driving current and output frequency was found to be linear (Traub *et al.*, 1996b, 1999b, figure 1.4A). This result was partially supported by *in vitro* model in which glutamate was focally delivered to stratum pyramidale of CA1. Increases in glutamate application time increased oscillatory frequency over the range of 20-50Hz, but further increases in time caused its reduction. This decrease in frequency was suggested to be due to activation of different subsets of interneurone whose $GABA_A$ receptor mediated effect has a longer time constant. In contrast, $T_{GABA(A)}$ and $g_{GABA(A)}$ was predicted in simulation studies to be inversely and non-linearly associated with oscillatory frequency (figure 1.4B and C). Indeed, increasing $T_{GABA(A)}$ by thiopental (2-20μM) or increasing $g_{GABA(A)}$ by diazepam (0.05-0.5μM) decreased the frequency of oscillation and led to eventual loss of synchrony (Traub *et al.*, 1996b, 1999b).

Aston University

Content has been removed for copyright reasons
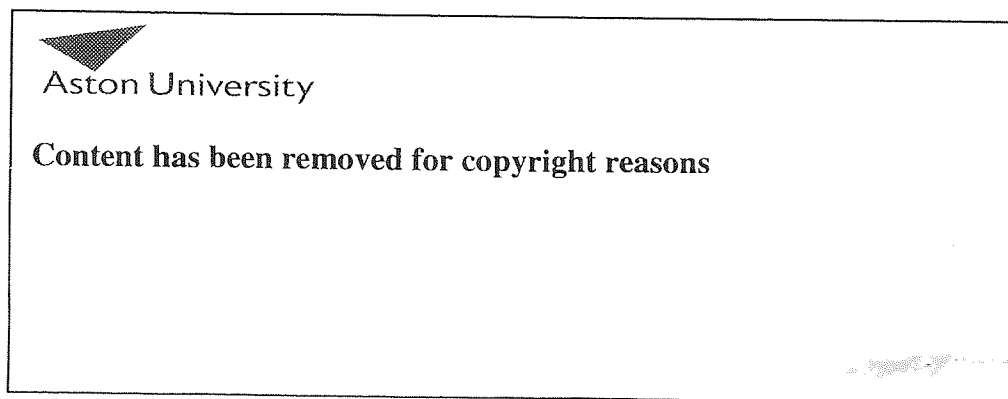
Figure 1.4 – The factors that influence frequency of ING. White dots indicate *in vitro* experimental data and black dots indicate computer simulation model (96 interneuron all-total connection). Graph shows **(A)** mean excitatory current **(B)** $T_{GABA(A)}$ **(C)** $g_{GABA(A)}$ against frequency. Figures from Traub *et al.* (1996b).

ING has been suggested to be implicated in hippocampal sharp wave[15] activity observed concurrently with theta oscillations *in vivo* (Traub *et al*, 1996b, 1999b). In both *in vitro* and *in vivo* models, ING-like activity has been observed after epileptiform bursts, suggesting a role in the neuropathology of seizures (Traub *et al.*, 1996b). Furthermore, its possible association with network activity within the thalamic reticular nucleus (nRT, which consists entirely of inhibitory GABAergic neurones), has been

---

[15] sharp waves can be observed during slow wave sleep, awake immobility, drinking, grooming, and eating in rat *in vivo*.

suggested (Traub *et al.,* 1996b, 1999b). However, ING would likely constitute a local phenomenon only, as the axonal length of interneurones is short (Traub *et al.,* 1996b, 1999b, 2001, 2004). Hence, long-range synchronisation would not be expected to occur via ING *in vitro* or indeed, *in vivo* (Whittington *et al.,* 1997b). For ING to be accomplished, the interneuronal network is required to be excited uniformly, which may appear unlikely in many biological systems. However, computer simulation of ING has suggested that these concerns can be eliminated when interneuronal networks were linked via dendritic gap junctions (Traub *et al.* 2001, 2003). Indeed, these electrical connections are known to exist between similar interneuronal subtypes (Galarreta and Hestrin, 1999; Gibson *et al.,* 1999; Beierlein *et al.,* 2000; Szabadics *et al.,* 2001). In addition to mutually connected interneurones, recently characterised autapses (i.e. a neurone making synaptic contact to itself) could also entrain a number of pyramidal cells (Cobb *et al.,* 1995) without receiving excitatory feedback, and also could enhance the regularity and spike-time precision of cortical interneurones (Bacci *et al.,* 2003, 2006).

Pyramidal-Interneurone Network Gamma (PING)
This mechanism was originally proposed by Freeman in 1968 who proposed a recurrent synaptic feedback loop between principal cells and interneurones as underlying network rhythms (Freeman, 1968; see also Fisahn *et al.,* 1998). In hippocampal CA3 slices, cholinergically induced gamma oscillatory activity seems to operate in this way, as pharmacological blockade of $GABA_A$ or AMPA receptors abolishes the synchronous network activity indicating that phasic inhibitory input, as well as phasic and/or tonic excitatory input plays significant role in rhythmogenesis, (Fisahn *et al.,* 1998; Buhl *et al.,* 1998). The involvement of glutamate and GABA synapses in oscillatory activity has since been replicated in the entorhinal cortex (Cunningham *et al.,* 2003).

Using cell-attached patch-clamp recordings from pyramidal neurones, Fisahn *et al.* (1998) dissected a temporal relationship between APs, excitatory postsynaptic currents (EPSCs) and inhibitory postsynaptic currents (IPSCs) with respect to PING. The group found that the AP of pyramidal neurones preceded an EPSC, which in turn, preceded an IPSC. This led to the suggestion that APs from a subset of pyramidal neurones generate monosynaptic EPSCs on neighbouring pyramidal cells,

but these EPSCs never reach threshold due to negating effect from delayed disynaptic IPSCs. This theory agrees with the observation that firing of pyramidal cells during PING rarely occurs in every field gamma cycle in both *in vivo* and *in vitro* (Fisahn *et al.*, 1998; Cunningham *et al.*, 2003).

The PING model is thought to be more biologically relevant compared to ING, especially for neocortical oscillatory activity where pyramidal cells and interneurones are highly connected. Moreover, this model is able to explain the spatial coherence of oscillatory activity (see section 1.3.4 below), which is thought to functionally bind spatially distributed cortical networks *in vivo*.

1.3.3 Oscillations driven by intrinsic neuronal properties

In contrast to ING and PING in which, firing pattern of cells are regulated by inhibitory and/or excitatory synaptic inputs, rhythmic activity may also be generated through intrinsic membrane properties of individual neurones. Here, synaptic inputs are only able to modulate a pre-existing activity pattern (Llinás *et al.*, 1991). Cells exhibiting intrinsic rhythmic behaviour produce subthreshold membrane potential oscillations via sequential activation of various ion channels. For example thalamic relay cells are able to spontaneously depolarise by activation of persistent Na^+ current or by voltage-dependent Ca^{2+} current, and are also able to spontaneously hyperpolarise by activation of delayed-rectifier K^+ or Ca^{2+}-activated K^+ currents (Llinás, 1988; Llinás *et al.*, 1991; McCormick and Bal, 1994)

Examples of intrinsic oscillators are now numerous. For example, stellate cells found in entorhinal cortex *in vitro* (Llinás *et al.*, 1991; Schmitz *et al.*, 1998) preferentially generate subthreshold oscillatory activity at theta frequency band (<10Hz) and activation of voltage-gated persistent Na^{2+} current is shown to underlie this activity. Similarly, stratum lacunosum-moleculare (LM) cells found in hippocampus also generate intrinsic theta rhythm in a similar manner (Chapman and Lacaille, 1999).

Llinás *et al.* (1991) reported that in layer IV frontal cortex *in vitro*, a small portion of interneurones exhibited an intrinsically oscillatory membrane potential. These cells

were categorised into two groups according to the frequency range exhibited upon depolarising current injection. One group of cells was capable of generating oscillations in a broad frequency range (10-45Hz), while a second group was limited within a narrow frequency band (35-50Hz).

Recently, Roopun *et al.* (2006) has shown that kainic acid-induced persistent beta2 (20-30Hz) network oscillation found in layer V of somatosensory cortex can operate via a non-synaptic mechanism. This activity was insensitive to AMPA receptor and NMDA receptor blockade. However, this group found some dependence of this network activity on $GABA_A$ receptors. Intracellular recording of the activity of different cell types during field beta2 oscillation found that FS cells were firing at almost every beta2 cycle, while IB cells generated spikelets (sub-threshold gap-junction mediated reflections of AP activity from neighbouring neurones) and spikelet-bursts at beta2 frequency. These spikelets recorded at the somata of IB cells appeared to be antidromically driven, as physical separation of layer IV and V regions, eliminating apical dendritic inputs, did not alter spikelet activity. The group have suggested that this $GABA_A$ mediated current may be providing axonal depolarisation. Indeed, increasing axonal excitability with 4-aminopyridine (K^+ channel blocker) in the presence of $GABA_A$, $GABA_B$, AMPA, kainate, and NMDA receptor antagonists generated transient beta2 oscillations. This beta2 oscillating network is, however, dependent on gap junctions, as their blockade by carbenoxolone eliminated oscillatory activity.

1.3.4 Long-range synchronisation

Cortical gamma oscillations are thought to be linked with higher cognitive function. Indeed, gamma oscillations generated upon sensory input are thought to work as a common language between related cortical areas, allowing information to be consciously perceived and/or attentionally selected. Any such processes, however, require spatiotemporal coupling of distant neuronal populations, which appears difficult considering the existence of axon conduction delay between distant circuitries. Indeed, hippocampal Schaffer collaterals were found to have conduction speeds of only ~0.5 m/s (Andersen *et al.*, 1978). Similarly, for neocortical pyramidal cell

collaterals, 0.15-0.55 m/s was estimated (Murakoshi *et al.,* 1993), while neocortical inhibitory neurone collaterals exhibited an even slower conduction speed of 0.06-0.2 m/s (Salin and Prince, 1996).

A number of *in vivo* studies in visual cortex have shown that long-range synchronisation is a physiological phenomenon (Gray *et al.,* 1989; Engel *et al.,* 1991). Traub *et al.* (1996b) demonstrated the possible mechanisms of such a spatial coherence using both computer simulation model and *in vitro* model. In simulation, five distant local networks, each containing 8 pyramidal cells and 8 interneurones, were used. Each cell received synaptic input from other cells within the same network, as well as neighbouring networks. All variables associated with synaptic input (e.g. $g_{GABA(A)}$, $\tau_{GABA(A)}$, and excitatory driving current) were adjusted so that frequency of network oscillation occured at gamma band (Traub *et al.,* 1996b, 1999b). Although the intra-network conduction delay was negligible (as network was too small to generate such phase lag), the inter-network conduction delay was manipulated independently to fall within the range of 0-10 ms. In this model, synchronous oscillations occurring in each network were found to be strongly coherent, with average lagging time between opposite networks close to 0.9ms. Importantly, this coherence between distant neuronal populations was accomplished via "spike doublet" interneuronal activity, which was also found in an *in vitro* model undertaken in same study (Traub *et al.,* 1996b, 1999b). This second spike is predicted to be produced by synchronisation of AMPA receptor-mediated excitatory input from a local and distant pyramidal cell (possibly several mm away). This EPSP is powerful enough to overcome the strong AHP occurring immediately after the first spike of an inhibitory interneurone, generating a pair of closely spaced interneuronal APs (a doublet). The resulting spike doublet summates IPSPs onto target pyramidal neurones, which subsequently delays the initiation of local pyramidal cell spiking. Consequently, phase lag of spike between the local and distant pyramidal cells is reduced, and cell firings become coherent.

1.4 MANIPULATION OF OSCILLATORY ACTIVITY IN THE TREATMENT OF PARKINSON'S DISEASE

1.4.1 Overview

Current treatments available for PD are pharmacological and/or surgical. Levodopa, a precursor of dopamine that crosses the blood-brain barrier, was introduced as most effective PD drug in 1960s, and has since been used for first-line treatment. However, single-dose potency of the drug declines over a period of time and in parallel to this, drug-induced complications, such as dyskinesia (involuntary writhing movements) and so-called "on-off" effect (i.e. rapid fluctuations in clinical motor state) begin to develop after 3 to 5 years. The underlying mechanism suggested for these side-effects is attributed to pharmacokinetic profile of levodopa: levodopa is know to have short plasma half-life and be absorbed rapidly from the gastrointestinal tract. This causes plasma concentration of levodopa to be oscillatory. In the early phase of PD, levodopa is taken up by surviving nigrostriatal terminals, where it is stored and gradually released. As disease progress, however, these surviving neurones begin to deteriorate, and as a result, the effect of levodopa becomes progressively shorter. Ultimately, the effect of levodopa becomes transient, mimicking the plasma concentration of administered levodopa, and leading to dyskinesia through inappropriate dopaminergic reward of aberrant motor patterns (see Jenner 2008 for review).

The surgical method (known as deep brain stimulation; DBS see section 1.4.2 below) seems to be effective in alleviating PD symptoms without the side-effects associated with pharmacological intervention (Wichmann and DeLong, 2006; Deuschl *et al.*, 2006). However, DBS is an invasive, expensive, stressful and high risk procedure. In addition, adverse effects such as haemorrhage (Seijo *et al.*, 2007), can be fatal (see Weaver *et al.*, 2006 for review). These factors restrict DBS to patients with advanced PD symptoms who do not respond to drug therapy or patients of young age with no sign of dementia or psychiatric co-morbidities. This is an obvious disadvantage in treatment of an ageing-related disease such as PD. Since none of above methods is risk-free, the search for better PD treatment is an urgent requirement.

1.4.2 Deep Brain Stimulation (DBS)

DBS involves high frequency stimulation (HFS, ~130Hz) of STN, GPi, or other regions by surgically implanted electrode(s) (Benabid et al., 1991; Limousin et al., 1995; Krack et al., 1998). The precise location of the electrode is identified using magnetic resonance image (MRI) or computed tomography (CT) scanning. The battery-operated neurostimulator, which is often set under the skin near the collarbone, generates the required stimulation pattern. The appearance of improved clinical state is thought to be dependent on the type of PD symptom; rigidity and tremor tend to fade away immediately after DBS (less than 1 minute) while bradykinesia and akinesia takes longer (a few minutes to a few days) (Krack et al., 2002). These positive effects of stimulation persist for at least several minutes after DBS termination (Temperli et al., 2003). Although this procedure has been used for 5 to 10 years to treat PD symptoms, the ways in which it alleviates the PD symptoms are still unclear. The similarity in clinical improvements produced by lesioning and HFS of subcortical areas has led to the hypothesis that HFS relieves PD symptoms by inhibiting the activity of the targeted structure (Bergman et al., 1990; Aziz et al., 1991; Hamada and Delong, 1992). Further support for this view was given by the electrophysiological observations that HFS of overactive STN/GPi reduced the mean firing rate of the stimulated site and BG output nuclei, and increased the activity of ventrolateral thalamus in vivo (Benazzouz et al., 1995, 2000). Critically speaking, the significance of these changes on clinical states has not been tested in these studies. There is, however, some evidence that confirms the coincidence of clinical improvement with HFS-induced inhibitory effects on activity in the stimulated site (Filali et al., 2004).

Microdialysis studies of anaesthetised rat EP and SNr found increased extracellular concentration of glutamate during STN stimulation, suggesting that DBS activated glutamatergic output from the STN to GPi (Windels et al., 2000). Moreover, increased mean firing rates of GPi neurones during chronic stimulation in the STN has been correlated with improved PD symptoms (Hashimoto et al., 2003).

It is clear, however, that none of the explanations for HFS effects through the classical PD model is entirely convincing, and this has led to new theories including

the modulation of pathological *oscillatory* network activity by HFS. In this context, Hashimoto *et al.* (2003) observed enhanced regularity in the firing pattern during STN HFS. Foffani *et al.* (2006) and Priori *et al.* (2006) recorded the STN LFPs a minute before, and a minute immediately after HFS of the STN. Consistent with previous reports, strong beta oscillatory activity was detected in STN of PD patients before stimulation. Interestingly, the application of 130Hz (10-15 minutes) stimulation did not have significant influence on this activity but enhanced lower frequency oscillation (1-1.5Hz), which coincided with clinical improvement. In another patient study, the stimulation of subthalamic area at 20Hz and >70Hz caused exacerbation and reduction of GPi beta band oscillatory activity respectively (Brown *et al.,* 2004). In support, stimulation of STN at 20Hz enhanced bradykinesia of patients with PD, suggesting excess synchrony in the BG-thalamo-cortical loop may be contributing to slowed movements (Chen *et al.,* 2007). Furthermore, Meissner *et al.* (2005) reported that HFS of STN reduced low frequency, oscillatory firing pattern in STN neurones in MPTP-treated parkinsonian primates. In addition, the correlated activity found between two simultaneously recorded STN neurones were also found to be reduced. These results indicate that HFS may indeed provide its therapeutic effect by reducing pathological low frequency oscillatory activity found in BG during PD.

1.4.3 Motor Cortical stimulation – Future treatment for PD?

The number of limitations associated with DBS encouraged exploration for alternative PD treatment methods. There is now evidence to suggest that M1-HFS may be a possible candidate therapy. A strong clinical result of M1-HFS was recently reported by Drouot *et al.* (2004). These authors performed epidural stimulation (130Hz) of M1 on MPTP-treated primates, and assessed its anti-parkinsonian effect by measuring the degree of akinesia (measured as total distance moved) and bradykinesia (measured as movement velocity) before and after the stimulation. From this study, it became apparent that beneficial effect of M1-HFS is positively correlated with severity of these symptoms. Furthermore, this HFS-induced alleviation is not due to modulation of dopamine release from nigrostriatal terminal, but rather, associated with reduction in number of synchronised neurones within the STN and GPi. Several other studies involving repetitive transmagnetic stimulation (rTMS) and extradural

stimulation of M1 in PD patients has also reported clinical motor improvement (Khedr *et al.,* 2003, 2006; Siebner *et al.,* 1999, 2000; Lefaucheur *et al.,* 2004). The electrophysiological effect of HFS on activity of M1 has not yet been analysed. Such an analysis is important in understanding how M1-HFS functionally affects subcortical activity.

1.5 HYPOTHESIS

In PD, exaggerated oscillatory activity becomes a prominent feature. It typically occurs within the theta-beta frequency band, and is abnormally synchronised across the BG system. Cortical activity also seems to participate in this pathological activity. This is likely to be accomplished by feedback mechanisms whereby pathological activity spreads from BG nuclei to cortex via thalamus. However, patterning of abnormal cortical activity to the STN may also play a significant role. If this is true, the beneficial effect of M1 HFS on PD can be explained as follows:

- Cortical HFS modulates the pathological beta oscillatory activity of M1, possibly suppressing it or shifting frequency to the gamma band.
- HFS evoked activity is transmitted to STN via the hyperdirect cortico-subthalamic projection, which disrupts abnormal synchronisation and restores normal activity.

1.6 AIMS

- In M1, to characterise persistent and transient oscillations and the neuronal networks responsible for such activity
- To determine the origin of oscillatory activity in M1
- To identify the possible mechanism(s) of network oscillation exhibited in M1
- To model DBS by electrical stimulation of the superficial layer of M1 and determine the effect on oscillatory activity

CHAPTER 2:
MATERIALS AND
METHODS

2.1 CORTICAL SLICE PREPARATION

Slices were prepared from male Wister rats of weight 40-60g (juvelinle, ~postnatal 20). They were anaesthetised with isoflurane and then decapitated after no heartbeat was detected in accordance with the Animals Scientific Procedures Act 1986, U.K. The brain was quickly and carefully extracted and incubated in ice-cold sucrose-based artificial cerebrospinal fluid (aCSF; containing (in mM) 20.6 sucrose, 2 KCl, 1.6 $MgSO_4$, 25.9 $NaHCO_3$, 1.25 NaH_2PO_4, 10 glucose, and 2.16 $CaCl_2$ at 310mOsm) saturated with 95% O_2 and 5% CO_2. The cyclooxygenase inhibitor, indomethacin (45μM), was also added into this aCSF to improve cell viability (Pakhotin et al., 1997). Subsequently, coronal slices (450μm) were cut using a microslicer (Campden Instruments, U.K.) and were stored in an interface chamber filled with oxygenated glucose-based aCSF containing (in mM) 126 NaCl, 2.95 KCl, 1.6 $MgSO_4$, 25.9 $NaHCO_3$, 1.25 NaH_2PO_4, 10 glucose, and 2 $CaCl_2$ at room temperature (20-25°C) for at least 60 minutes. Slices were then transferred to recording interface chamber (Scientific System Design Inc, Canada, figure 2.1A and B) and continuously perfused with 100ml glucose-based aCSF or modified glucose-based aCSF (where KCl and $MgCl_2$ concentrations were increased to 4.0mM and reduced to 0.5mM, respectively), at flow rate of ~1.4ml/min for 60 minutes. The temperature of aCSF was maintained at 33-34°C using a PTC03 proportional temperature controller (Scientific System Design Inc., Canada).

2.2 ELECTROPHYSIOLOGICAL RECORDINGS

2.2.1 Extracellular recording

The extracellular recording technique was employed to measure the local field potentials (LFPs) of neuronal networks. These potentials are believed to correspond to the weighted sum of somatodendritic synaptic currents flowing through the extracellular medium (Logothetis, 2003). Additional contributions from voltage-dependent membrane oscillations and spike after-potentials have also been suggested (Logothetis, 2003).
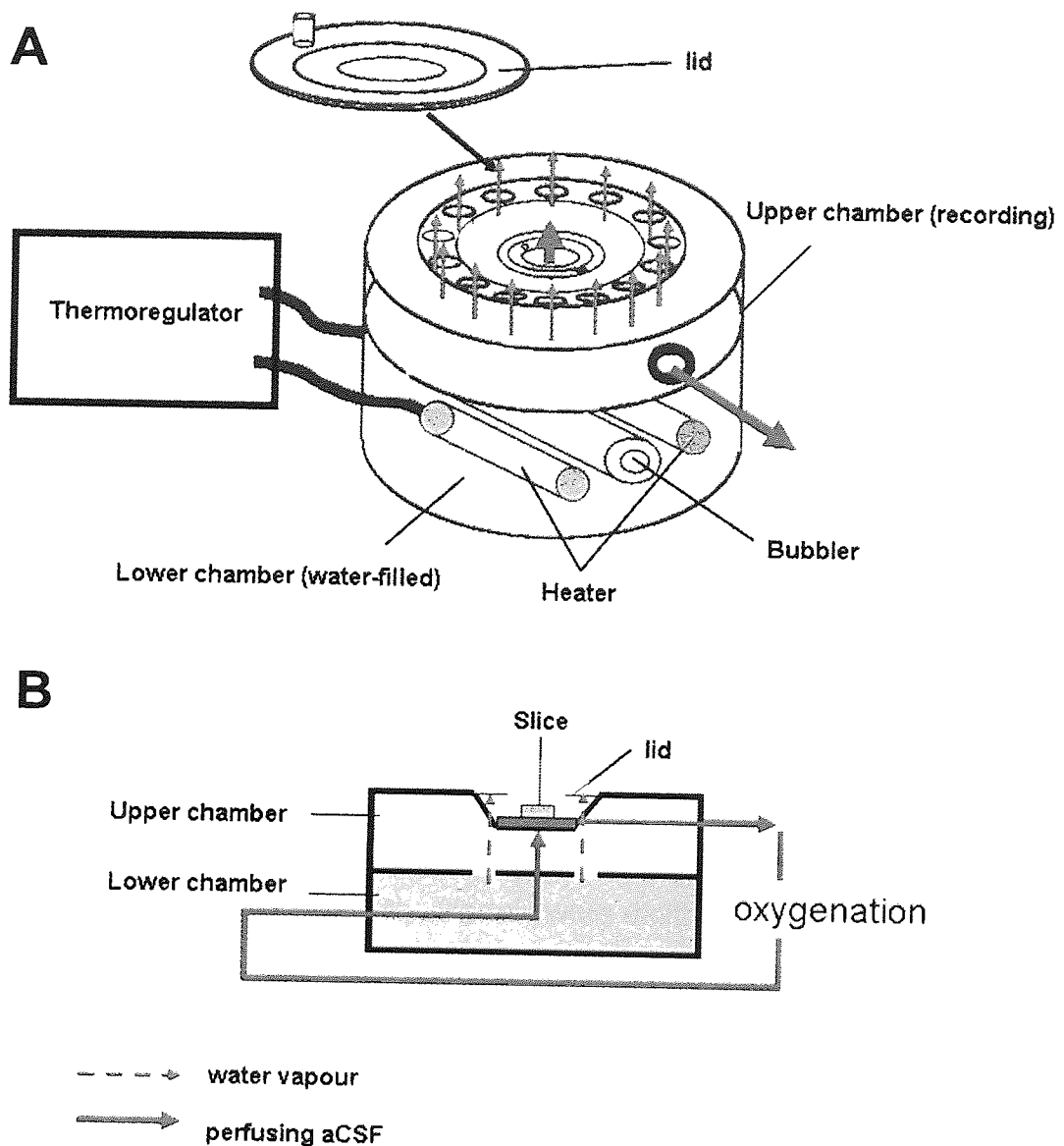
Figure 2.1 – Recording chamber. (A) Diagram of recording chamber. It consisted of two compartments. The slice was placed on upper compartment at the interface between perfused aCSF and humidified air. The lower chamber was filled with distilled water, the temperature of which was controlled by a thermoregulator. Water was constantly bubbled with 95%O_2 - 5%CO_2 in order to ensure full oxygen saturation. **(B)** Schematic diagram of (A).

LFPs were recorded using borosilicate glass microelectrodes filled with glucose-based aCSF. These electrodes were prepared using a Flaming/Brown micropipette puller (P-97, Sutter instrument Co, U.S.A.). A silver wire coated with silver chloride was inserted into this glass microelectrode, which was then mounted on to the

manually-operated micromanipulator (Kanetec, Japan). The microelectrode resistance was chosen to be in the range of 1-3MΩ. This resistance range is thought to be able to detect the synchronised synaptic signals of neuronal population within a sphere of approximately 0.5 - 3.0 mm of the microelectrode tip (Mitzdorf, 1987; Juergens, 1999; Rasch et al., 2007).

Microelectrodes were placed into deep primary motor cortex (M1), which was located using a dissecting microscope with reference to the rat brain atlas of Paxinos and Watson. For dual extracellular recording, an additional microelectrode was placed in superficial M1 as shown in figure 2.2. The electrical current signal was initially amplified by 50 times through AI402 ultra-low noise amplifier headstage (Molecular Devices, U.S.A.). Signals were further amplified by 100 times and low-pass filtered at 200Hz through CyberAmp 380 (Molecular Devices, U.S.A). This low-pass filtration was applied to expose the slow waveform component (i.e. LFP) and to separate our recording from extracellular "multiunit" activity (which is representative of weighted sum of the extracellular action potentials of neurones within the 140 to 300μm radius of electrode tip (Henze et al., 2000). Alternating current (AC) signals of neuronal network activity were visualised at 40MHz on a HM305-2 oscilloscope (Hameg Instruments, U.K.). Simultaneously, signals were digitized at 10 kHz sampling rate by an analogue to digital converter (CED micro-1401 mk II; Cambridge Electronic Design, U.K.). Spike2 software (CED, U.K.) was used for online recording and analysis (figure 2.3).
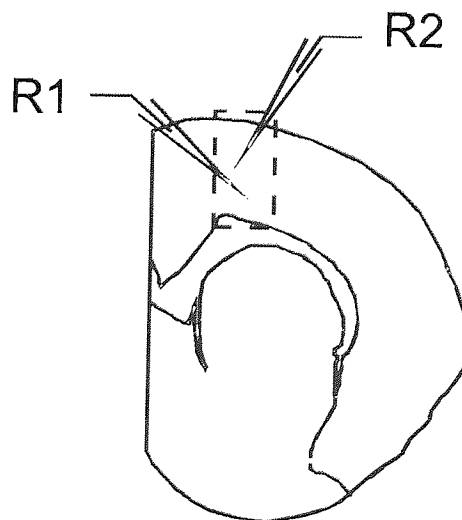
Figure 2.2 – Location of M1 in coronal slice and location of recording electrodes placed within M1. R1 = recording electrode 1, placed in deep (layer V) M1. R2 = recording electrode 2, placed in superficial (layer II/III) M1.
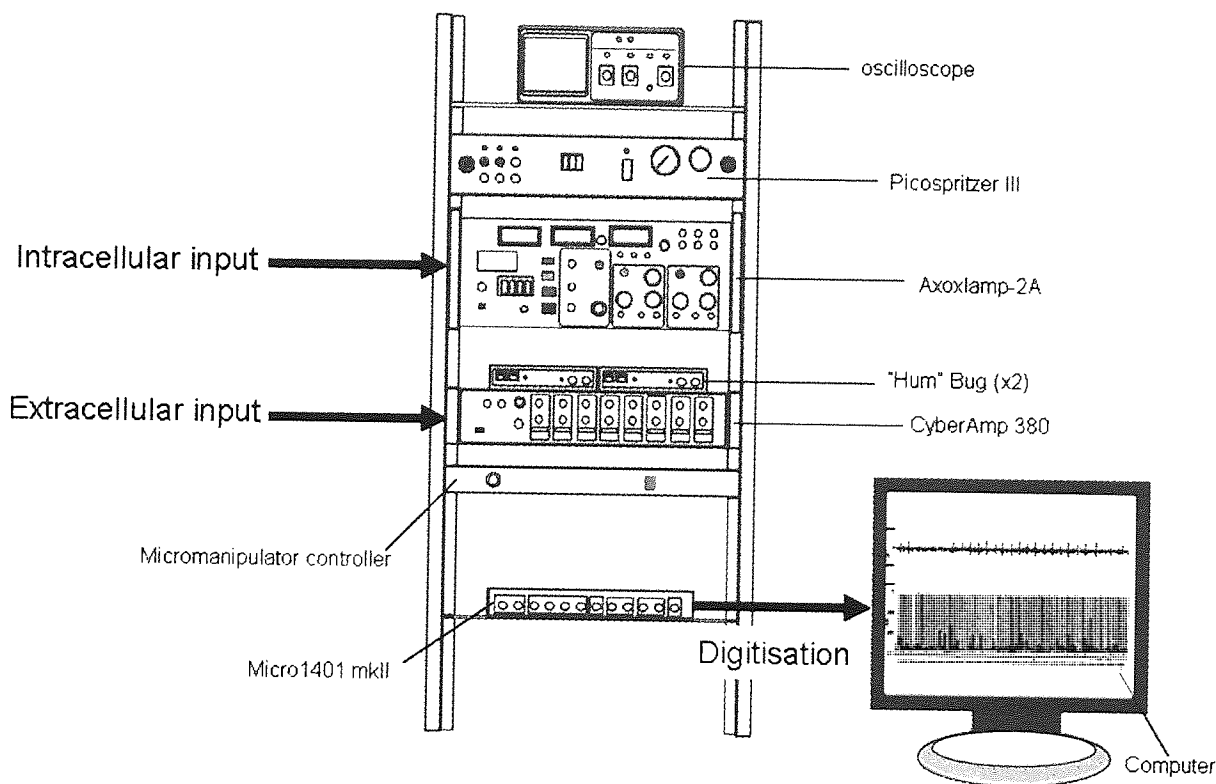
Figure 2.3 – Arrangement of rig set up for extracellular and intracellular sharp electrode recording. Extracellular signals detected from recording electrode(s) were amplified by a headstage before being fed into a Cyberamp 380. Similarly, signals from sharp electrodes were amplified via a headstage before being fed into an Axoclamp-2A amplifier.

2.2.2 Intracellular recordings

In order to characterise single-cell activity during neuronal network oscillations, current-clamp intracellular recordings were made simultaneously with extracellular recordings. Sharp borosilicate glass microelectrodes with resistance of 70-150MΩ were selected, as it allowed the required electrical current to be injected into the cell for membrane potential control, while being "sharp" enough to allow penetration without damage to single neurones. Sharp microelectrodes were filled with 2M potassium acetate (KAc) and attached to a microelectrode holder. The microelectrode holder was then connected to a HS-2 headstage (gain 0.1; Molecular Devices, U.S.A.).

The Axoclamp-2A amplifier (Molecular Devices, U.S.A.) set in current-clamp mode was used to process both input signal and externally generated output command. Square current pulses (amplitude 10nA, duration 0.5s) constructed through Signal 2.10 software (CED, U.K.) were continuously injected into the microelectrode via the amplifier at 1Hz. The microelectrode was initially placed into the aCSF bath before any attempt to find a cell, in order to apply bridge balance. This process allowed subtraction of the voltage drop produced at micropipette upon current flow, which may have caused inaccurate measurement of membrane potential if not compensated. The capacitance of the microelectrode was also neutralised.

Each microelectrode was placed into the M1 area of the coronal brain slice, and subsequently advanced at the rate of $2\mu m$ per step by using a computer operated manipulator (PCS 5000, Scientifica, U.K.). The approach of the manipulator was software controlled to ensure that the microelectrode was advanced along its axis in the z-plane.

Signal 2.10 software (CED, U.K.) was used to search for a cell and for recording of the membrane potential of cell. The offset was first set at zero mV through the input offset command. The microelectrode was considered to be in close proximity, or attached to cell membrane when sudden voltage drop was noted (due to increased tip resistance). Once this was observed, strong current injection (1.0-2.0 ms duration) was applied to penetrate the cell membrane. This "buzz" generated at the tip of microelectrode is thought to attract bound charges on the inside of the cell membrane, providing electrostatic force to break through it (Axon Guide). Penetration was confirmed with appearance of action potentials. At this point, negative current was injected to hold membrane potential between -90 to -110 mV, a value more negative than expected resting membrane potential in the majority of cells. This compensated for the membrane depolarisation caused by leakage of cations into the cell and provided time for the cell membrane to form a tight seal around the microelectrode.

Typically, the tip of microelectrode was obstructed or cleared slightly upon penetration. This caused a change in the microelectrode resistance and hence, the precise membrane potential to be recorded. This error was negated through a

second bridge balancing operation. After 5-10 minutes of "sealing" time, the injected negative DC current was withdrawn gradually and the membrane potential found at zero current injection was recorded as resting membrane potential of cell. The viability of the cell for subsequent experiments was determined by electrophysiological characterisation of the cell, details of which are described in Chapter 4.

2.2.3 Noise concerns

During electrophysiological recording, the biological signals of interest may be subject to physical and electrical interferences. Vibration, which could disrupt the recording, was nullified by a stable air-floating anti-vibration table (TMC, USA). In addition, the use of a computer-operated micromanipulator ensured no destructive hand vibration was transmitted to the cell. Electrical noise could be derived from external and intrinsic (to the recording) sources. Interference may consist of radiative electrical pickup (e.g. 50Hz noise from lights/power sockets), magnetically-induced pickup, or ground-loop noise[16]. Electrical noise was negated by shielding recording devices with a Faraday[17] cage (TMC, USA) and connecting shielding to the common ground (e.g. microelectrode amplifier). In addition, all signals from microelectrodes were processed through a Humbug (Quest Scientific, Canada), which removes line noise (at 50Hz) without filtering biological signals.

2.3 CORTICAL STIMULATION

In order to activate a large area of M1, stimulation of the superficial cortical layers of M1 was made through simultaneous activation of two bipolar electrodes made from 80/20 nichrome wire, separated by approximately 1mm and equidistant from recording electrodes in layer V (figure 2.4). On occasion, an additional recording electrode was also inserted into layer II/III. Stimulation (0.5-2.0mA) was applied simultaneously via Spike 2 software at frequency of 125Hz, 20Hz, or 4Hz. 125Hz

---

[16] noise induced when shielding is grounded at more than one place. If the different grounds have slightly different potential, then it will allow electrical current to flow creating noise
[17] made of stainless steal frame with copper-mesh wall

stimulation consisted of 20 square pulses. Each square pulse had a duration of 2ms, with 7ms inter-pulse interval (IPI). For 20Hz and 4Hz stimulation, 10 square pulses were applied.
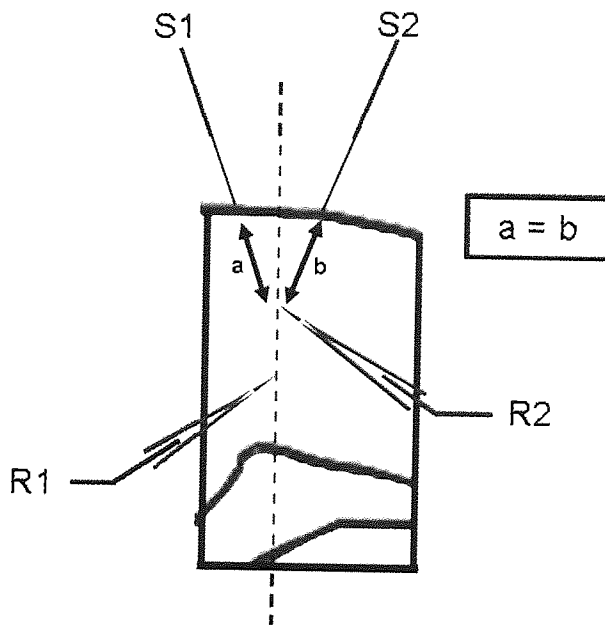
Figure 2.4 – Schematic diagram of M1 stimulation protocol. Area of M1 is magnified from figure 2.2. R1 = extracellular recording electrode placed in layer V region. R2 = extracellular recording electrode placed in layer II/III region. S1 and S2 indicate stimulating electrode 1 and 2, respectively. The position of each stimulating electrode was aimed to be approximately same distance away from R2 electrode.

2.4 DRUG PREPARATION AND APPLICATION

Stock solutions of each drug (purchased from Sigma or Tocris) were prepared and stored at -20 $^{\circ}$C before use. Drugs were applied directly to the perfusing aCSF after recording stable control oscillatory activity. Subsequent population events were recorded for between 20 and 180 minutes,

2.5 DATA ANALYSIS

All electrophysiological data were digitally acquired in waveform format in Spike 2. Time-series analysis was undertaken to examine these data. Two approaches, the frequency-domain method (Fourier transform and spatial coherence) and the time-domain method (auto- and cross-correlation), were used for this purpose. The former

approach involves the decomposition of the sampled waveform into constituent frequency components, which highlights any distinct periodic component in the data. In contrast, the time-domain method describes the pattern of signal or signals over time. The sampling rate employed in current study was chosen to be 10 KHz, which is sufficient for reconstructing the original signal of below 200Hz, according to Nyquist-Shannon sampling theory[18]. All acquired data were low-pass filtered at 80Hz off-line in order to clarify the low-frequency components of network activity.

2.5.1 The power spectrum (Fast Fourier Transform)

The Fast Fourier transform (FFT), is an efficient algorithm to compute one type of Fourier transform (the discrete Fourier transform; DFT) and was used to determine the dominant frequency of oscillatory activities occurring in M1. The DFT is a Fourier series coefficient for a sampled periodic signal, which decomposes complex wave signals into a number of constituent sine/cosine waves. The amplitude of respective waves is expressed as power of that particular frequency.

The FFT block size of 1.6384 seconds was used, as it gave a spectral resolution (frequency resolution of each bin) of 0.61Hz, a highest available in Spike 2 software. Unless otherwise stated 60 s epochs of sampled data were analysed.

Pooled data are presented in two ways: as averaged power spectra or as mean peak power values ± SEM. Since averaged spectra are aligned by frequency bins and not by peak, the averaged peak may not match the mean peak value. All statistical analyses have been performed using mean peak values, and, unless otherwise stated, it is these values that are reported in the text.

2.5.2 Auto- and Cross-correlation analysis

Auto-correlation is a measure of the intrinsic periodicity of a signal (*x(t)*), and summarises its time-domain structure. Mathematically, its function is the average

---

[18] states that the analog signal which has been digitized can be perfectly reconstructed if the sampling rate was 1/(2W) seconds, where W is highest frequency of the original signal.

product of the sequence *x(t)* with a time shifted *m*, version of itself. Figure 2.5 describes way in which this analysis operates, using two different signals as an example. This analysis was used as an alternative to FFT, to identify oscillatory activity in sampled signals.

Cross-correlation analysis was used to reveal a temporal relationship between two different signals x(t) and y(t). In addition to this, information regarding common frequency components as well as phase differences between two signals can be obtained. It is calculated by multiplying two waveforms together and summing the products. The results are expressed as cross-correlation coefficient by Spike 2 (i.e. normalised valued, allowing all measures to lie between -1 and +1).

Aston University

Illustration removed for copyright restrictions
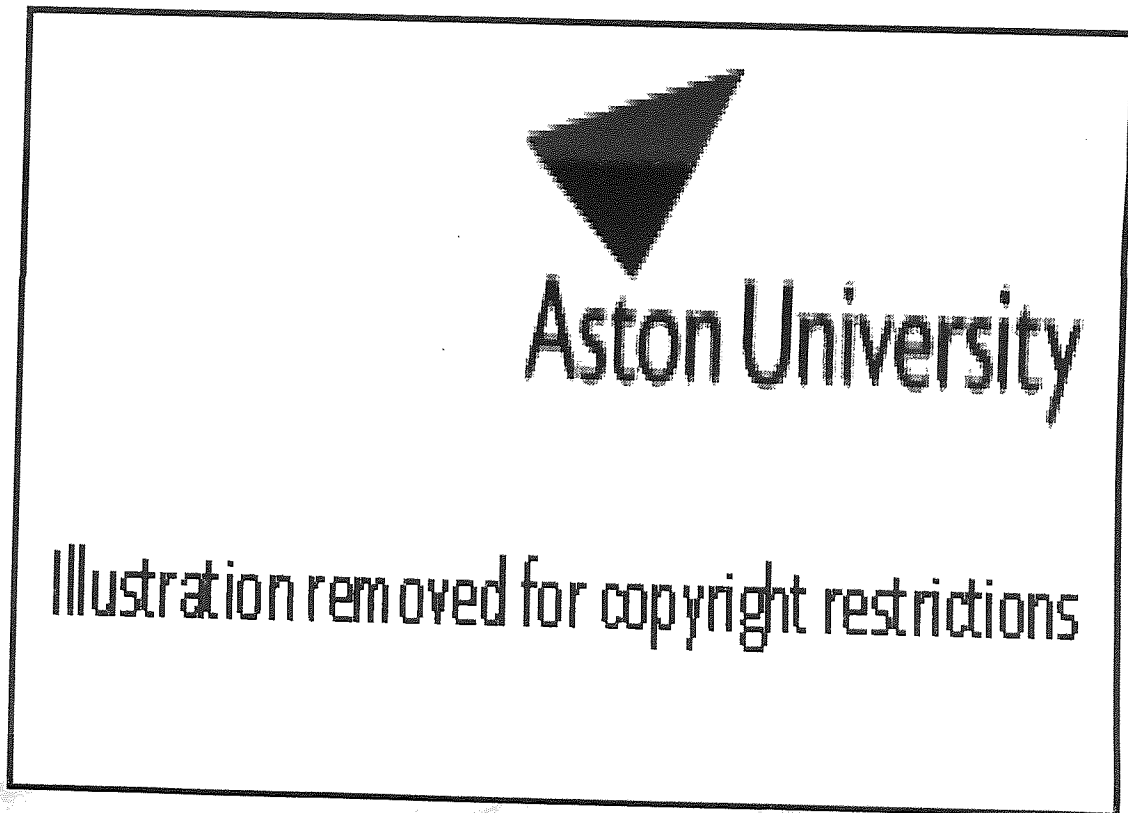
Figure 2.5 – Example of auto-correlation analysis. (A) Digital sequence. **(B)** Auto-correlation of digital sequence (A). At *m*=0 (i.e. zero time-lag, where the digital sequence is aligned exactly with a version of itself), perfect auto-correlation always exhibits a positive peak of 1.0. When *m* is gradually shifted, and if there are particular pattern of fluctuation in signal as in (A), then multiplication and averaging would cause auto-correlation to be decreased gradually from 1.0, passing through 0 and reaching -1.0 (i.e. anti-phase) where peak positivity of a trace is aligned with peak negativity of version of itself. **(C)** Digital sequence with no pattern. **(D)** Auto-correlation of (C) showing no pattern of distribution. Figures from http://www.staff.ncl.ac.uk/oliver.hinton/eee305/Chapter6.pdf

2.5.3 Spatial coherence

In order to identify and statistically evaluate the phase relationship between two signals concurrently occurring at close, but separated space, spatial coherence analysis was undertaken. The Spike2 script required for this analysis was provided by Dr. P.J. Magill (MRC Unit, Oxford).

2.5.4 Spectrogram analysis

Spectrogram analysis was used to calculate spectral power over time. In this plot, dominant activity patterns were shown as "hot" colours (i.e. red/orange/yellow) while less active state was represented by "cold" colours (i.e. blue). Matlab was used for this analysis. A period of extracellular or intracellular signal recorded in Spike 2 was selected and stored initially as a notepad file. These data were subsequently converted into DataEditor file format by a Matlab script written by Dr. S. D. Hall (Aston University). Data were then resampled down to 1000Hz to facilitate spectrogram analysis in Matlab.

2.5.5 Statistical analysis

Student's t-test (paired) was used to determine statistical significance between two sets of data. One-tailed P values were selected when certain assumptions were made regarding the outcome, and two-tailed P values were used when no assumptions were made. All data are shown as mean ± SEM (standard error of mean) unless otherwise stated.

2.6 MAGNETOENCEPHALOGRAPHY (MEG)

2.6.1 Instrumentation for MEG

The use of MEG as a non-invasive device for recording brain activity was introduced by David Cohen in 1968. He obtained α band brain rhythms using MEG, similar to those first described by Hans Berger using an EEG system 40 years earlier (Berger, 1929). In 1968, only single channel MEG was available, limiting the area of the brain from which activity could be recorded at any one time. Significant improvements have now been made to MEG systems such that, current standard MEG employs several hundred channels, allowing the observation of the brain activity occurring at multiple locations within the same temporal frame.

The MEG system at Aston contains 275 channels or, more specifically, Superconducting Quantum Interface Devices (SQUIDs)[19]. Each SQUID functions by means of superconducting devices called flux transformers, which are highly sensitive to extremely small magnetic fields (~10^{-15} Teslas) generated by neuronal network activity. Each SQUID consists of a pick up coil (magnetic field detectors), lead (superconducting wire), and coupling coil attaching to the flux transformer. The pick up coils (also called gradiometers) are situated in the inner surface of a helmet into which the subject's head is accommodated, ensuring that they remain in close proximity to the cortical surface in order to maximise the signal amplitude detected (Biot and Savart's law[20]). Magnetic noises originating from more distant sources (e.g. cardiac and skeletal muscles) are removed by 3rd order arrangement of gradiometers (figure 2.6). These filtered magnetic signals generate electrical current at SQUID ring circuits. Outputs from the SQUID are subsequently amplified and digitally reconverted into magnetic oscillatory signals by the MEG supercomputer system, before visualisation and recording online by acquisition (ACQ) software.

The MEG sensors are submerged in the liquid helium, as they are only capable of maintaining superconductivity at a temperature of 4K (-269°C). In order to preserve the optimal performance of the SQUID sensors, liquid helium is stored in the

---

[19] comprises a loop of superconductng metal (i.e. metal with no electrical resistance)
[20] describes the relationship of magnetic field strength to distance and polarity of the current source

superinsulating, magnetically-neutralised vacuum container called a "Dewar" (figure 2.7)

Aston University

Content has been removed for copyright reasons
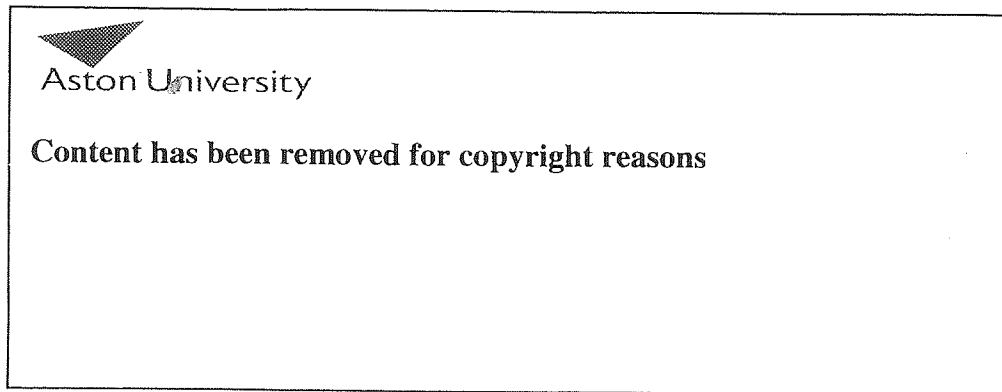
Figure 2.6 – Schematic diagram of 3rd order symmetric gradiometer. Figure from Vrba and Robinson (2001).

Aston University

Content has been removed for copyright reasons
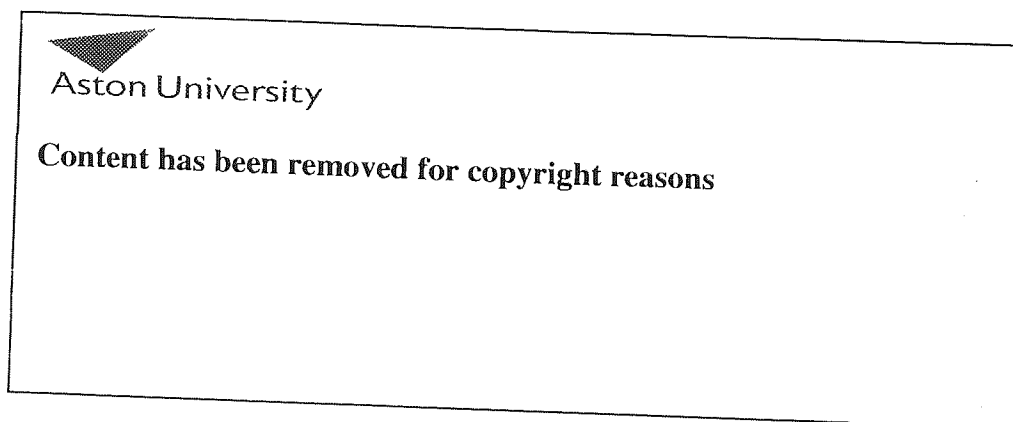
Figure 2.7 – Schematic diagram of MEG system. Figure from Vrba and Robinson. (2001).

The MEG recordings were undertaken in μ (mu) metal[21] shielded room, to further restrict the transfer of magnetic fields to the MEG system to increase signal-to-noise ratio.

---

[21] nickel-iron alloy that has very high magnetic permeability, attenuating transmission of magnetic fields from external sources to the MEG by attracting magnetic field lines

2.6.2 Source of magnetic signals detected by MEG

The magnetic fields are produced upon current flow in one particular direction. Because the brain can be considered as a highly dense network of conducting wires in which current flows constantly in various directions, specification of the magnetic sources detected by MEG has been debated for some time. At the cellular level, the magnetic product of current propagating along the cell membrane is thought to contribute to MEG signals, which can be classified into intraneuronal, intraglial, and extracellular current. However, magnetic field from current flowing across the membrane is believed to be negligible, if any, due to the thinness of the cell membrane and likely symmetry of the current (Okada et al., 1987).

The way in which current is distributed within the cell is also thought to be an important factor for determining its contribution to the MEG signal. To this end, the most significant contributor to MEG has been suggested to be a current dipole that is oriented parallel or tangential to the overlying scalp. It is a current dipole because the magnetic field derived is far greater than those derived from higher polar order (e.g quadrupole) according Biot and Savart's law (for a dipole, intensity of magnetic field decrease with $1/R^2$ from its source but for quadrupole, this value is $1/R^4$, where R is distance Okada et al., 1987). The apical dendrites and somata of pyramidal neurone show directionality in current flow and is hence, dipolar. Conversely, structures such as stellate cells, whose dendrites radiate from the cell body in all directions, are not expected to contribute to MEG signals, as currents dipoles are distributed almost every direction, thus, cancelling each other out (Okada et al., 1987).

The cortex is a highly convoluted structure with numerous sulci and gyri, and as such, current flow can be tangential or radial depending on anatomical location (figure 2.8). Considering the brain as a uniform conducting sphere, it was suggested that only tangential currents would produce magnetic field outside the sphere whereas the radial currents would not (Vrba and Robinson, 2001). Finally, for magnetic fields to be detectable outside the scalp, it is reported that almost simultaneous activation of a large number of cells, typically 10^4 and 10^5 are required (Vrba and Robinson, 2001).

Figure 2.8 – A dipole induced by tangential and radial current. (A) Coronal section of brain **(B)** Tangential dipole occur parallel to skull but radial dipole occur perpendicular to skull. Figure from Vrba and Robinson, 2001.

2.6.3 Source localisation and head movement

In order to reduce the possible location bias associated with head movement during recording, it is necessary to track the position of the head with respect to the SQUID sensors. This is accomplished by attaching a set of reference coils directly on to subject's head at three locations, specifically one on the forehead (nasion) and one behind each ear (pre-auriculars). Each location is then defined in space using a Polhemus Isotrak digitisation system (Kaiser Aerospace Inc. U.S.A.). The position of these coils is monitored continuously throughout the experiment to ensure that the maximum head motion (3mm) is not exceeded.

2.6.4 Co-registration

MEG measures only brain activity, and hence, used alone it lacks information about the spatial location of magnetic sources. Therefore, construction of an anatomical image is required using magnetic resonance imaging (MRI), which can then be co-registered with MEG data (Adjamian *et al.*, 2004). This co-registration process can be

accomplished by aligning the reference points of both MEG and MRI data. LuckyCoreg software was used for this process.

2.6.5 Limitations of MEG

Although MEG has the considerable advantage of being non-invasive over *in vitro* and *in vivo* recording methods, and has better spatiotemporal resolution than other non-invasive techniques such as functional magnetic resonance image (fMRI) and EEG, two limitations are said to be associated with this system. First of all, it is thought to be unable to detect magnetic field accurately from deep sources, due to the law of Biot and Savart. Secondly, if simultaneously occurring currents flow in opposing directions, corresponding magnetic fields will not be detected by MEG due to mutual cancellation, meaning that even signals close to the sensors may be lost (Hillebrand and Barnes, 2002).

2.6.6 Data analysis

SAM (synthetic aperture magnetometry)
SAM is a spatial filtering technique that is based on the beamforming technique. The beamforming, or "focusing" involves selective weighting of the contribution that each of the MEG sensors make to overall output (Hillebrand *et al.*, 2005). These weights can also be defined for a specific anatomical location, based upon an individual's anatomical MRI, to reconstruct a virtual electrode (VE).

Virtual Electrode Analysis
This approach uses beamformer weights computed for a predetermined location to reconstruct the time course of the activity at that location. These data can then be processed further using time-frequency analyses to compare, for example, drug and baseline periods, providing a profile of power change across the complete frequency range. The anatomically discrete fluctuations in a specific frequency band are visualised by band-pass filtering the virtual electrode trace, generating a specific envelope of oscillatory power during drug uptake which can be directly compared to control data.

CHAPTER 3:
SYNAPTIC MECHANISMS UNDERLYING BETA OSCILLATIONS IN M1

3.1 INTRODUCTION

Since the discovery of rhythmic neuronal network activity in human brain in 1929 (Berger, 1929), numerous efforts have been made to understand its functional implications and underlying mechanisms. One approach involves recording of brain activity in the awake/behaving animal, using both invasive and non-invasive techniques. However, for mechanistic evaluation, *in vitro* techniques have been used as these allow component analysis of network oscillatory activity through direct pharmacological and electrophysiological dissection so that types of cells, receptors, and ion channels can be identified.

Many *in vitro* studies to date have concentrated on gamma oscillations. Indeed, areas of the brain where gamma oscillations have been found include the hippocampal CA1 region (Whittington *et al.*, 1995), CA3 (Fisahn *et al.*, 1998), and dentate gyrus (Towers *et al.*, 2002), entorhinal cortex (Cunningham *et al.*, 2003), somatosensory cortex (Buhl *et al.*, 1998; Roopun *et al.*, 2006), and auditory cortex (Cunningham *et al.*, 2004; Traub *et al.*, 2005). Despite such extensive research, no *in vitro* study of oscillatory activity within M1 has been reported to date.

Early *in vivo* studies showed that motor cortex expresses beta oscillations (usually within 15-35Hz), which occur intermittently with varying amplitude in the awake behaving monkey (Murthy and Fetz, 1992, 1996a, 1996b; Sanes and Donoghue, 1993; Baker *et al.*, 1997, 1999). The amplitude of this beta oscillation was found to be enhanced before voluntary movement and during sustained muscle contractions. By contrast, beta was suppressed during the dynamic phase of voluntary movements (Murthy and Fetz, 1992; Sanes and Donoghue, 1993; Baker *et al.*, 1997, 1999). Interestingly, recent MEG data from motor cortex confirmed oscillatory activity in the beta frequency band, which was modulated during preparation and performance of voluntary movement (Salmelin *et al.*, 1995). Due to this sensory input-induced desynchronising of beta oscillatory activity, it is suggested that beta oscillations reflect an idling state of cortex, which is prevalent in the absence of sensory input (Jurkiewicz *et al.*, 2006). Furthermore, in the dopamine-depleted state as seen in PD, beta oscillatory activity is abnormally enhanced (Sharott *et al*, 2005a; Silberstein *et al.*, 2005), which coincides with the emergence of movement disorders such as

akinesia. These observations led to suggestion that the modulation of beta oscillations is functionally associated with motor behaviour.

Although the functional implication of oscillatory activity in motor cortex has been examined, its underlying mechanism is yet to be unveiled. In this chapter, we investigated this question using the rat brain slice preparation to pharmacologically determine the mechanism(s) by which synchronous network activity occurs in M1.

3.2 SYNCHRONOUS NETWORK OSCILLATIONS IN M1

3.2.1 Induction of synchronous network activity in M1

We commenced our initial investigations with the question; "is there any spontaneous oscillatory activity within M1?" On no occasion was such activity observed (figure 3.1A and B) and hence an approach involving pharmacological manipulation was undertaken. Synchronous network activity in the gamma frequency range has previously been detected in brain slices using pharmacological manipulations (Fisahn et al., 1998; Cunningham et al., 2003), and with electrical stimulation protocols (Whittington et al., 1995, 1997a, 1997b). The activation of kainate receptors by nanomolar concentrations of receptor agonist kainic acid (KA) was reported to be able to generate sustainable network oscillations, which possesses in vivo oscillation-like characteristics as seen in the hippocampus (Hormuzdi et al., 2001), entorhinal cortex (Cunnigham et al., 2003) and somatosensory cortex (Roopun et al., 2006). However, addition of KA alone did not reliably generate oscillation in our study [22] (figure 3.1A and B). Buhl et al. (1998) investigated the properties of gamma oscillatory activity in mouse somatosensory cortex in vitro. In their study, the application of nanomolar concentration of KA alone was not sufficient to generate gamma network activity but co-addition of micromolar concentration of muscarinic M1 receptor agonist carbachol (CCh) generated persistent gamma oscillations. Replicating this procedure in M1 produced synchronous network activity (figure 3.1A and B). Power spectrum analysis of this activity revealed that it was at beta frequency band[23] (27.8 ± 1.1 Hz in layer V, n=6, figure 3.1C and D). Previous studies of gamma oscillatory activity in vitro also indicated that this oscillation can last for several hours (Dickinson et al., 2003). The stability of beta oscillations over time was therefore assessed by recording its power and frequency for 1 hour. There was a tendency for oscillatory power to increase after the extracellular electrode penetration into the slice for 20 minutes. Oscillatory power then slowly declined and became

---

[22] rarely, we have observed beta oscillatory activity on application of KA alone. When observed, it required an induction period of over 3 hours, and was typically of very low power (shown in appendix I). Characterisation of this oscillation revealed that it was essentially identical to KA/CCh induced oscillation (appendix I). Hence, we have used KA/CCh oscillation as a standard for subsequent experiments.

[23] in our study, the term "beta oscillation" refers to oscillatory activity in 15-35 Hz frequency band.

steady after 40 minutes. The frequency also fluctuated within a narrow band, but this was not found to be statistically significant (figure 3.1F).
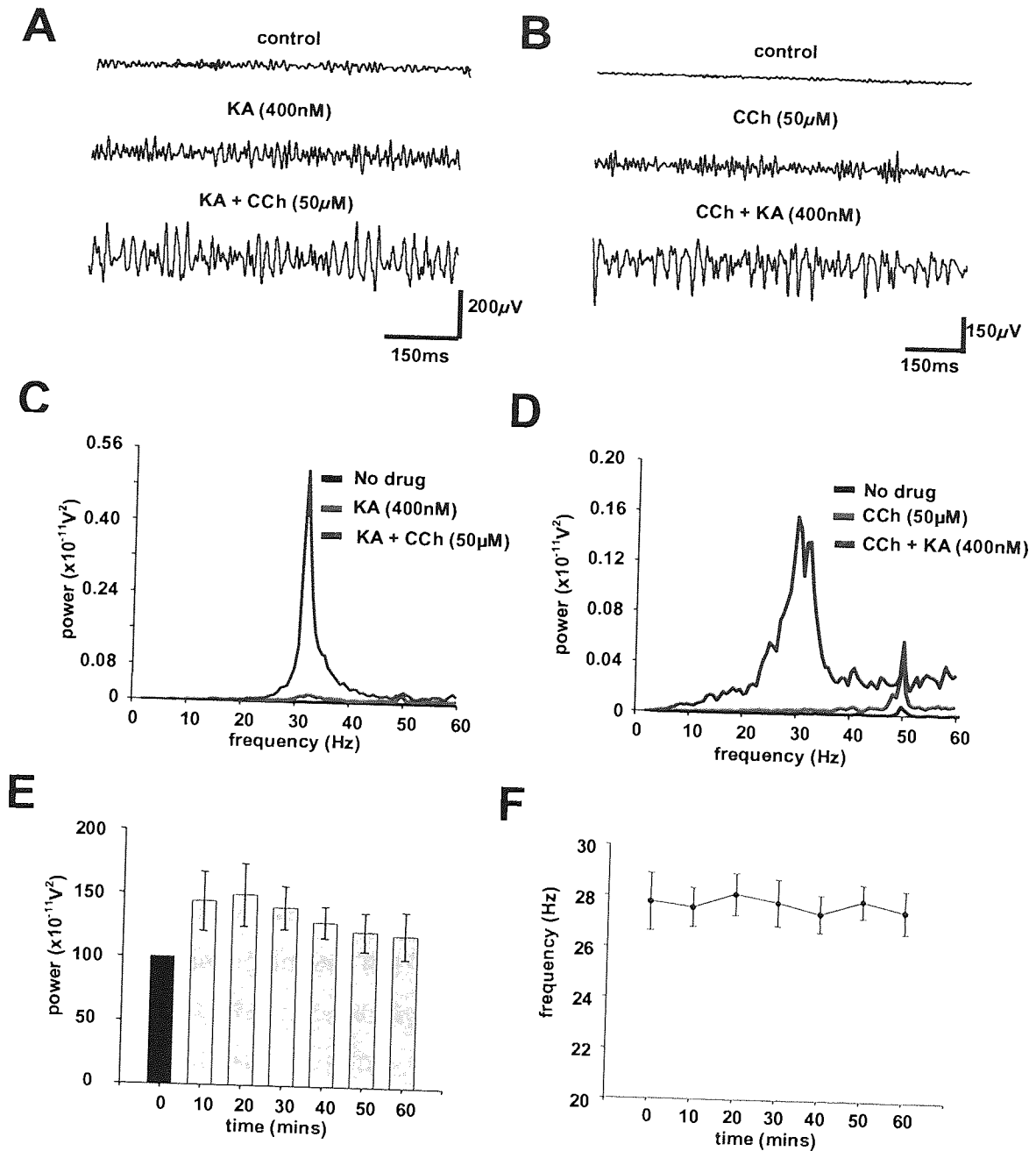
Figure 3.1 – Co-application of kainic acid (KA) and carbachol (CCh) reliably generated beta oscillations in M1 layer V. (A and B) Top – No spontaneous oscillations. Middle – KA or CCh alone was insufficient to induce synchronous network activity. Bottom – Co-application of KA and CCh reliably induced network oscillations. **(C and D)** Power spectrum analysis showing pharmacologically induced network oscillations in the beta frequency band. **(E)** Averaged and normalised power of beta oscillation over 1h from electrode insertion (n=8). Black bar represents reference. **(F)** No change in oscillatory frequency during same time period as (E).

3.2.2. Origin of beta oscillation in M1

All layers showed beta oscillatory activity except layer I (figure 3.2A and B). Sequential placement of the recording electrode revealed that the relative strength of oscillatory activity declined from a peak in deep to superficial layers such that layer V exhibited the most powerful oscillatory activity (figure 3.2A and B). This result led to the assumption that layer V was driving the oscillatory activity of the other layers. In support of this, layer V has been reported to be the source of cortical activity in somatosensory cortex (Sanchez-Vives and McCormick, 2000). To further test this hypothesis, we performed dual extracellular recordings in M1. The data obtained from each layer were analysed employing a cross-correlation algorithm using activity recorded in layer V as a reference point. This revealed that the beta oscillations occurring in layers II/III were always phase lagged relative to those of layer V (figure 3.2C, D, E, and F). The average lag time was found to be 1.13 ± 0.71 ms for layer III ($n=8$, $P<0.05$), and 2.36 ± 1.52 ms for layer II ($n=8$, $P<0.05$). Against our expectations, however, the phase of layer VI beta oscillation was found to precede that of layer V by 3.02 ± 0.75 ms ($n=8$, $P<0.01$).

As the peak power of beta oscillation in layer V is substantially greater than layer VI, it seems unlikely that the layer VI oscillatory activity is the source of the beta oscillation. However, it remains possible that activity in layer V is paced by layer VI, such that the latter exerts indirect control over superficial layers. Due to technical difficulties in distinguishing the exact boundary between layer V and VI, we were unable to test this possibility by pharmacological isolation of these layers. Nevertheless, it was possible to explore oscillatory drive through more general manipulation of activity in deep or superficial M1. Thus, tetrodotoxin (TTX, $10\mu M$) was focally applied to superficial and deep layers while simultaneously recording oscillatory activity from each site.
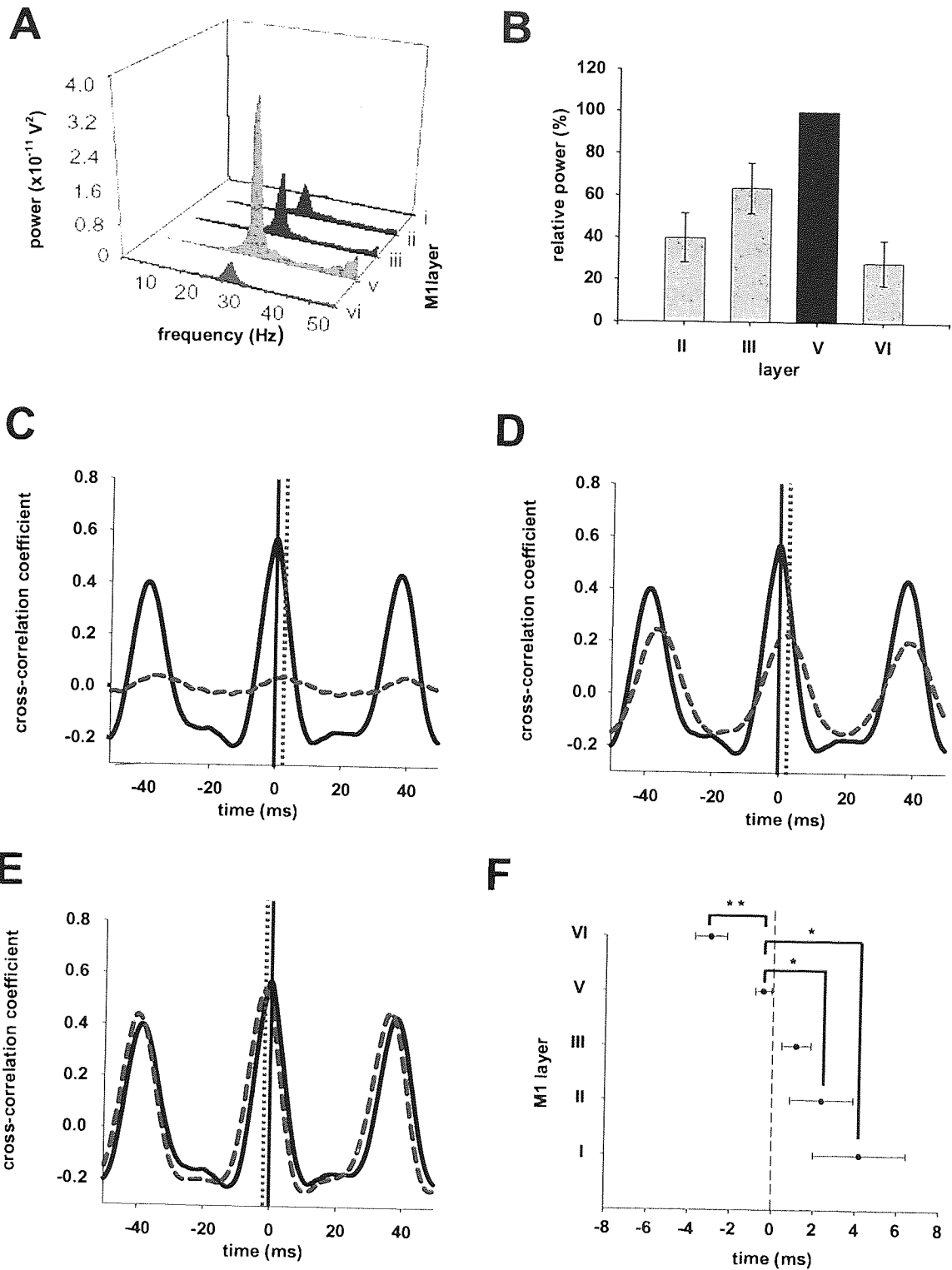
Figure 3.2 – Deep layers are the origin of beta oscillations in M1. (A) Power spectrum of oscillatory activity in each layer in a single slice. (B) Relative power from each layer averaged and normalised with respect to layer V activity. (C) Cross-correlation analysis of beta oscillation between layers II/V (red) and layers V/V (black). (D) Cross-correlation analysis of beta oscillation between layers III/V (red) and layers V/V (black). (E) Cross-correlation analysis of beta oscillation between layers VI/V (red) and layers V/V (black). (F) Averaged phase delay plotted across M1 layers with respect to layer V.

When TTX was focally applied to superficial layers for 20ms, ongoing beta oscillatory activity disappeared approximately 300ms after the pressure ejection artefact. Although the peak power of activity in the deep layers was also affected in some experiments, activity always persisted beyond the time point where no superficial activity was observed (figure 3.3A). In contrast, focal application of TTX to deep layers caused immediate cessation of beta oscillations which always coincided with abolition of rhythmic activity from the superficial layers (figure 3.3B).
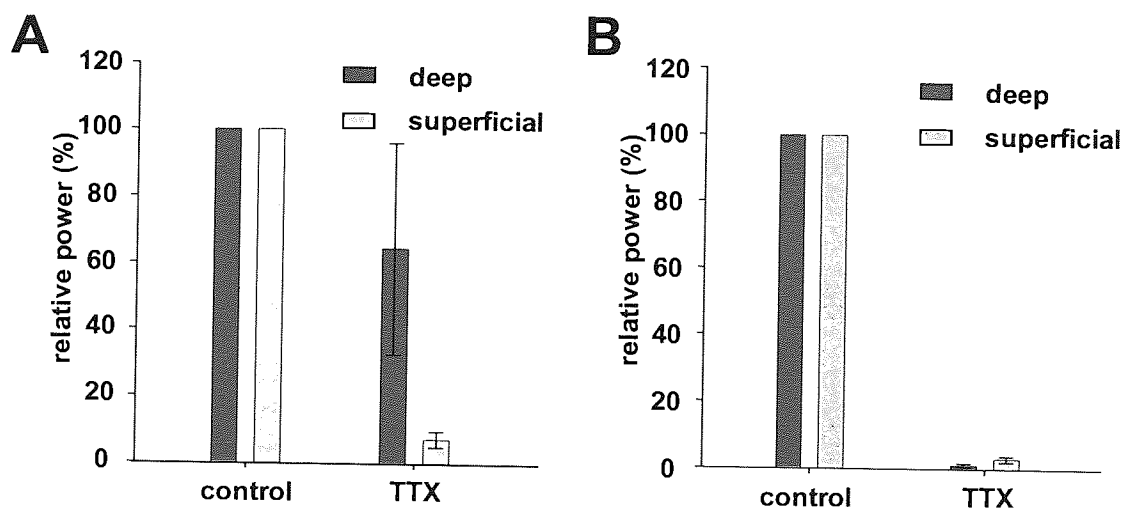
Figure 3.3 – Activity in deep layers drives M1 beta oscillations. (A) Change in relative power induced 300ms after picospritzer application of TTX to superficial layers. Red bar represents normalised power of layer V beta oscillatory activity. Grey bar represents normalised power of layer II/III beta oscillatory activity. (B) Change in relative power induced 300ms after by picospritzer application of TTX to deep layers. Red bar represents normalised power of layer V beta oscillatory activity. Grey bar represents normalised power of layer II/III beta oscillatory activity.

3.2.3 Effect of slice orientation and experimental setup

In neocortical slices, the frequency of synchronous network oscillation is known to be affected by variables such as the temperature of perfusing aCSF (Dickinson *et al.,* 2003). In addition, slice orientation of brain has been suggested to have some impact on oscillatory activity due to presence or absence of local and distant connectivity (Trudel and Bourque, 2003). Although experimental conditions used here are consistent with previous studies of gamma oscillation *in vitro*, many of these have been carried out in horizontal slices. In order to replicate these studies and also test whether beta oscillatory activity is characteristic of M1 or an artefact of slice orientation, horizontal slices were prepared. At 33-34°C addition of KA alone to

horizontal slices induced oscillations in the beta-gamma range in granular area of somatosensory cortex (n=2, figure 3.4B) consistent with previous reports by Roopun *et al.* (2006). No oscillatory activity was observed in M1 under these conditions, however, further addition of CCh promoted beta oscillations (figure 3.4A). No other frequencies of activity were observed confirming that beta oscillations are the predominant feature of M1 oscillatory activity. We have confirmed that it is possible to obtain gamma oscillatory activity using our experimental set-up by recording from the CA3 region of hippocampus in horizontal slices using CCh as reported by Fisahn *et al.* 1998 (n=3, figure 3.4C). These indicate that slice orientation does not matter for beta synchronous network activity.
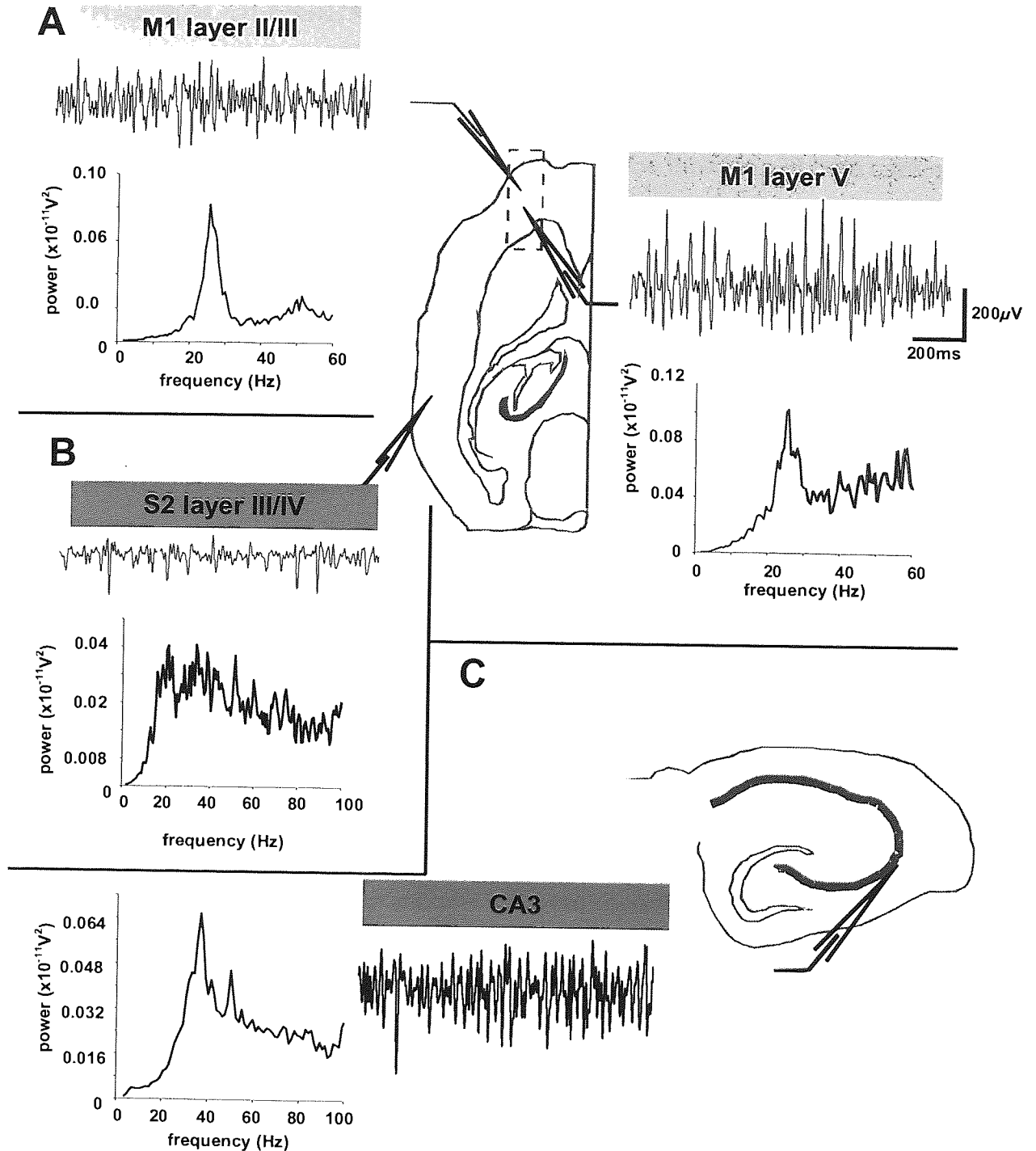
Figure 3.4 – Validity of the experimental setup. (A) Raw traces of synchronous network activities and associated power spectra obtained from layer II/III and layer V of horizontal M1, induced by co-application of KA and CCh. **(B)** Raw traces and associated power spectrum analysis of synchronous activity in somatosensory cortex induced by KA alone. Grey shadow indicates beta frequency band. **(C)** CCh-induced gamma oscillations in hippocampal CA3 region, as reported in Fisahn et al. (1998, appendix II). aCSF temperature and flow rate was identical to that used in the generation of beta oscillations in coronal slices of M1.

3.3 PHARMACOLOGICAL CHARACTERISATION OF BETA ACTIVITY IN M1

I have shown that deep layers of M1 are the likely to be the origin of beta oscillations. In this section, I have used the beta oscillation in layer V to characterise synaptic mechanisms involved in this activity. Layer V was selected as it generated beta oscillation of large power, hence, any drug-induced change would be easily observable.

3.3.1 The role of GABAergic receptors on beta network oscillation

In order to investigate the involvement of $GABA_A$ receptors in oscillatory activity in M1, picrotoxin (PTX, $50\mu M$), a $GABA_A$ receptor antagonist that blocks the chloride channel was bath applied. Addition of PTX abolished beta oscillatory activity, indicating a significant contribution of $GABA_A$ receptor-mediated synaptic input (n=5, figure 3.5A and B). Application of the $GABA_A$ receptor modulators pentobarbital (PENT, $20\mu M$) and the $\alpha1$-subunit specific $GABA_A$ receptor modulator zolpidem (ZOL, 100nM), which increase the chloride channel opening time and frequency respectively, also affected the nature of beta oscillation. PENT reduced beta frequency from 27.4 ± 1.3 to 24.1 ± 1.0 Hz ($P<0.001$, n=6, figure 3.5C) without significant change in oscillatory power. ZOL reduced the frequency from 26.7 ± 0.7 to 25.4 ± 0.8 Hz ($P<0.001$, n=11, figure 3.5E) whilst increasing the peak oscillatory power from $0.75 \pm 0.27 \times 10^{-11}$ to $1.05 \pm 0.32 \times 10^{-11}$ V^2 (two cells in particular showed large enhancement in power, $P<0.05$, n=11, figure 3.5F).
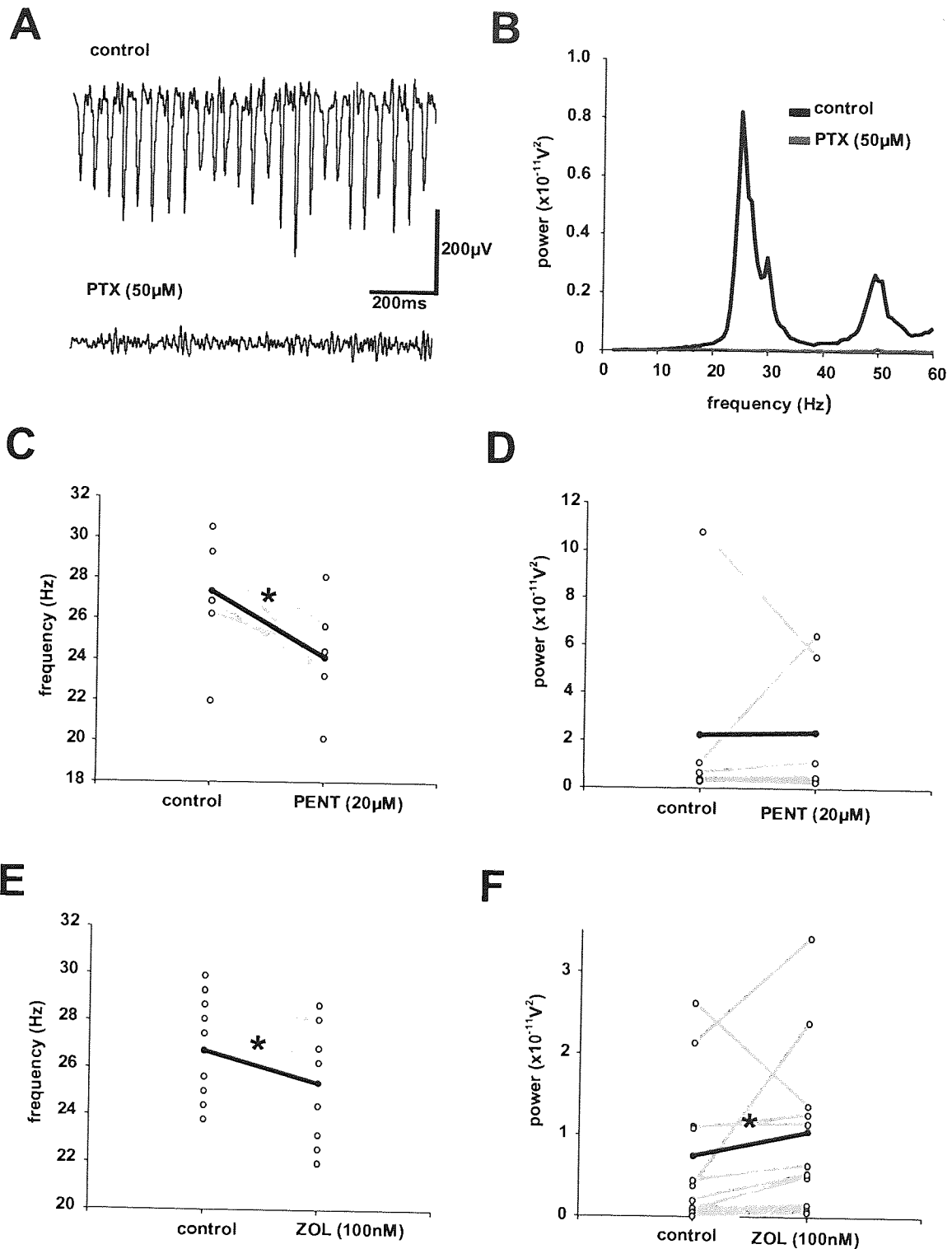
Figure 3.5 – The role of GABA$_A$ receptors in layer V beta oscillations. (A) Representative trace showing beta oscillation before (top trace) and after (bottom trace) application of PTX. (B) Averaged power spectrum (n=5) showing blockade of beta oscillation by PTX. (C and D) Plots showing application of PENT significantly reduced frequency of oscillatory activity but without significantly affecting its power. Grey represents changes observed in individual recordings and the black line indicates average change (E) Plot showing application of ZOL similarly reduced frequency of beta oscillation. (F) ZOL significantly increased oscillatory power.

Previous studies have indicated that GABA$_B$ receptors are not required for persistent oscillatory activity induced by CCh (Williams and Kauer, 1997). However, there is a report that suggests involvement of GABA$_B$ receptors in determining duration of transient, electrically evoked gamma oscillation (Whittington *et al.*, 1995). We therefore investigated the effect of the competitive GABA$_B$ receptor antagonist CGP55845 on M1 persistent beta oscillations. Bath application of this drug at 100nM concentration did not affect oscillatory frequency (mean control 27.1 ± 0.7 Hz vs. 25.5 ± 0.9 Hz in CGP55845 for layer V, figure 3.6A and B), but increased oscillatory peak power from 0.44 ± 0.14 x10^{-11}V^2 under control conditions to 0.70 ± 0.17 x10^{-11}V^2 in CGP55845 (*P*<0.02, n=5, figure 3.6A and B).
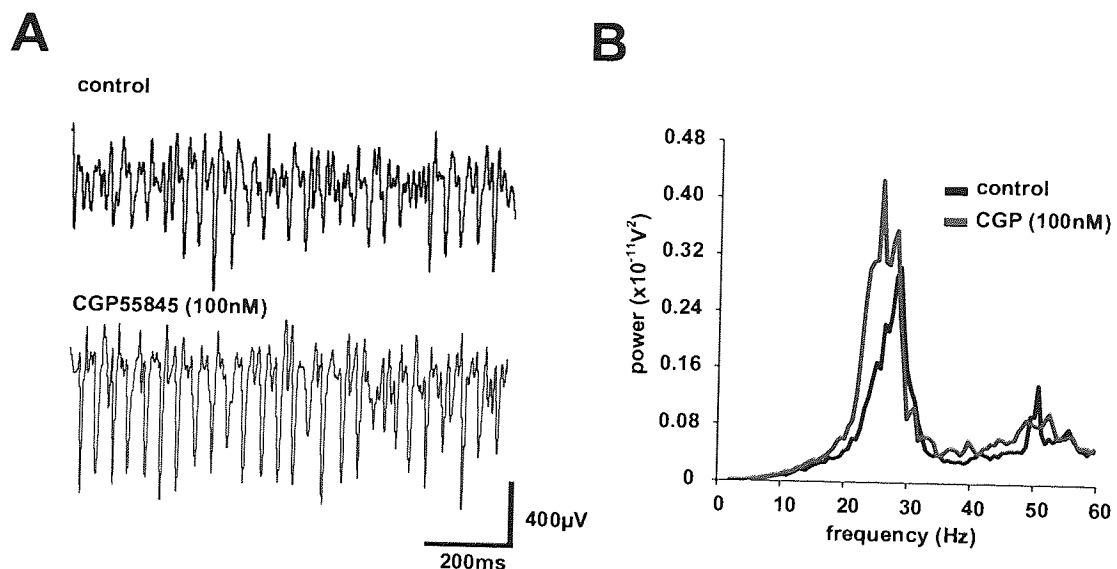
Figure 3.6 – The role of GABA$_B$ receptors in layer V beta oscillations. (A) Representative traces of beta oscillation recorded in layer V before (top) and after (bottom) application of CGP55845. **(B)** Averaged power spectrum (n=5) of beta network activity before and after CGP in layer V.

3.3.2 The role of glutamatergic receptors in beta oscillations

Previous studies indicated that both fast ionotropic glutamate receptors (i.e. AMPA and kainate) and mGluRs (Whittington *et al.*, 1995) may be involved in rhythmic network activity. Fast ionotropic glutamate receptors provide phasic recurrent excitatory input to both pyramidal and FS cells, thereby sustaining ongoing rhythmic activity (as seen in PING). mGluRs, in contrast, provide tonic excitation essential for ING. To determine whether the beta oscillation in M1 employs any of these mechanisms, CNQX (10µM), which blocks both AMPA and kainate receptors, was

applied. This drug abolished M1 beta oscillations, indicating the requirement at least one of these receptors (n=5, figure 3.7A and B). Bath application of AMPA receptor-specific antagonist SYM2206 (100μM) did not change ongoing beta oscillatory peak power (from 1.05 ± 0.25 x10^{-11} to 1.02 ± 0.31 x10^{-11}V^2, P>0.05, n=6) or frequency (from 25.9 ± 1.3 to 25.4 ± 0.9 Hz, P>0.05, n=6), suggesting AMPA receptor activation is not required and provides evidence for a significant contribution of kainate receptor-mediated excitation to neuronal network oscillation in M1 (figure 3.7C and D).

Application of MK801 (50μM), a non-competitive antagonist of NMDA receptors, significantly reduced peak power (from 2.53 ± 1.33 x10^{-11} to 1.65 ± 0.88 x10^{-11}V^2, n=5, P<0.05, paired, one-tailed) and oscillatory frequency (from 27.4 ±1.2 to 24.5 ± 0.7 Hz, n=5, P<0.05, paired, one-tailed, figure 3.7E and F). These data suggested that NMDA receptors may play a role in generation of beta oscillatory activity.

I next examined the role of mGluRs in the M1 beta oscillation. Previous reports indicated a role for these receptors in transient gamma oscillations evoked by tetanic stimulation (Whittington et al., 1995, 1997a, 1997b). However, application of MPEP (10μM), a specific antagonist of Group I mGluRs, to M1 beta oscillation had no effect on oscillatory power (from 0.19 ± 0.06 to 0.22 ± 0.06 x10^{-11}V^2, P>0.05, paired, two-tailed) or frequency (27.6 ± 2.5 to 25.8 ± 2.3 Hz, P>0.05, paired, two-tailed, figure 3.8A and B). Palhalmi et al., (2004) reported that activation of Group I mGluRs by DHPG induced gamma oscillations (30-100 Hz) in the CA3 region of hippocampus, whose properties was different from CCh-induced gamma oscillations in same region. Therefore, activation of mGluR alone may be able to generate mechanistically distinct synchronised network activity in M1. To test this, DHPG was applied to perfusing aCSF. Although gamma oscillatory activity was observed from simultaneously recorded CA3 hippocampal slice confirming the viability of drug (figure 3.8C and D), no synchronous network activity was observed in any layer of M1 even when pre-incubated for more than 1 hour.
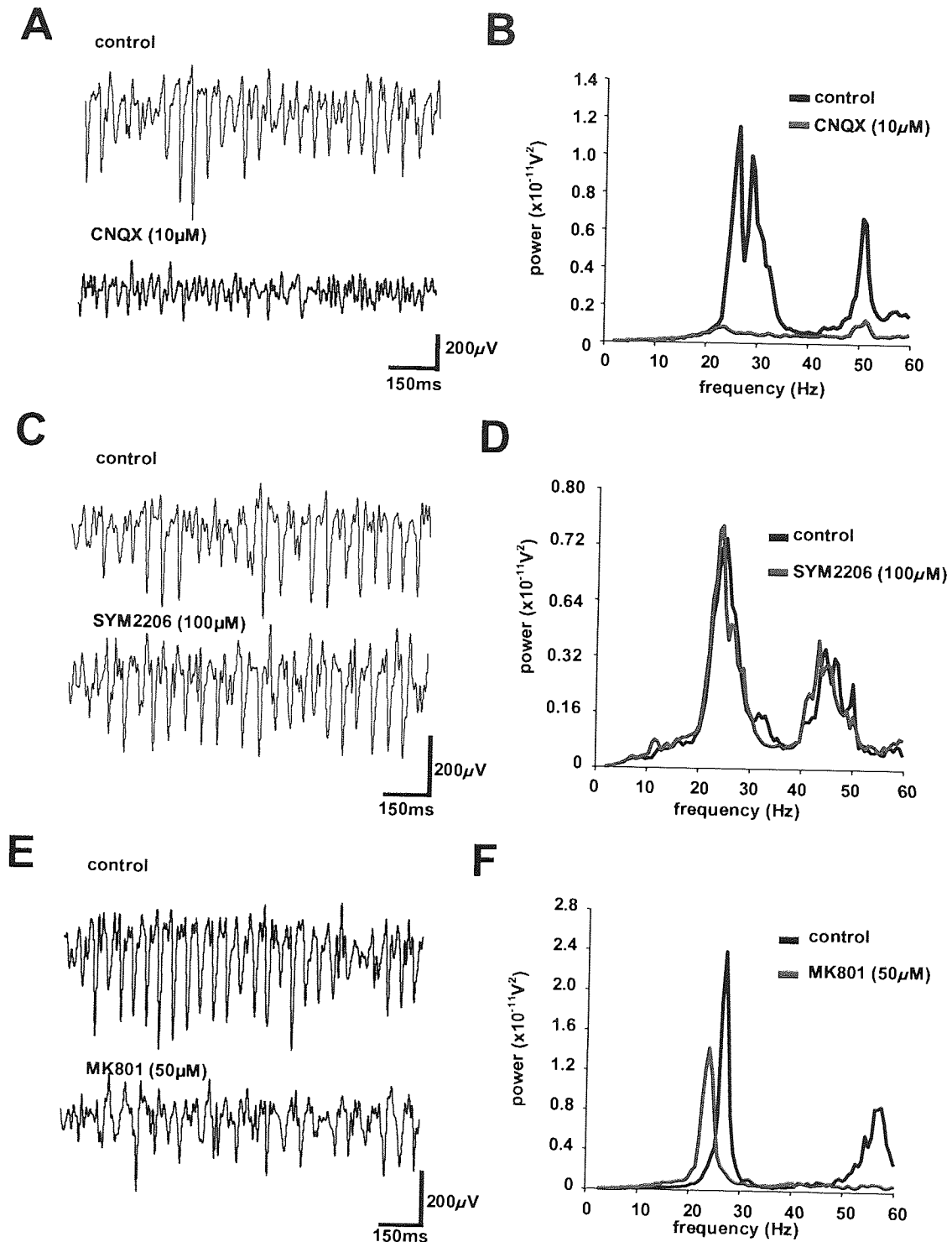
Figure 3.7 – The role of ionotropic glutamatergic receptors in layer V beta oscillations. (A) Raw traces showing beta oscillation before (top) and after (bottom) application of AMPA/KA receptor antagonist CNQX. **(B)** Averaged power spectrum showing removal of beta oscillation by CNQX. **(C)** Raw trace obtained before and after the application of AMPA receptor specific antagonist SYM2206. **(D)** Averaged power spectrum (n=6) analysis revealed no effect of SYM2206 on beta oscillation. **(E)** Raw trace of beta oscillation before and after addition of NMDA receptor antagonist MK801. **(F)** Averaged power spectrum analysis showing that MK801 significantly reduced both power and frequency of beta oscillation in layer V.
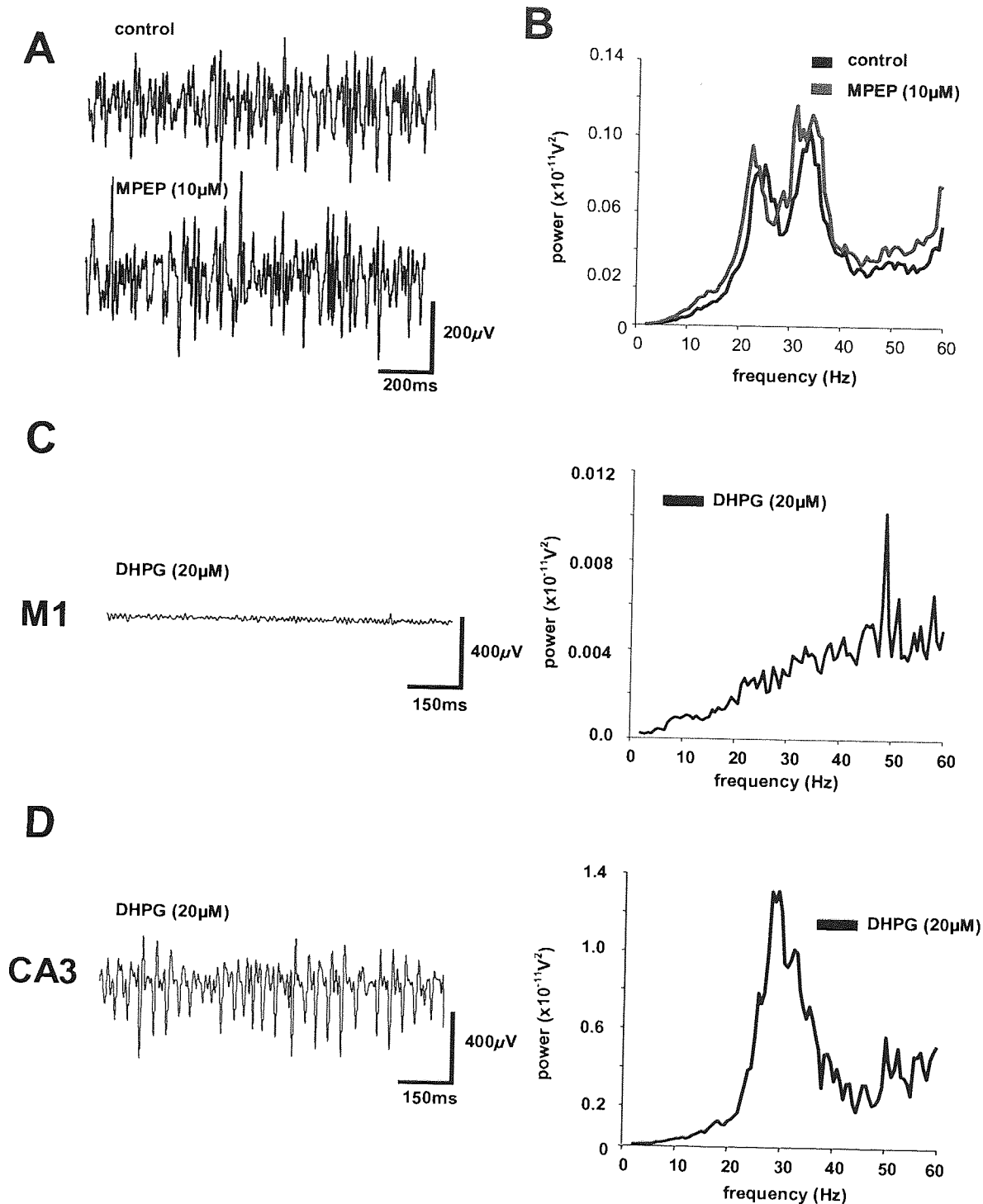
Figure 3.8 – The role of mGluR receptors on beta oscillations in layer V. (A) Raw traces showing beta oscillation before (top trace) and after (bottom trace) application of mGluR receptor antagonist MPEP. **(B)** Averaged power spectrum (n=6) clarifying that beta oscillations were not affected by MPEP. **(C)** Raw trace (left) and its power spectrum (right) showing no effect of DHPG on M1 network activity. **(D)** Raw trace and associated power spectrum of simultaneously recorded network oscillation in CA3 induced by DHPG.

3.3.3. The role of gap junction coupling on beta oscillation

A number of previous studies have indicated the involvement of gap junction-mediated electrical coupling of neurones in enhancing synchrony of network activity (Draguhn *et al.*, 1998; Galarreta and Hestrin, 1999; Traub *et al.*, 2000, 2001, 2003). I investigated gap junction mediated activity in M1 by applying the gap-junction blocker carbenoxolone (100μM). Persistent beta oscillations were entirely blocked by this drug (figure 3.9A and B), decreasing peak power from 1.17 ± 0.27 to 0.16 ± 0.04 x10^{-11}V^2 P>0.05, paired, two-tailed) and indicating the importance of gap junction activity to beta oscillations.
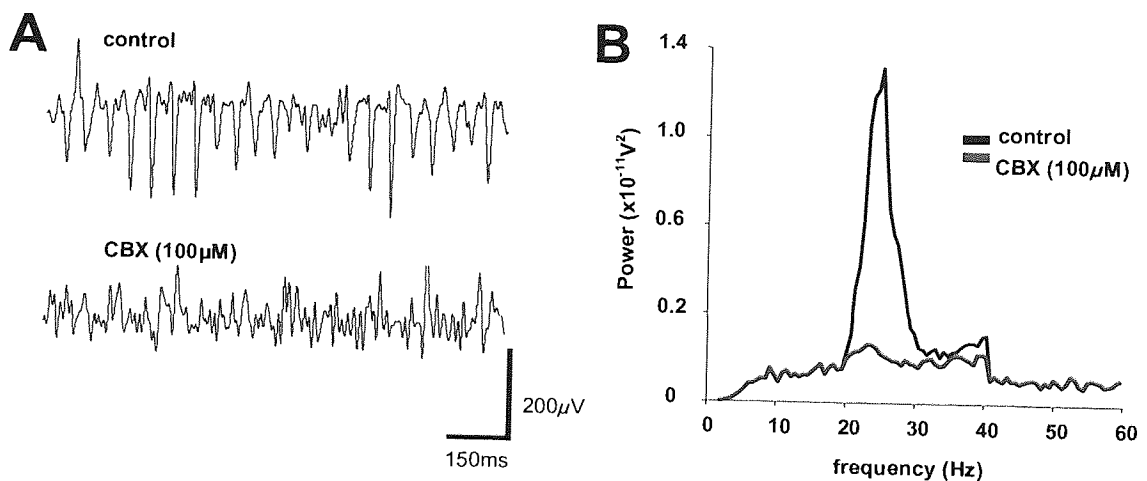
Figure 3.9 – The role of gap junctions in emergent beta oscillations in layer V. (A) Representative raw traces showing beta oscillation before (top trace) and after (bottom trace) application of gap junction blocker carbenoxolone. **(B)** Averaged power spectrum (n=5) clarifying that beta oscillations were abolished by carbenoxolone.

3.3.4. The role of acetylcholine receptors in beta oscillations

Synchronous oscillatory activity at theta or gamma frequency band can be observed upon cholinergic activation of neuronal network in CA3 region of hippocampus *in vitro* (Williams and Kauer, 1997; Fisahn *et al.*, 1998). In M1, however, addition of CCh (50μM) alone was insufficient to generate synchronous network activity and required co-application of KA. Nevertheless, this result indicated necessity of muscarinic receptor activation for M1 beta oscillation generation. In order to further probe the role of AChRs in oscillatory activity, the acetylcholine (ACh) receptor antagonist,

atropine (5μM), was bath applied. Application of this drug abolished synchronous network activity, decreasing peak power from 1.17 ± 0.27 to 0.16 ± 0.04 $\times 10^{-11} V^2$ implying an important role for AChR (n=5, figure 3.10A and B). However, as atropine affects a broad spectrum of ACh receptors, there was a possibility that the observed effect may be derived from blockade of nicotinic receptors (nAChR). To clarify this, TMPH (1μM), a selective antagonist for nAChR, was bath applied to oscillatory activity. However, this has no effect on the peak power (from control 0.36 ± 0.09 $\times 10^{-11}$ to 0.48 ± 0.13 $\times 10^{-11}$ V^2 in TMPH, $P>0.05$, paired, two-tailed) or frequency (from 25.2 ± 0.7 to 25.1 ± 0.7 Hz, $P>0.05$, paired, two-tailed) (figure 3.10C and D).
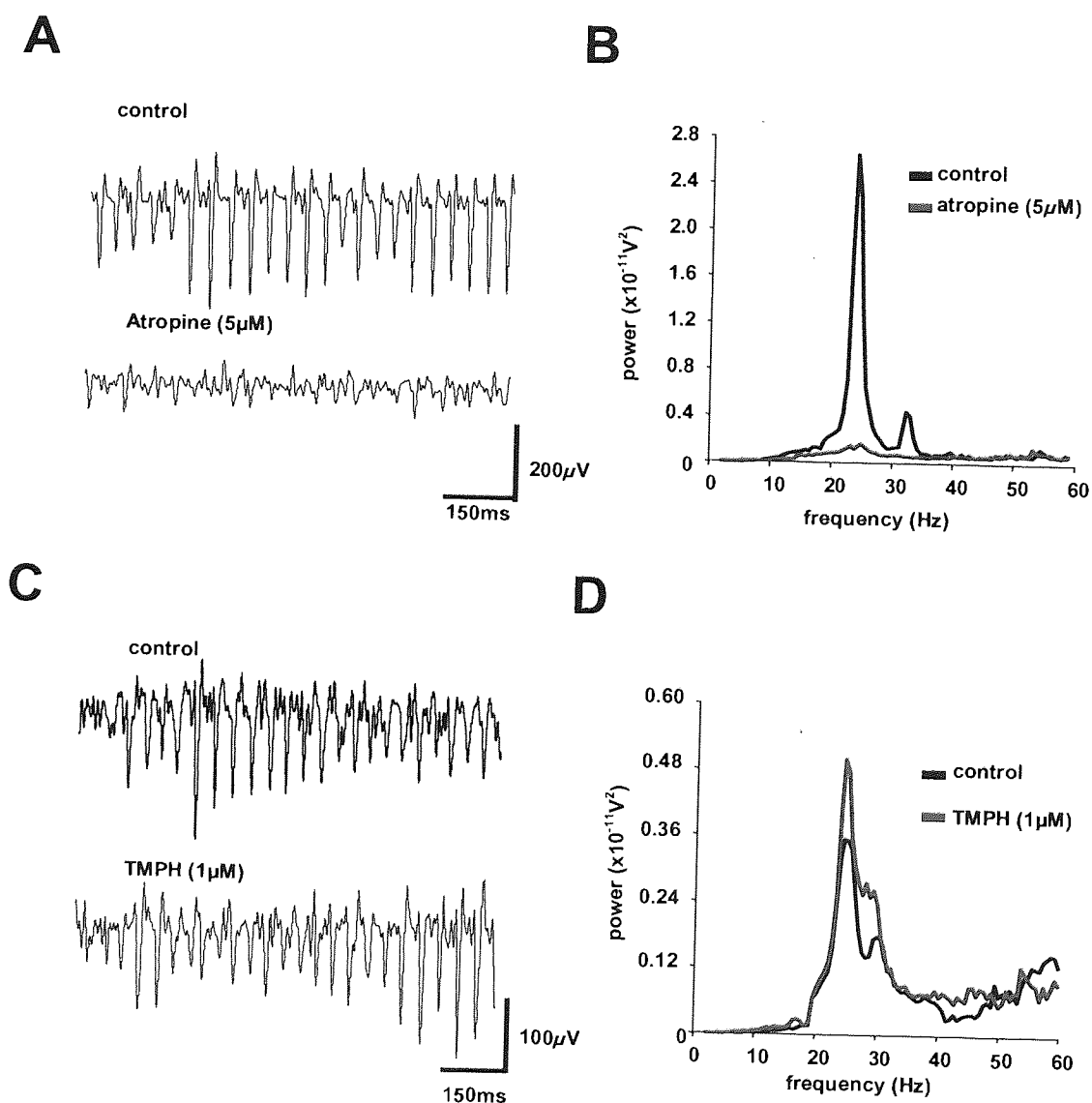
Figure 3.10 – The role of ACh receptors in beta oscillations in layer V. (A) Raw traces showing beta oscillation before (top) and after (bottom) application of the ACh receptor antagonist atropine. (B) Averaged power spectrum (n=5) clarifying that beta oscillations were abolished by atropine. (C) Raw traces showing beta oscillation before (top traces) and after (bottom traces) the addition of specific nicotinic receptor antagonist TMPH. (D) Averaged power spectrum from TMPH experiment (n=8).

3.3.5 Influence of dopaminergic input on beta oscillations

Dopamine (DA) is a neuromodulator released by dopaminergic neurones, whose cell bodies lie principally in SNc and ventral tegmental area (VTA) of the midbrain. Projections from these sites arrive at cortex and striatum, where they are thought to regulate cognition, motivated behaviour, and motor behaviour. Previous studies involving LFP recordings revealed that beta oscillations are abnormally enhanced in motor cortex in DA-depleted state, perhaps, implying a role for DA in synchronous network activity. Bath application of DA (100μM) had no effect on the power of beta oscillations (from 27 ± 0.10 to 0.31 ± 0.09 $\times 10^{-11}$V^2, $P>0.05$, figure 3.11B) but significantly reduced oscillatory frequency (25.1 ± 0.85 to 23.6 ± 0.77 Hz, $P<0.05$, figure 3.11C).
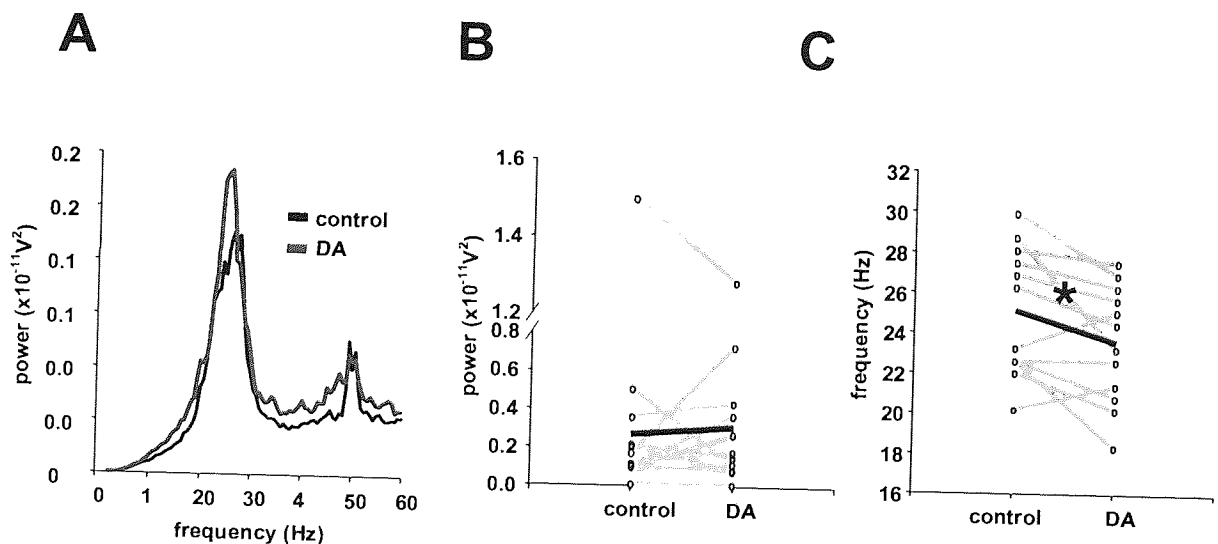
Figure 3.11 – The effect of dopamine on beta oscillations in layer V. (A) Averaged power spectrum (n=14) in control (black) and in DA (red). (B and C) Plots showing individual change (grey line) and averaged change (black line) of oscillatory power and frquency. * indicates $P <0.05$.

3.4 DISCUSSION

3.4.1 Overview

Consistent with previous *in vivo* studies (e.g. Murthy and Fetz, 1992, 1996a, 1996b; Jensen *et al.*, 2005), M1 preferentially generates synchronous network oscillatory activity at beta frequencies *in vitro* consistent with conditions required for induction of persistent oscillations in other *in vitro* models (Fisahn *et al.*, 1998; Buhl *et al.*, 1998; Cunningham *et al.*, 2003; Roopun *et al.*, 2006). However, application of both KA and CCh was necessary to observe this persistent synchronous network beta activity. The power distribution and phase relationship of the beta oscillation between layers suggested that it was likely to be generated in layer V in the M1 slice preparation. Persistent beta oscillations in layer V were dependent on fast synaptic inhibition mediated by $GABA_A$ receptors and fast/tonic excitation mediated by kainate receptors, NMDA receptors and muscarinic M1 receptors. A contribution from $GABA_B$ receptors was also observed while electrical coupling of the neuronal network by gap junctions appeared necessary for robust rhythmogenesis. Dopamine was found to be able to modulate this network activity via activation of D1 receptor but not D2 receptors.

3.4.2 The role of KA and CCh

The kainate receptor family contains glutamate receptor subunits GluR5, GluR6, or GluR7. Activation of kainate receptors with nanomolar concentration of KA increases excitability of neurones and enhances AP-independent release of glutamate or GABA. Indeed, at inhibitory synapses, KA depolarises interneurones leading to continuous neuronal firing, thereby increasing frequency of sIPSCs on pyramidal neurones (Cossart *et al.*, 1998; Frerking *et al.*, 1998). Significant increases in AP-independent miniature (m)IPSC frequency by KA have also been reported, indicating some direct pre-synaptic effect (Cossart *et al.*, 2001).

Similar effects have also been reported at excitatory synapses, where nanomolar concentration of KA increased both sEPSCs and mEPSCs frequency recorded on

pyramidal cells (Campbell *et al.,* 2007). Kainate receptors have been reported to contribute to synaptically evoked currents in hippocampus (Vignes and Collingridge, 1997), although the contribution of kainate receptor-mediated currents to evoked EPSC amplitude was found to be negligible in layer V pyramidal cells of motor cortex (Ali, 2003). In fact, in M1 increases in extracellular glutamate concentration via pharmacological blockade of glutamate uptake were required to observe any KA-mediated current, suggesting an extrasynaptic location of kainate receptors in these cells.

In order to induce network oscillations in M1, CCh was co-applied with KA to enhance neuronal excitability. CCh activates the muscarinic M1 receptor, which is G-protein coupled and thought to be expressed post-synaptically (Muller and Misgeld, 1986). Generally, this receptor exerts its depolarising effect by inhibiting various K^+ channels, such as the rectifying outward current (I_M), Ca^{2+}-dependent K^+ current (I_{AHP}), and the leak K^+ current (I_{K-leak}) (Lucas-Meunier *et al.,* 2003). The effect of muscarinic receptor activation however, seems to be different between cells. Indeed, cortical interneurones are more rapidly depolarised than pyramidal cells (McCormick and Prince, 1986).

The need for both KA and CCh to induce robust beta oscillations most likely reflects the reduced local neuronal network excitability in slice compared with that which may be found *in vivo.* Each cortical pyramidal cell receives 5,000-60,000 synapses (DeFelipe and Fariñas, 1992; Destexhe and Paré, 1999), 70% of which originate from projection neurones *in vivo* (Szentagothai 1965; Gruner *et al.,* 1974). During sectioning of the brain for *in vitro*, these synaptic inputs will be removed, causing a large reduction in spontaneous background activity, and this normally contributes to increasing network responsiveness (Destexhe and Paré, 1999; Hô and Destexhe, 2000).

In contrast to a number of previous studies of gamma oscillations in hippocampus, entorhinal, and somatosensory cortex, (Fisahn *et al.,* 1998; Cunningham *et al.,* 2003; Roopun *et al.,* 2006), the application of KA or CCh alone did not reliably generate oscillatory activity in M1 in our study. Our experimental setup was found to be sufficient to induce oscillatory activity in CA3 similar to that described by Fisahn *et al.*

(1998), indicating that slice viability or differences in perfusion were unlikely to explain our findings. It is possible that the structural and functional resilience of pyramidal cells and interneurones in M1 after slicing may be less compared to other cortical areas. This may lead to a requirement of stronger excitation for M1 to compensate for damage induced during slice preparation and storage. However, it is notable that Buhl et al. (1998), using coronal slices of mouse somatosensory cortex, found a similar requirement for KA and CCh in generation of persistent gamma oscillations. The Buhl study (Buhl et al., 1998) also highlights the fact that I was unable to observe robust oscillatory activity at frequencies other than beta using this preparation and alteration of the plane of section from coronal to horizontal orientation did not abolish the induction of beta oscillations or reveal any activity in other frequency bands. These data indicate strongly that beta oscillations are a characteristic and defining feature of M1 in vitro, and this is entirely consistent with previous reports of the role of beta activity in physiological and pathological states such as movement (Murthy and Fetz, 1996a; Donoghue et al., 1998) and PD (Sharott et al., 2005a; Silberstein et al., 2005) where M1 has a prominent role.

3.4.3 The origin of oscillatory activity

In present study, the power of beta oscillations was found to gradually increase from superficial to deep layers, reaching its maximum in layer V. This finding is consistent with in vivo studies in which, the amplitude of beta LFPs was found to increase with depth to a peak corresponding to layer V region (Murthy and Fetz, 1996a; Donoghue et al., 1998).

Layer V may show greatest oscillatory power simply due to its relatively high density of large pyramidal cell bodies. Secondly, the power of layer V beta oscillations may be attributed to the morphology of pyramidal cells. Betz cells in layer V have large cell bodies and extensive dendritic arborisations relative to other cortical layers. In particular, the type 1 Betz cell is known to extend its dendrites up to layer I where they form an apical dendritic tuft (Molnár and Cheung, 2006). Since the LFP is thought to reflect the weighted sum of somatodendritic potential (Logothetis, 2003), the power of beta oscillation recorded from layer V region may reflect greater

summation of synaptically-driven oscillatory activity impinging on the extensive dendritic tree.

Dendritic gap junctions amongst the interneurones of similar subtype are thought to reduce differences in intrinsic membrane properties thereby enhancing synchrony (Galarreta and Hestrin, 1999; Gibson *et al.,* 1999; Traub *et al.,* 2000, 2001, 2003). Furthermore, gap junctions between axons of pyramidal cells have been suggested to amplify the synchronous output of these neurones (Schmitz *et al.,* 2001; Traub *et al.,* 2003). A study of the distribution of mRNA encoding connexin 36 (Cx36), the most abundant subunit of gap junction in mammalian neurones (Condorelli *et al.,* 2000, LeBeau *et al.,* 2003), reported high expression in deep compared to superficial layers (Condorelli *et al.,* 2000).

The cross-correlation analysis and TTX experiments indicate the origin of pharmacologically induced beta oscillation lies within deep layers. This is consistent with the reported source of oscillatory activity in deep somatosensory cortex *in vitro* (Sanchez-Vives and McCormick, 2000). However, *in vivo,* the polarity of the beta oscillations was found to completely reversed 0.5-1mm from the surface, suggesting a superficial origin of oscillatory activity (Murthy and Fetz, 1996b). The difference between *in vitro* and *in vivo* reports may be attributed to the preserved connection of subcortical inputs to superficial cortex *in vivo.* Indeed, numerous excitatory synaptic inputs from VL thalamus arrive at superficial layers of M1 *in vivo* (Douglas and Martin, 2004; Shipp, 2005).

3.4.4 All layers of M1 express beta oscillatory activity

In all layers, oscillatory activity at beta frequencies was observed, indicative of oscillatory resonance within the extended network. However, unlike the somatosensory cortex (Roopun *et al.,* 2006), no pharmacologically induced gamma activity was observed in superficial layers. This difference may reflect different network structure between our coronal slices and the horizontal slices used by Roopun *et al.* (2006), or a fundamental difference between the two cortical regions. Indeed, we know M1 is agranular (i.e. no layer IV). Nevertheless, coherent gamma frequency oscillations in specific regions of motor cortex have been demonstrated

81

during strong contractions (e.g. Brown *et al.,* 1998) and recently, one study has suggested that the 'piper frequency' (40 Hz) oscillatory activity in non-homologous and contralateral muscles constitutes evidence of 'occult' gamma oscillation in motor cortex at rest (Funk and Epstein, 2004). Several studies indicate that in man, 20 Hz activity in M1 is associated with inactive cortical states, and is suppressed prior to and during movement (Murthy and Fetz, 1992; Donoghue *et al.,* 1998), but that such activity is progressively recruited during sustained isometric muscle contraction (Penfield, 1954; Conway et al., 1995). These data suggest that beta oscillatory activity in M1 is part of the idling process in cortex, but can also be dynamically related to function. In this scenario, both beta and gamma activity may be present at rest, with the former highly suppressed and the latter enhanced during voluntary movement, but both beta and gamma may be enhanced during sustained contraction.

3.4.5 A possible mechanism for beta oscillations in M1

Previous studies of persistent gamma oscillatory activity in neocortex *in vitro* indicated that neuronal network activity is patterned by recurrent inhibition from local interneurones (Whittington *et al.,* 1995; Traub *et al.,* 1996b; Fisahn *et al.,* 1998; Buhl *et al.,* 1998; Cunningham *et al.,* 2003; Roopun *et al.,* 2006). Beta oscillations found in M1 layer V are also likely to be governed by interneurones, as pharmacological blockade of $GABA_A$ receptors completely abolished this activity. Furthermore, pharmacologically induced beta oscillations were modulated by pentobarbital and zolpidem, which bind directly to $GABA_A$ receptors. The action of zolpidem at a concentration of 100 nM also indicates the involvement of $GABA_A$ receptors containing the α1 subunit (Crestani *et al.,* 2000). The increase in oscillatory power indicating the recruitment and synchronous activation of pyramidal neurones may be related to the enhanced beta activity or 'beta buzz' observed during EEG recordings upon administration of certain benzodiazepines and barbiturates (Glaze, 1990).

The persistent gamma oscillations observed in neocortical slices can be generated by two distinct mechanisms: (1) those that require recurrent excitatory feedback from pyramidal cells to interneurones to preserve network rhythm (Fisahn *et al.,* 1998; Buhl *et al.,* 1998; Cunningham *et al.,* 2003) or (2) those that do not require such a

feedback (Whittington *et al.,* 1995; Traub *et al.,* 1996b). The former mechanism, known as "PING" (Traub *et al.,* 1999a), requires fast excitatory synaptic inputs, which are mediated by AMPA receptors. In the current study, application of CNQX abolished the beta oscillation presumably due to loss of AMPA/kainate receptor function. However, specific blockade of AMPA receptors alone using SYM2206 had no effect on oscillatory activity. These observations indicate that the mechanism of M1 beta oscillation may not be PING-like. For the latter mechanism, known as ING, tonic depolarisation provides a persistent diving force for rhythmogenesis between mutually inhibiting interneuronal network. Activation of metabotrophic glutamate or muscarinic receptors are necessary for this mechanism (Whittington *et al.,* 1995). The requirement of muscarinic M1 receptor activation for generation of beta oscillation in M1, as well as absence of AMPA mediated current indicates that beta oscillation in M1 is mechanistically similar to ING. Kainic acid may as well contribute to such a tonic excitation of neuronal network via activation of extrasynaptic receptors (Ali *et al.,* 2003) or direct activation of interneurone and pyramidal cells (Cossart *et al.,* 1998; Frerking *et al.,* 1998; Semyanov and Kullmann, 2001). However, the possibility that kainate receptors provide some recurrent excitatory feedback or presynaptic function cannot be ruled out.

Despite the mechanistic similarity between M1 beta activity and ING, pharmacological manipulation of M1 did not generate gamma frequency network activity. In Traub *et al.* (1996b) model, the frequency of interneuronal network oscillation was shown to be dependent on mean excitatory drive to network, decay time of $GABA_A$-mediated IPSPs, and $GABA_A$-mediated current (Traub *et al.,* 1996b). According to this model, beta oscillations would be preferred when (1) the mean excitatory drive is low (2) the decay time of $GABA_A$-receptor mediated IPSPs are slow and (3) the $GABA_A$-receptor conductance is high. The lack of AMPA mediated current in M1 layer V may be indicative of relatively low excitatory drive present in M1 layer V. Confirmation of the other possibilities outlined above requires further investigation using intracellular recording.

Our pharmacological studies indicated that $GABA_B$ receptors are involved in this beta oscillation, as blockade of this receptor type significantly enhanced beta oscillation. Presynaptically expressed $GABA_B$ receptors are thought to reduce the GABA release

from terminal, while postsynaptically expressed $GABA_B$ receptors generate slowly decaying IPSPs. Hence, postsynaptic $GABA_B$ receptors may be contributing to slowing of IPSPs decay mediated by $GABA_A$. Furthermore, we observed a contribution of NMDA receptors in the beta oscillation which decreased power and frequency consistent with previous studies (Cunningham *et al.*, 2003; Roopun *et al.*, 2006). Overall, beta oscillations show an absolute dependence on kainate receptors, muscarinic M1 receptor, and $GABA_A$ receptors and are modulated by $GABA_B$ and NMDA receptors.

3.4.6 The role of gap junctions

Gap junctions have been shown to occur between dendrites of FS cells (Galarreta and Hestrin, 1999; Gibson *et al.*, 1999), dendrites of RSNP cells (Szabadics *et al.*, 2001), dendrites of LTS cells (Gibson *et al.*, 1999; Beierlein *et al.*, 2000), and axons of pyramidal cells (Schmitz *et al.*, 2001). Such an electrical connectivity was found to be rare between different interneuronal subtypes (Gibson *et al.*, 1999; Szabadics *et al.*, 2001). Pharmacological blockade of gap junction function with carbenoxolone (CBX), has been shown to abolish ultrafast oscillation (80-200Hz, Draguhn *et al.*, 1998) and gamma/beta oscillation *in vitro* (Traub *et al.*, 2000; Deans *et al.*, 2001; Hormuzdi *et al.*, 2001; Cunningham *et al.*, 2003; Roopun *et al.*, 2006). Consistent with these observations, application of 100µM of CBX suppressed pharmacologically induced beta oscillation in M1 layer V. At this concentration it does not appear to influence the intrinsic properties of hippocampal pyramidal neurones while diminishing gap junction-mediated spikelets (Schmitz *et al.*, 2001), suggesting that the observed effects were purely due to gap junction blockade.

It has been demonstrated, by computer simulation model, that dendritic and axonal gap junctions contribute differently to KA induced gamma oscillatory activity (Traub *et al.*, 2003). Indeed, dendritic gap junctions have been suggested to reduce heterogeneity"[24] of excitability among individual interneurones, thereby enhancing their coherent firing (Traub *et al.*, 2001, 2003). Axonic gap junctions, on the other

---

[24] Such a heterogeneity may occur due to different excitatory inputs source as well as different intrinsic properties of interneurones

hand, have been reported to provide a mechanism which create gamma frequency outputs from the pyramidal cell axons despite the somatic AP frequency being low (Traub *et al.*, 2003). Interestingly, blockade of axonic gap junctions abolishes gamma oscillations, but blockade of dendritic gap junctions only suppresses their power (Traub *et al.*, 2003). Indeed, it has been shown that hippocampal slice prepared from mice knocked out with Cx36, a major subtype of gap junction protein expressed highly in interneurones (Condorelli *et al.*, 2000; Deans *et al.*, 2001; Hormuzdi *et al.*, 2001; Traub *et al.*, 2003), could still generate gamma oscillations albeit with reduced power (Deans *et al.*, 2001; Hormuzdi *et al.*, 2001). Therefore, it is possible that the high conductivity of gap junctions between interneurones in layer V, relative to other layers, may contribute to the distinctively large beta oscillatory power.

3.4.7 Functional implications of dopamine

Beta oscillatory activity is thought to be strongly associated with motor behaviour. Indeed, several *in vivo* and MEG studies show beta oscillatory activity before, during, and after the voluntary movements (Murthy and Fetz, 1992, 1996a, 1996b; Donoghue *et al.*, 1998). In addition, during dopamine-depleted state, such beta activity is abnormally enhanced, and this enhancement correlates with symptoms including bradykinesia and akinesia (Brown *et al.*, 2001; Sliberstein *et al.*, 2005).

Previously, Weiss *et al.* (2003) reported that gamma oscillatory power was consistently reduced by the application of dopamine. This effect was mimicked by dopamine D1-like receptor agonist (SKF-38393), and suppressed by D1-like receptor antagonist (SCH-23390). D2-like receptors were found to play no role. In our studies, the effect of dopamine on beta oscillations was rather inconsistent. In 8 out of 14 slices, dopamine significantly enhanced beta power, but a reduction in power was seen in 5 out of 14 slices. These observations led to the conclusion, that overall, DA had no significant effect on the power of beta oscillations.

Interestingly, it appeared that the effect of dopamine on layer V oscillatory power was dependent on the initial beta power. When control beta oscillatory power was low, dopamine enhanced oscillatory power however, when initial oscillatory power was high, dopamine had a suppressive effect. A number of previous studies indicated

complex effects of dopamine at the cellular level (Yang and Seamans, 1996; Shi et al., 1997; Gulledge and Jaffe, 1998; Henze et al., 2000). For example, Gulledge and Jaffe (1998) reported that firing rate of layer V pyramidal cells, at given depolarising current injection, was significantly reduced by dopamine, and this effect was correlated with reduced input resistance. However, others indicated that dopamine increases the membrane excitability of both pyramidal cells and interneurones (e.g. Yang and Seamans, 1996; Shi et al., 1997; Zhou and Hablitz, 1999). Thus, the diverse actions of dopamine may be due to a number of factors, site of action, receptor subtype being activated and ion channels affected (Gulledge and Jaffe, 1998; Gonzalez-Islas and Hablitz, 2003).

In present study, the enhancement of oscillatory power induced by dopamine may reflect an increased neuronal population available for synchronisation. Such an elevation could be achieved simply due to participation of pyramidal cells and/or interneurones, that have failed to reach threshold before dopamine application. Indeed, in the absence of synaptic inputs, dopamine was reported to enhance the duration of slow inactivation Na^+ current while attenuating a slowly inactivating outward rectifying K^+ current via D1-like receptors, thereby lowering the spike threshold of pyramidal cells (Yang and Seamans, 1996). The excitability of interneurones is also increased by dopamine via suppression of the leak K^+ current, inward rectifying K^+ current, and slowly inactivating K^+ current (Gorelova et al. 2002; Zhou and Hablitz, 1999; Wu and Hablitz, 2005).

Reduction of oscillatory power, on the other hand, reflects reduced synchrony. The amplitude of oscillations has been shown to be sensitive to the electrical coupling of interneurones (Deans et al., 2001; Hormuzdi et al., 2001). Recently it was found that electrical coupling between amacrine cells in mammalian retina was significantly reduced by dopamine, which involved phosphorylation of Cx36 by protein kinase A (Hampson et al., 1992; Urschel et al., 2006). Hence, a negative effect of dopamine on oscillatory power in M1 may possibly be related to reduced conductivity of gap junctions by dopamine. However, a recent study of FS-FS cell coupling in M1/M2 layer V indicated that D1-like or D2-like receptor activation has no effect on electrical communication (Towers and Hestrin, 2008). In same study, a D1-like receptor agonist, SKF-38393, reduced the amplitude of evoked IPSCs on FS cells (Towers

and Hestrin, 2008), which may indicate decreased inhibitory synaptic coupling between FS-FS cells. Furthermore, dopamine has been reported to reduce the evoked inhibitory synaptic influence of FS cells on pyramidal cells (Gao *et al.*, 2003). These results may suggest that dopamine reduces the ability of FS cells to entrain a large population of neurones in the current study.

CHAPTER 4:
CELLULAR MECHANISMS UNDERLYING BETA OSCILLATIONS IN M1

4.1 INTRODUCTION

In the pervious chapter, I revealed that M1 preferentially generates persistent synchronous network oscillations at beta frequency upon KA and CCh application. This activity is generated in layer V, and propagates towards layer II/III. In addition, the oscillation was found to be strongly dependent on $GABA_A$, kainate, and muscarinic M1 receptors, and modulated by $GABA_B$, dopamine and NMDA receptors. Furthermore, neurones participating in synchronised network activity appeared to be linked by gap junctions.

Although this information allowed us to speculate how the activity of thousands of neurones might be synchronised, analysis of individual cell behaviour with respect to network beta oscillatory activity would provide a more detailed and precise picture of the underlying mechanism. Sensorimotor cortex has been reported to contain glutamatergic cells that can be classified into regular-spiking (RS) cells or intrinsically-bursting (IB) cells, depending on the firing properties (Connor et al., 1982; Chen et al., 1997). GABAergic cells also exhibit electrophysiological diversity, which divides them into regular spiking non-pyramidal (RSNP), fast-spiking (FS), late-spiking (LS), or low threshold-spiking (LTS) cells (Kawaguchi, 1995; Cauli et al., 1997). Each of these cells contribute differently to shape the spatial pattern of transient and persistent gamma oscillations (e.g. Whittington et al., 1995; Fisahn et al., 1998; Buhl et al., 1998; Klausberger et al., 2003). In this chapter, I have explored the cellular mechanisms of beta oscillations by simultaneously recording field and single cell activity in layer V. Coherence analysis was used to reveal the relationship between these two signals.

4.2 CELLULAR MECHANISMS OF BETA OSCILLATIONS

4.2.1 Electrophysiological characterisation of different cell types

Passive and active membrane properties were characterised using a current step protocol. In response to a series of 500ms current steps in increments of +40 pA from an initial holding current of -0.4nA until threshold for AP firing was reached. Three different electrophysiological cell types were observed in present study (figure 4.1). A summary of their electrophysiological characteristics are shown in table 1. RS cells (n=12) exhibited spike frequency adaptation, while IB cells (n=7) were characterised by an initial spike burst followed by low frequency, non-adapting APs. For spike analysis, non-bursting APs were chosen. Finally, FS cells (n=2) were identified by their high firing frequency with fast but profound AHPs.

Cell type	Resting membrane potential (RMP)	Spike threshold (mV)	Spike amplitude (mV)	AP width (mV, at base)	AHP (mV, from threshold to amplitude)
RS (n=12)	-72,0 ± 2.1	-54.8 ± 2.3	54.0 ± 1.6	2.06 ± 0.20	7.6 ± 1.1
IB (n=7)	-77.1 ± 3.2	-60.4 ± 3.5	57.3 ± 1.2	3.04 ± 0.61	8.5 ± 1.7
FS (n=2)	-65.7 ± 11.4	-54.2 ± 8.6	38.3 ± 5.3	1.55 ± 0.35	11.7 ± 1.5

Table 4.1 – Electrophysiological characteristics of RS, IB and FS cells
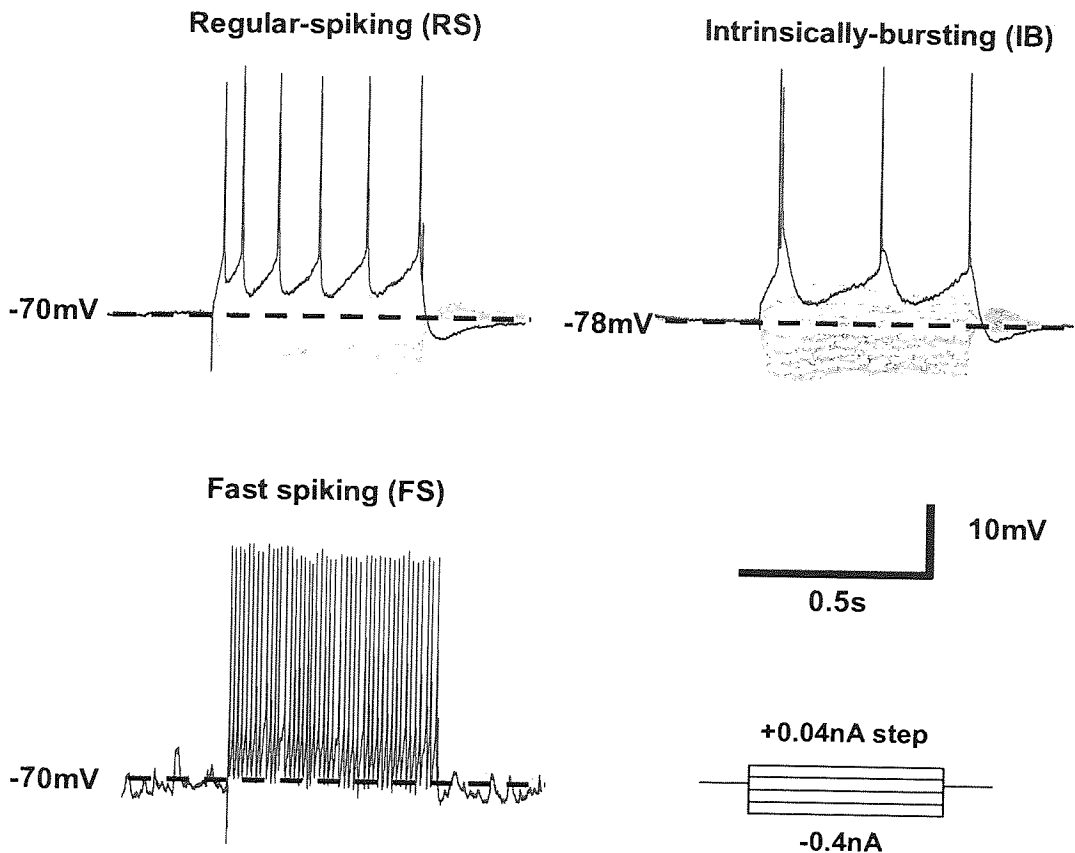
Figure 4.1 – Spiking behaviour of RS, IB and FS cells in M1 layer V. RS cells were characterised by spike frequency adaptation and single spike, in contrast to IB cells, which showed spike bursts, little adaptation and a membrane voltage sag characteristic of I_h. FS cells we characterised by fast spiking and extensive background synaptic activity.

4.2.2 Firing behaviour of excitatory neurones during beta oscillations

During beta field oscillations (24.9 ± 0.8 Hz), most RS cells fired spontaneously (figure 4.2A). The firing frequency of these cells was found to be much slower than beta oscillations at 9.6 ± 1.2 Hz (figure 4.2B). Although RS cells exhibited different AP frequency to the field, they were spatially related. To test this, coherence analysis was undertaken. In 11/12 RS cells, a significant peak at beta frequency was found (average coherence of 0.31 ± 0.04 at 23.7 ± 1.5 Hz) (figure 4.2C). In one cell, however, such a positive association of APs with respect to beta field activity was not found figure 4.2D). I then investigated the pattern of synaptic input received by RS cells. Previous studies of persistent gamma oscillation *in vitro* indicated that excitatory cells received IPSPs at gamma frequency, which were spatially coupled with gamma field activity (Fisahn *et al.,* 1998; Buhl *et al.,* 1998; Cunningham *et al.,*

2003). Depolarising cell membrane potential to -30mV exposed pure rhythmic IPSPs (figure 4.3A). Power spectrum analysis of these IPSPs revealed that they were occurring at beta frequency (23.4 ± 0.7Hz, figure 4.3B). It was confirmed that these were IPSPs, as application of bicuculline (20μM) eliminated them completely, together with beta field oscillations (n=6, figure 4.4C, and 4.4D). Coherence analysis of IPSPs and field activity indicated that they were significantly dependent on each other at beta frequency (average coherence of 0.51 ± 0.76 at 25.1 ± 0.8 Hz, figure 4.3C). Interestingly, one cell which did not show any coherent spiking behaviour received IPSP input which was coherent with the field (figure 4.3D).
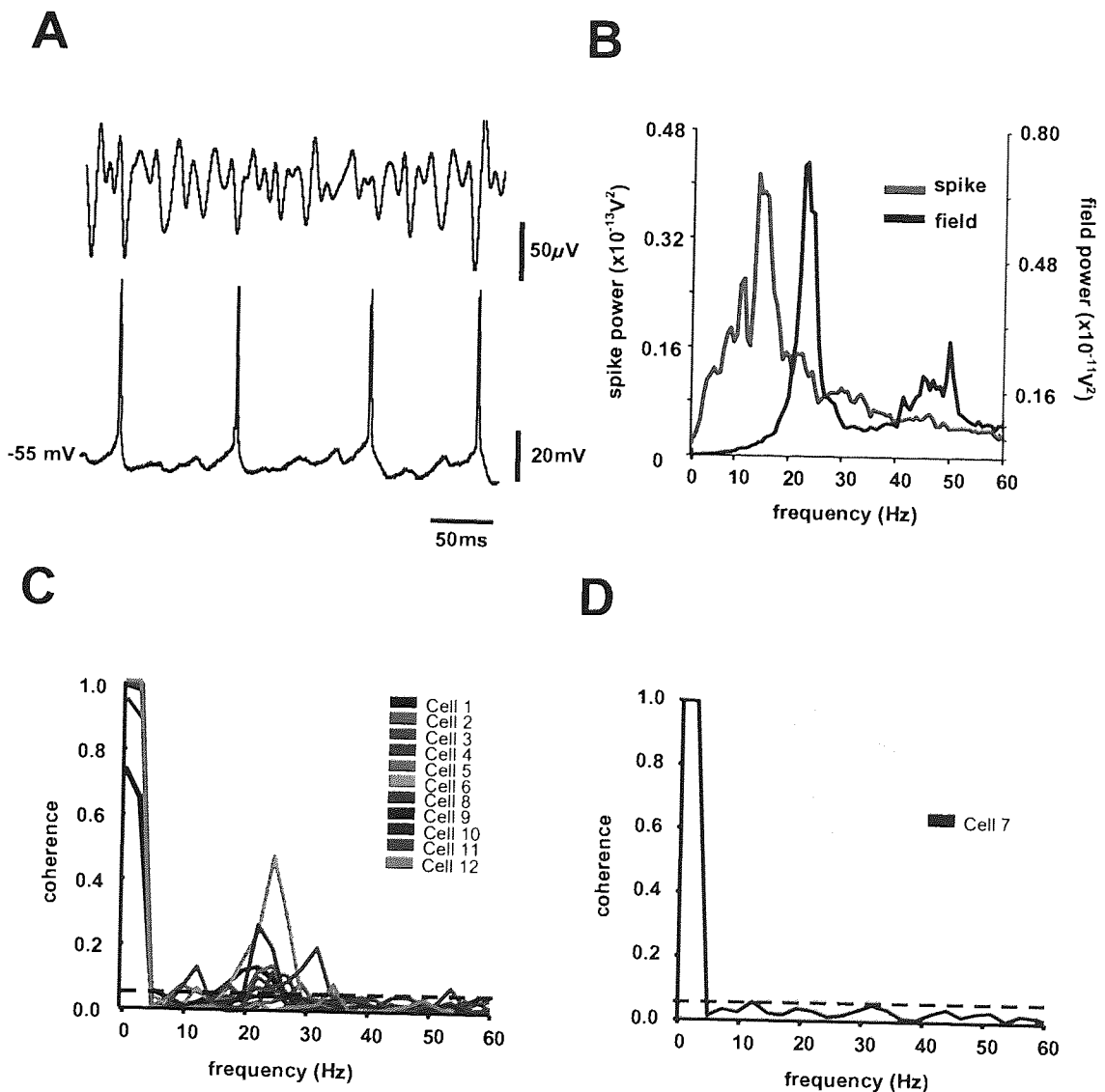
Figure 4.2 – Relationship between beta field oscillations and RS cell APs. (A) Representative example traces of beta field oscillations (top) and simultaneously recorded firing behaviour of RS cell (bottom). (B) Averaged power spectra (n=12) of APs (red) and field activity (black). Coherence analysis between APs and field oscillation (C) with correlation at beta frequency (n=11), and (D) without (n=1). Dashed line indicates significance threshold calculated by coherence analysis script for Spike2 software. Grey shadow indicates beta band of 15-35 Hz.
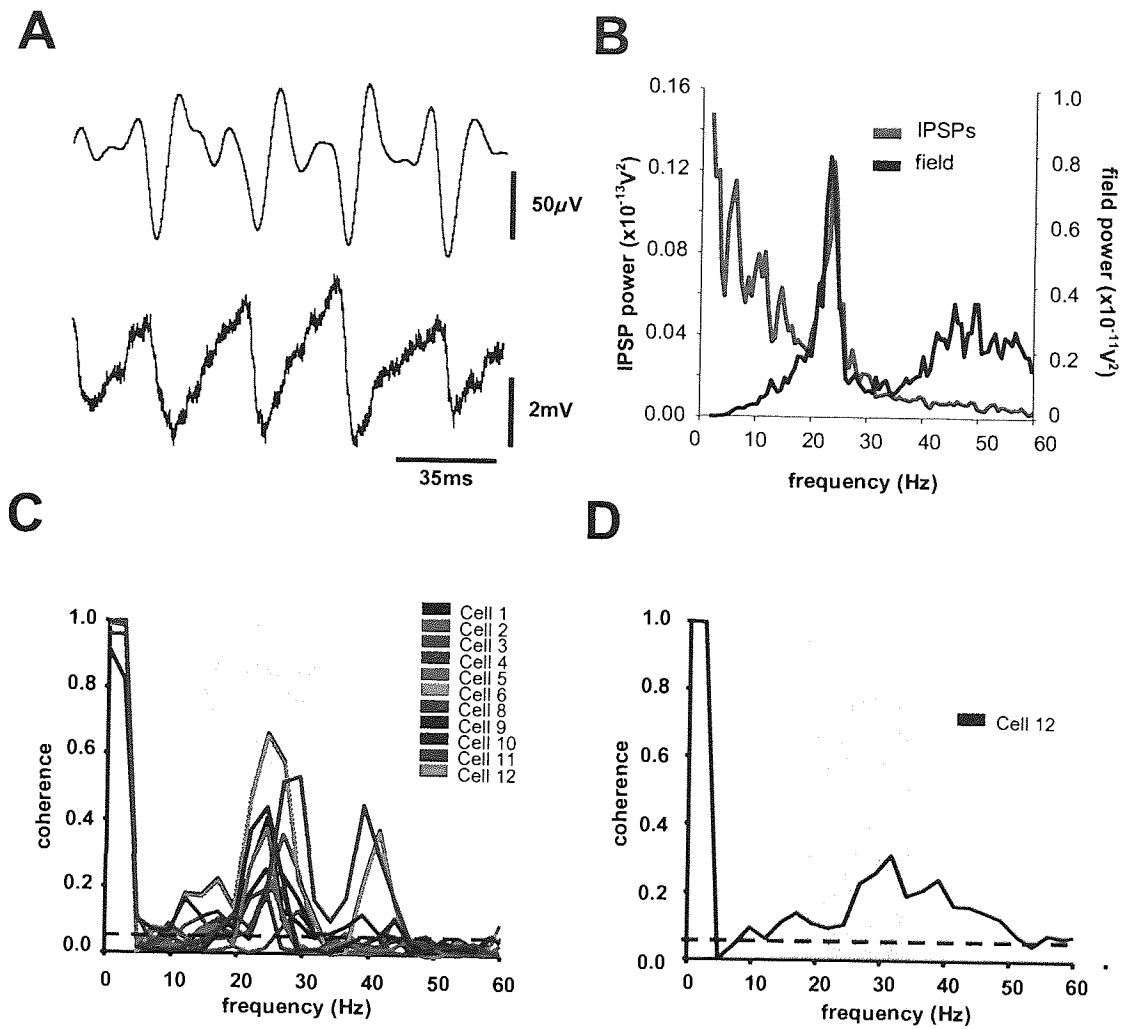
Figure 4.3 – Relationship between beta field oscillations and IPSPs received by RS cells. (A) Example traces of simultaneously recorded beta field activity (top) and IPSPs (bottom). **(B)** Example power spectrum of IPSPs (red) and field activity (black). **(C and D)** Coherence analysis of IPSPs received by RS cells and field activity (same cells as in figure 4.2C and D). Dashed line indicates significance threshold calculated by coherence analysis script written for Spike2 software. Grey shadow indicates beta band of 15-35 Hz.
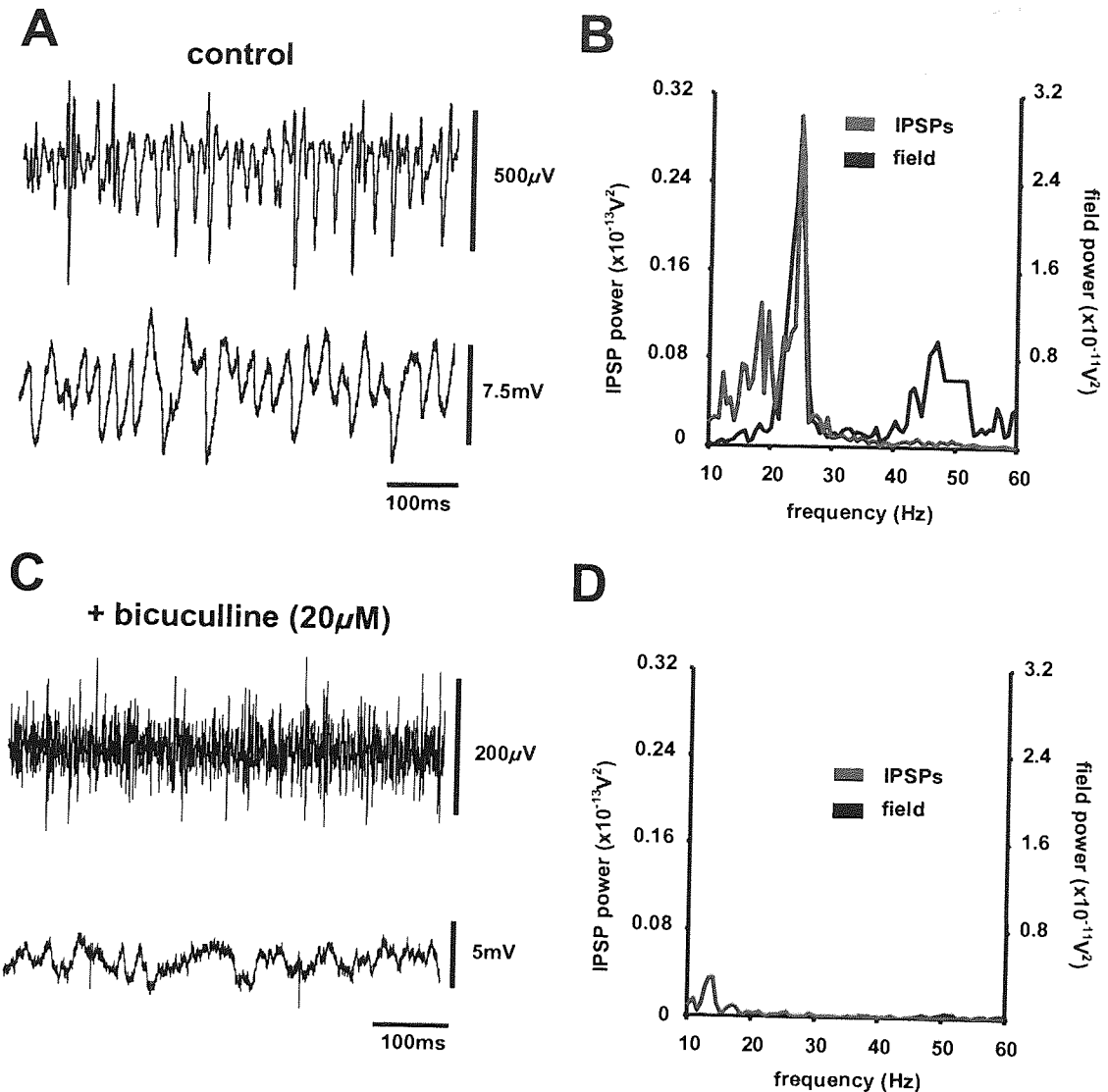
Figure 4.4 – IPSPs received by RS cells. (A) Example traces of simultaneously recorded beta field oscillation (top) and membrane potential fluctuation recorded at -30mV from a RS cell (bottom). **(B)** Power spectrum analysis of each trace shown in A. **(C)** Same recording as A, but after application of the GABA$_A$ receptor antagonist bicuculline (20μM). **(D)** Power spectrum analysis of traces shown in C.

IB cells fired APs spontaneously at a rate of 9.8 ±1.2 Hz during beta field oscillation (27.4 ± 1.0 Hz, figure 4.5A and B). These APs were found to be coupled with beta field oscillation, as significant coherence peak of 0.29 ± 0.03 was found at 27.3 ± 1.0 Hz, (figure 4.5C). Again, one cell exhibited no significant coherence at beta frequency (figure 4.5D). Exposing fast inhibitory synaptic input received by this cell type by depolarising to -20mV revealed that they are also under the influence of beta frequency IPSPs (23.6 ± 1.2Hz, figure 4.6A and B). Coherence analysis of these signals showed a significant peak of 0.51± 0.08 at 27.0 ± 0.8Hz (figure 4.6C and D).

As in RS cells, the one cell which exhibited no correlation between spike and field activity was still shown to be receiving IPSPs at beta frequency (figure 4.6D).
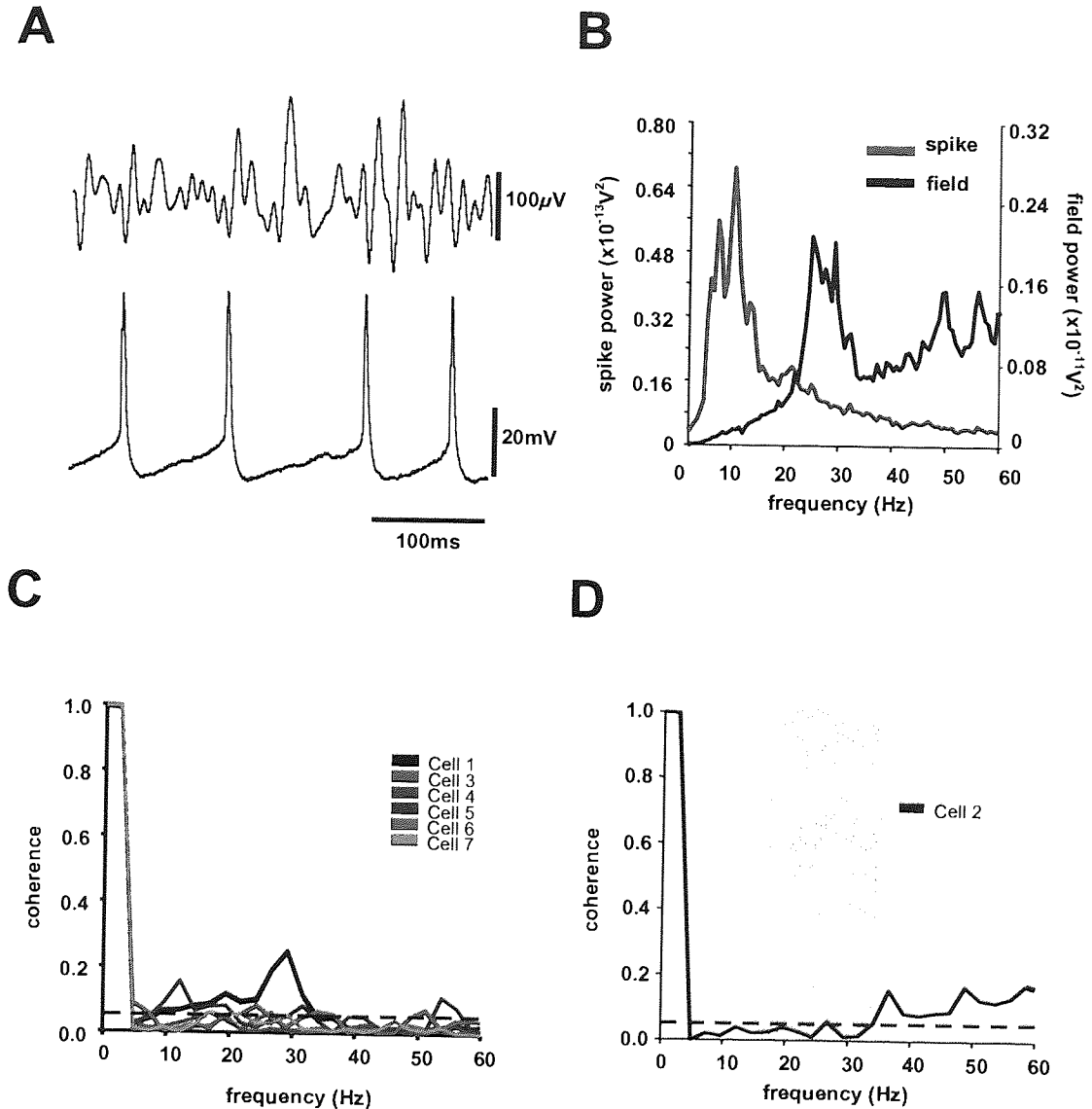
Figure 4.5 – Relationship between beta field oscillations and IB cell APs. (A) Example traces of simultaneously recorded beta field activity and APs **(B)** Averaged power spectra of beta population activity and IB cell spiking. Coherence analysis of APs and field activity divided IB cells into two types as for RS cells. **(C)** Those which exhibited correlation (n=6) and **(D)** those which did not (n=1). Dashed line indicates significance threshold calculated by coherence analysis script for Spike2 software. Grey shadow indicates beta band of 15-35 Hz.
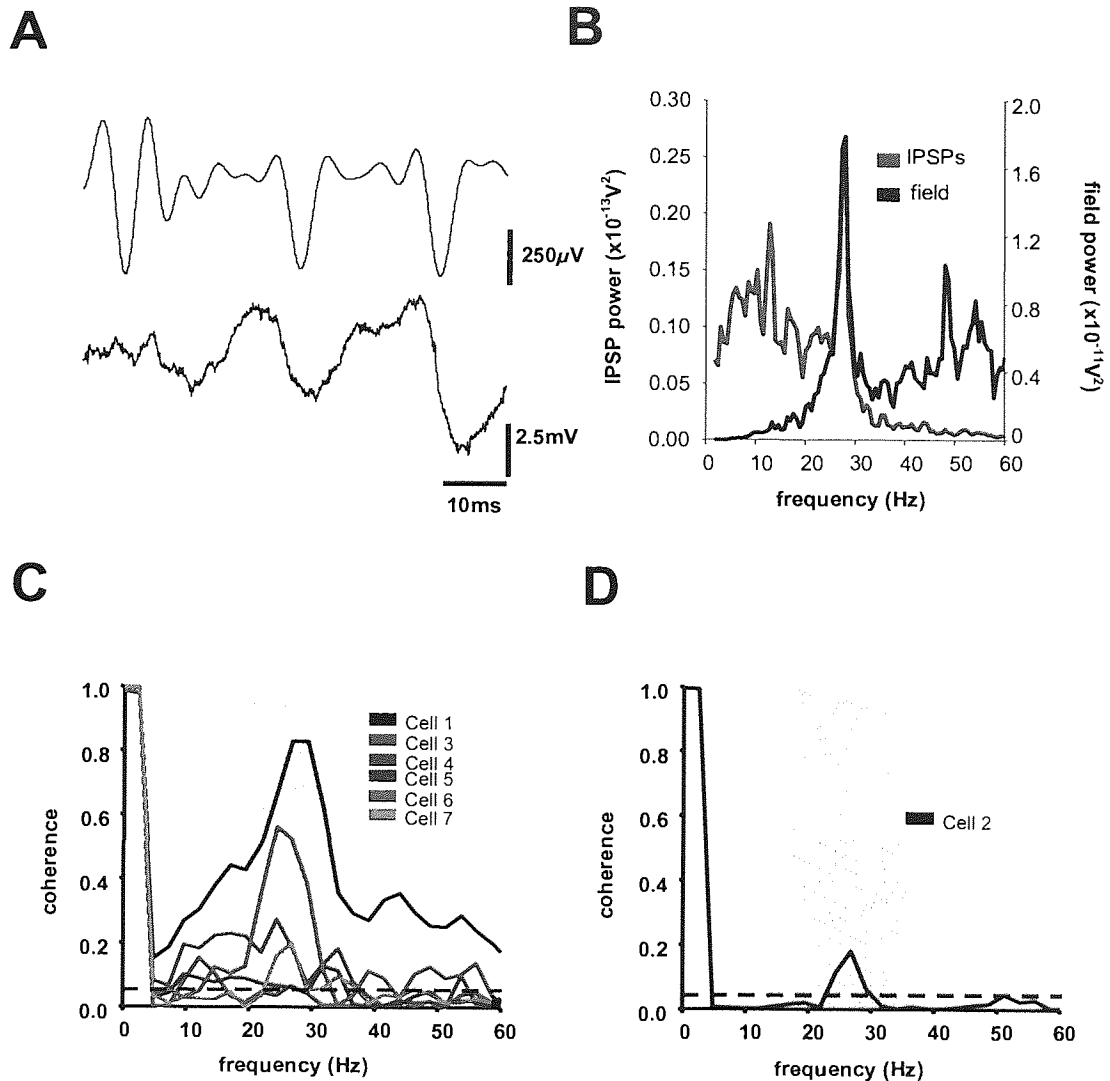
Figure 4.6 – Relationship between beta field oscillations and IPSPs received by IB cells. (A) Representative example traces of simultaneously recorded beta field activity (top) and IPSPs (bottom). **(B)** Representative example power spectrum of IPSPs and network activity. **(C and D)** Coherence analysis between IPSPs received by IB cells and field (same cells as in figure 4.5 C and D). Dashed line indicates significance threshold calculated by coherence analysis script for Spike2 software. Grey shadow indicates beta band of 15-35 Hz.

4.2.3 Firing behaviour of FS cells during the beta oscillations

Two FS cells were identified, both of which generated APs spontaneously during beta field oscillation in layer V. Power spectrum analysis of this spontaneous firing revealed that APs were occurring at beta frequency (23.2 ± 0.6 Hz), similar to activity simultaneously recorded from field (22.6 ± 1.2 Hz, figure 4.7A and B). Coherence analysis of these two signals showed a significant peak at beta frequency (average coherence of 0.66 ± 0.12 at 23.5 ± 0.3 Hz), indicative of their strong phase relationship (figure 4.7C). In order to examine the pattern of inhibitory input received by recorded FS cells, IPSPs were exposed by hyperpolarising membrane potential to -90mV. Power spectrum analysis of these IPSPs revealed that they were occurring at 23.8Hz, a similar frequency of simultaneously recorded field oscillation (23.2 Hz, figure 4.7D and E). This indicates that FS cells were under rhythmic inhibition at beta frequency. The phase relationship between IPSPs and field activity in FS cells was found to be particularly robust with a coherence of 0.83 at 24.4 Hz.
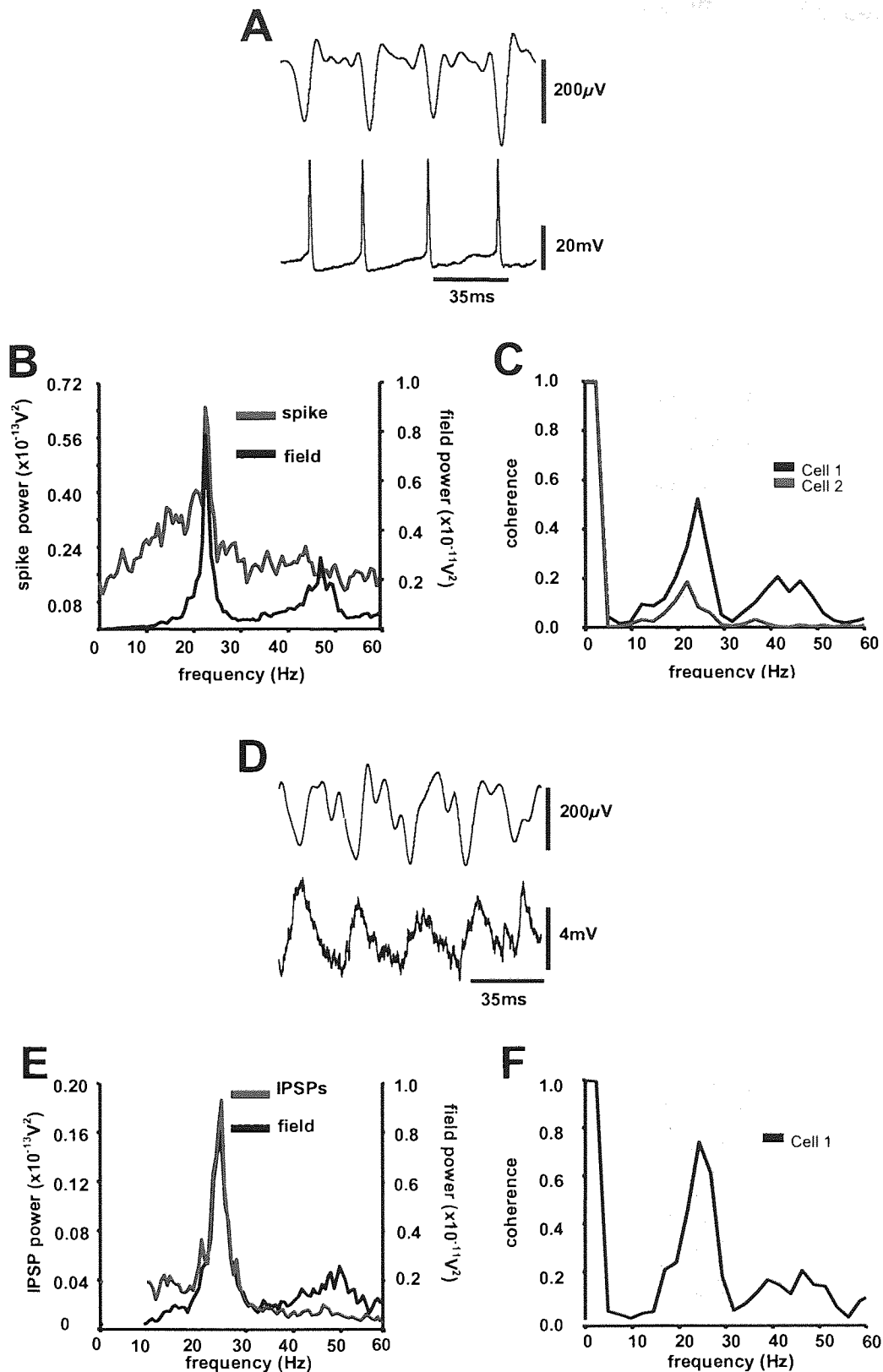
Figure 4.7 – Relationship between beta field oscillations and APs/IPSPs of FS cells. (A) Example traces of simultaneously recorded beta field activity (top) and APs (bottom). **(B)** Averaged power spectrum (n=2) of field activity (black) and APs (red). **(C)** Coherence analysis of field and APs from each recording. **(D)** Example traces of simultaneously recorded beta field activity (top) and reversed IPSPs (bottom, cell held at -90mV). **(E)** Power spectrum of field and IPSPs received by FS cells. **(F)** Coherence analysis of field activity and IPSPs received by FS cell. Grey shadow indicates beta band of 15-35 Hz

4.2.4 Verification of observed spiking behaviour of RS, IB, and FS cells with respect to beta field oscillations

In one non-spiking RS cell recorded during beta oscillatory activity, a mixture of IPSPs and EPSPs was clearly observed at a membrane potential of -75mV (figure 4.8A). I analysed these potential fluctuations over time by plotting the data on a spectrogram. This analysis showed two distinct synaptic input patterns received by this cell, one at beta frequency (25.4Hz) and another at theta frequency (12.2Hz, figure 4.8C). In addition, coherence analysis of membrane potential and field activity was found to be strongly correlated at beta frequency (0.42 at 24.4 Hz, figure 4.8B). This observation supports our findings of firing behaviour of FS cells (at beta frequency) and RS and IB cells (at theta frequency range) during beta field oscillation.
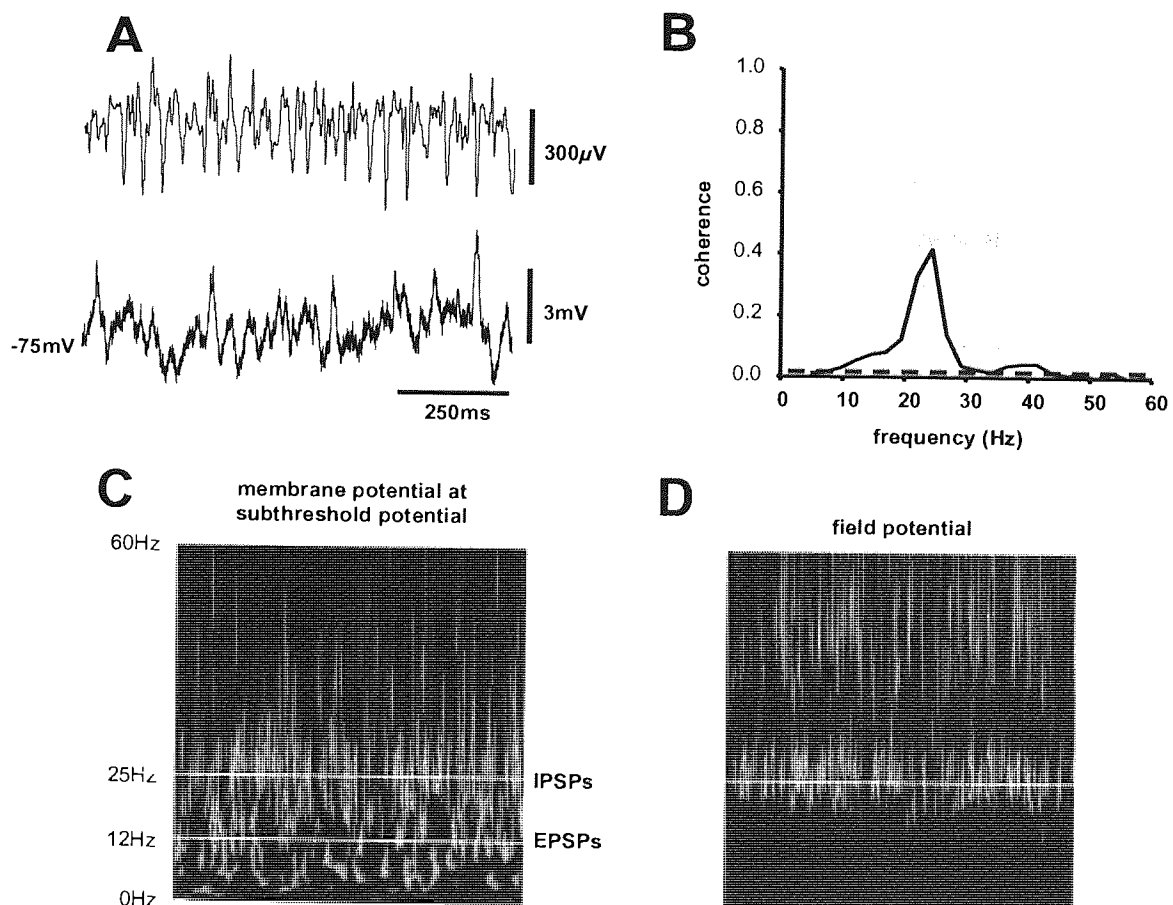
Figure 4.8 – Simultaneous recording of EPSPs and IPSPs at subthreshold membrane potential. (A) Representative traces of simultaneously recorded beta field oscillations (top) and membrane potential fluctuation recorded at -75mV from a RS cell (bottom). (B) Coherence analysis of traces shown in A. Dotted line shows significance threshold. Grey shadow indicates beta band of 15-35 Hz. (C) Spectrogram analysis of membrane potential fluctuation exhibited by cells in A. x-axis is 10 seconds. (D) Spectrogram analysis of field activity traces shown in A.

99

4.2.5 Coherence between EPSPs and field beta oscillations

I next investigated contribution of excitatory synaptic inputs to beta field oscillation. From chapter 3, it was expected that kainate receptors were likely to be involved for phasic/tonic excitation in M1. Pure EPSPs were found to be difficult to expose in our study; however, in 3 cells, they were observable at membrane a potential slightly greater than resting membrane potential, with small amplitude IPSPs (figure 4.9A and B). Power spectrum analysis of these signals revealed predominant low frequency activities (peak power of 8.7 ± 1.6 Hz). Simultaneously recorded LFPs were shown to be at beta frequency (26.0 ± 1.4 Hz, figure 4.9D, black line). Coherence analysis of these signals showed a peak of 0.09 ± 0.03 at 28.5 ± 4.3 Hz (figure 4.9E). Application of the AMPA receptor selective antagonist SYM2206 (20μM) did not have a significant effect on membrane potential fluctuation, beta oscillation, or coherence (figure 4.9B for membrane fluctuation and red line in 4.9D and E for beta oscillation and coherence). Subsequent application of CNQX (10μM) significantly reduced beta field power (from 0.25 ± 0.12 (n=3) to 0.08 ± 0.07 $\times 10^{-11} V^2$, n=2, $P<0.05$), figure 4.9D, blue line) without changing frequency (26.3 ± 1.5 to 26.8 ± 1.8 Hz, $P>0.05$) and also reduced EPSP amplitude and power (figure 4.9C). Correlation between field activity and membrane potential fluctuation was also reduced by application of CNQX. In addition, the coherence peak was shifted to a lower frequency (0.08 ± 0.01 at 16.3 ± 2.2 Hz, blue line).
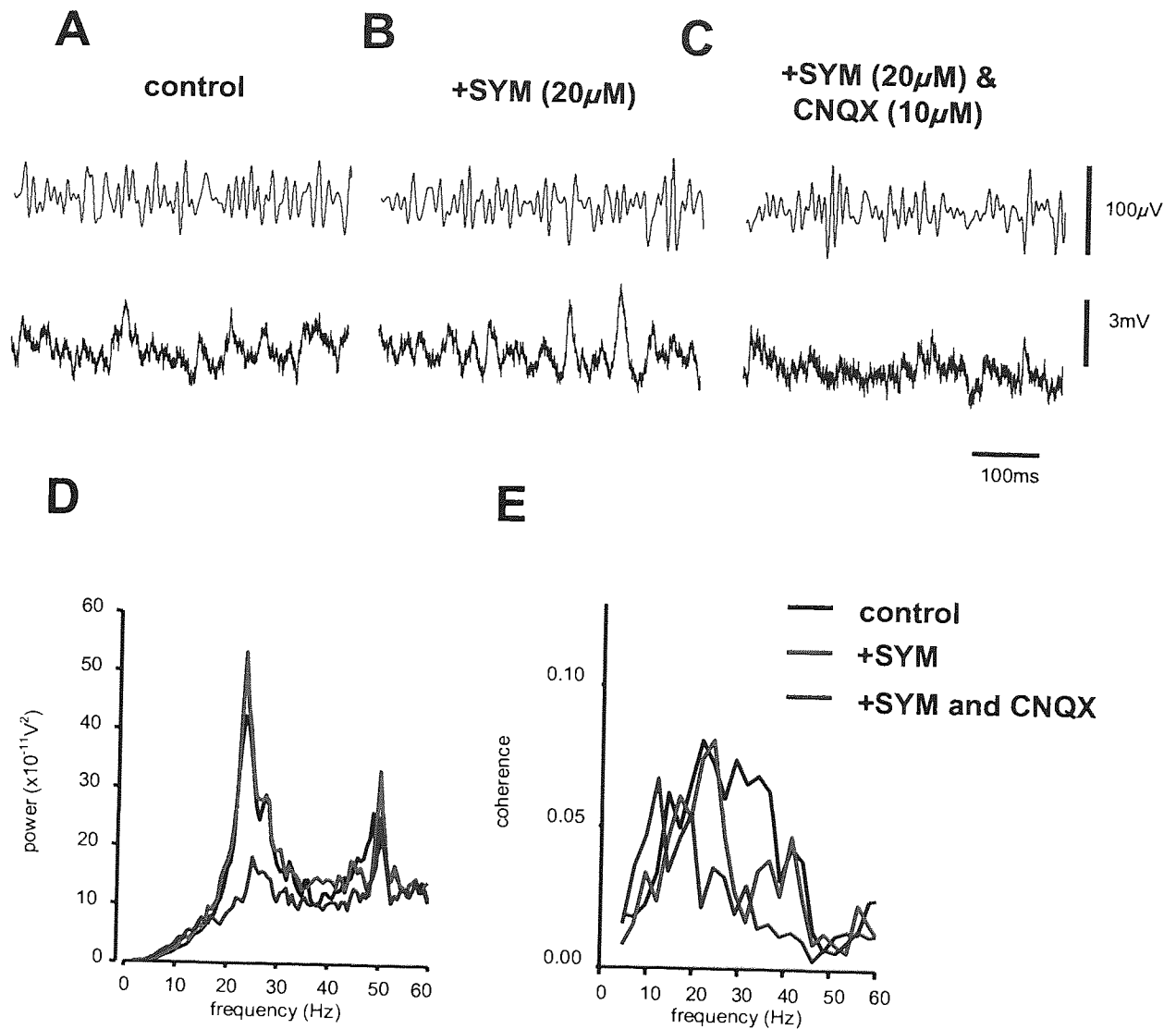
Figure 4.9 – Phase relationship of EPSPs on RS cells and field beta activity. (A) Representative raw traces of beta oscillations and EPSPs with small amplitude IPSPs on RS cell. Membrane potential -82mV. **(B)** After SYM2206 application. **(C)** After CNQX application. **(D)** Average power spectrum of LFP simultaneously recorded in control, SYM and CNQX. **(E)** Averaged coherence between synaptic activities and field oscillation. Grey shading indicates beta frequency band.

4.3 DISCUSSION

4.3.1 Summary

In Chapter 3, it was shown that phasic inhibitory and phasic/tonic excitatory synaptic inputs were required for persistent beta oscillations in M1 layer V. In the experiments presented in this chapter, I have shown that phasic $GABA_A$ receptor-mediated inhibitory inputs are likely to be delivered from FS cells. This is because (1) FS cells fired APs on every beta cycle but RS and IB cells only fired, on average, every other beta cycle and (2) all electrophysiological cell types recorded in the present study (RS, IB and FS) received IPSPs at beta frequency, which were strongly phase-locked with concurrently occurring field beta activity. Since FS cells receive IPSPs at beta frequency, it seems likely that tonically excited FS cells are mutually inhibiting each other, and by doing so, sustaining the beta frequency pattern. These mutually connected interneurones would then, provide their beta frequency inputs to a population of pyramidal cells.

4.3.2 Mechanistic thoughts – comparison with previous studies

Pharmacologically induced beta oscillations observed in M1 appeared to be different to the so called beta2 oscillations observed in layer V somatosensory cortex (Roopun et al., 2006). In somatosensory cortex, the beta oscillation appears less sensitive to $GABA_A$ receptor antagonists than the one described here, while IB cells generated spikes/spikelets at beta frequency on every cycle.

The beta oscillations observed in this study are also different from those beta oscillations induced by tetanic stimulation, in which pyramidal cells fire at every beta cycle while interneurones are firing at gamma frequency (Whittington et al., 1997a; Traub et al., 1999a, 1999b; Bibbig et al., 2001). Rather, the pattern of excitatory and inhibitory cell firing observed during beta oscillations in our study resembled the pharmacologically induced persistent gamma oscillation described by Fisahn et al. (1998) and Cunningham et al (2003). Indeed, pyramidal cells were found to fire at lower frequency than field gamma oscillation, while FS cells were found to fire every

gamma cycle (Fisahn *et al.,* 1998). Furthermore, pyramidal cells and FS cells were found to receive IPSPs at gamma frequency, which correlated with field activity. Such firing behaviour of pyramidal cells was also reported in behaving rats (Csicsvari *et al.,* 1999a, 1999b). The mechanism by which less frequent firing of pyramidal cells with respect to field oscillation occurs has been investigated by Fisahn *et al.* (1998). This group has postulated that APs generated by pyramidal cells produce monosynaptic EPSPs on dendrites, while simultaneously activated interneurones generate disynaptic IPSPs perisomatically, limiting the time window for EPSPs to generate APs on pyramidal cells. This possible shunting mechanism explains the mismatch observed between pyramidal cell spiking and EPSCs. Cunningham *et al.* (2003) also encountered similar mismatching between phasic excitatory drive and AP output. Here, interneurones fired at gamma frequency which corresponded to the field activity, but the frequency of EPSPs received by interneurones was lower.

In present study, although difficult, manipulation of membrane potential was used to expose EPSPs in the presence of small amplitude IPSPs. The difficulty in obtaining EPSPs during beta oscillatory activity may be due to significantly less involvement of recurrent phasic excitation from pyramidal cells to both pyramidal cells and interneurones. Indeed, in contrast to gamma oscillation found in studies of Fisahn *et al.* (1998) and Cunningham *et al.* (2003), beta oscillations in M1 were found to be AMPA current-independent, but kainate current-dependent (Chapter 3, section 3.3.2). In addition, muscarinic M1 receptor activation was required for its induction (Chapter 3, section 3.3.4). Since these two receptors would generate strong tonic excitation of all cell types, phasic recurrent excitatory inputs may play less of a role in M1 beta oscillations. Conversely, the longer decay time of IPSPs (compared to decay time of IPSPs seen during gamma oscillation) may be causing shunting of activity impinging on pyramidal cell dendrites, making dendritic EPSPs more difficult to observe. Perhaps, firing can only occur when EPSPs coincide with activation of an intrinsic membrane conductance (e.g. activation of I_h leading to activation of T-type current), or gap junction mediated spikelets. In support of this possibility, intrinsic properties of the postsynaptic neurones have been suggested to interact effectively with GABAergic inputs in shaping supra-threshold activity (Tamas *et al.,* 2004). Further experiments will be required to determine involvement of recurrent excitation and the pattern of EPSPs received by FS cells.

Although both RS and IB cells were found to fire less frequently than field oscillatory cycle, APs were phase-locked with field activity, suggesting a contribution of these cells to measured network activity. This observation was consistent with *in vivo* studies in which activity of layer V pyramidal cells was phase-locked with beta LFP (Murthy and Fetz, 1996b; Baker *et al.*, 1999). Thus, the field oscillation appears constructed by a population of pyramidal neurones whose membership is dynamic (i.e. a particular set of pyramidal neurones fire at phase of beta while others fire in a different temporal window).

Most pyramidal cell activity was phase-locked to field activity; however, we observed a small number of cells whose AP activity was not. Paradoxically, these cells were receiving IPSPs at beta frequency, which were phase-locked to field activity. One possibility is that these pyramidal cells are receiving excitatory inputs from other pyramidal cells, which are not patterned by the same interneurones. This is likely, if (1) the activity of functional fields representing particular movements are governed by local FS cells, but these fields are synaptically linked via pyramidal cells, and (2) inputs from pyramidal cells can overcome beta frequency inhibitory inputs. The functional association of related somatotopical fields for specific movements could then be achieved by increasing the excitatory input from distant pyramidal cells onto FS cells (i.e. long-range synchronisation). In addition, if there is an overlap between such topographical fields, then output cells existing in a specific functional area may receive non-phase locked IPSPs and EPSPs (figure 4.10). Indeed, Marsden *et al.* (2000) found a strong tendency for coherence between EcoG (recorded from sensorimotor region) and EMG activity during various motor activities in human, and suggested the possibility that neuronal populations contributing to a given action are characterised by their tendency to resonate at specific frequencies.

Figure 4.10 – Possible functional interactions within M1. Two networks of neurones receiving different excitatory inputs expressing beta oscillatory activity but in different phase. Each network represents a functionally different field, with some overlap. Output of pyramidal cells from one field to dendrite of pyramidal cells in another field may then result in generation of spike not phase-locked to field, while IPSPs phase-locked to field (Model first described by Traub *et al.*, 1996a)

4.3.3 Which FS cell?

In the CA1 region of hippocampus, FS cells target both apical dendrites (e.g. bistratified cells and oriens-lacunosum moleculare (O-LM) cells) and perisomatic regions (e.g. basket and axo-axonic cells). In this study we have not determined the domains of postsynaptic pyramidal cells where synaptic contact are made by FS cells. However, in sensorimotor cortex, Kawaguchi and Kubota (1997) and Cauli *et al.* (1997) have shown that FS cell terminals are preferentially located at perisomatic region of postsynaptic pyramidal cells. It has been thought that interneurones which innervate pyramidal cell dendrites control the efficacy and plasticity of glutamatergic synaptic inputs whilst perisomatic targeting interneurones are responsible for regulating overall output (for review, see Freund and Katona, 2007). In support of this interpretation, *in vitro* studies have shown that perisomatic-targeting interneurones

are likely to produce stronger influence on the output of pyramidal cells, as they induce IPSPs with faster kinetics and greater amplitude than those induced by dendrite-targeting interneurones (Miles *et al.*, 1996). Furthermore, perisomatic-targeting interneurones were reported to have larger synaptic terminals, more synaptic vesicles and mitochondria and larger active zones (Miles *et al.*, 1996) and have the ability to generate simultaneous IPSPs at different postsynaptic cells in absence of excitatory synaptic inputs (Miles, 1990; Freund and Katona, 2007).

However, the literature is not clear-cut, and it has been shown that dendritic-targeting bistratified cells fire APs at gamma frequency, which was strongly phase-locked with field activity in CA1 (Tukker *et al.*, 2007). Perisomatic-targeting cells, in contrast, were found to be moderately/weakly coupled, while O-LM cell activity was found to be suppressed during the gamma oscillation period. Nevertheless, these authors suggested that contribution of perisomatic-targeting inhibitory neurones towards gamma oscillation may be significant, due to their high number of synaptic contacts per pyramidal cell. These factors suggest that fast-spiking, perisomatic-targetting cell are likely to be responsible for recruiting and pacing the activity of populations of neurones in M1 layer V.

4.3.4 Possible involvement of other interneurones

Whether interneuronal subtypes other than FS cells participate in beta network oscillations remains to be determined. It has been suggested that the large number of interneuronal subtypes in neocortex have distinct roles in shaping network activity (Klausberger *et al.*, 2003). Indeed, Klausberger *et al.* (2003, 2004) have shown that different types of interneurone in CA1 fired at different phases of the theta oscillation (4-8 Hz) and sharp wave (120-200 Hz) in rats under urethane anaesthesia. These authors described basket cells which generated several spikes during the descending phase of theta and axo-axonic cells which fired at the peak of theta oscillation while O-LM and bistratified cells generated their spikes at the trough of theta oscillation. In contrast, during sharp-wave activity basket cells fired clusters of spikes at the trough of ripple but axo-axonic cells generated one or two spikes at the beginning of the sharp wave. O-LM cells were silent during this period.

Gloveli et al. (2005) studied the spike-timing of a distinct type of interneurone during gamma oscillation occurring in stratum oriens/pyramidale layer of CA1 in vitro. They found that O-LM cells fire at theta frequency despite receiving EPSPs at gamma frequency. Other types of interneurones examined included tri-laminar, basket and bistratified cells. These also received gamma EPSPs and produced APs at gamma frequency, indicating their significant involvement in synchronising pyramidal cell activity.

Apart from FS cells, RSNP, LTS, and LS interneurones have been reported in sensorimotor cortex in vitro (Kawaguchi and Kubota, 1997; Cauli et al., 1997). Szabadics et al., (2001) have shown that RSNP cells, which synapse onto the dendritic shaft of other RSNP cells, are capable of timing somatic AP generation. However, RSNP cells could not be persistently entrained at beta or gamma frequency by recurrent excitatory inputs, as repetitive stimulation leads to activity-dependent depression and switch from phasic to tonic excitation which allows RSNP cells to depolarise and fire APs at ~4Hz. Therefore, if RSNP cells are tonically exited in our M1 studies their involvement in pacing beta oscillations would appear unlikely.

The contribution of LTS and LS cells to beta rhythmogenesis in M1 is difficult to predict. The decay time constant of IPSPs mediated by these types of interneurones is slow and the amplitude (and hence charge transfer) of IPSCs much lower than FS cells (Bacci et al., 2003a, Tamas et al., 2003), which may indicate their involvement in a slower network oscillation. These differences between LTS and FS cell were attributed to the selective activation, by LTS cells, of GABA$_A$-receptor lacking β2-3 subunits whilst FS cells selectively active GABA$_A$ receptors expressing α1-subnit (Bacci et al., 2003a). However, both LTS and LS cells are thought to preferentially target apical dendrites (Kawaguchi and Kubota, 1997, Tamas et al., 2003) and may strongly shape the location-specific spatiotemporal pattern of excitatory input (Miles et al., 1996; Tamas et al., 2003) especially at low frequencies (Beierlein et al. 2000). Recent computer simulations and in vitro studies have indicated that LTS cells may have an ability to concatenate the gamma and beta2 oscillations into beta1 oscillations (13-18Hz, Kramer et al., 2008; Roopun et al., 2006, 2008). In addition, Martinotti cells (a type of LTS cell) have been shown to strongly influence activity of

layer V IB cells in frequency-dependent manner (Silberberg and Markram, 2007). Therefore, a contribution of LTS cells can not be ruled out.

CHAPTER 5:
EFFECT OF CORTICAL STIMULATION ON BETA OSCILLATORY ACTIVITY IN M1

5.1 INTRODUCTION

In the previous two chapters I outlined the underlying mechanism of beta oscillatory activity in M1. My next focus was to investigate if the pharmacologically-induced persistent beta oscillation can be modulated by externally applied HFS designed to mimic DBS, and stimulation at 20Hz and 4Hz which have been shown to exacerbate movement deficits.

DBS is a well-established method for the treatment of advanced PD. It involves high frequency (130Hz) electrical stimulation often of the STN but its application to other structures within the cortico-BG-thalamo-cortical motor loop also appears effective (Hassler et al., 1960; Benabid et al., 1996; Canavero et al. 2000, 2002, 2003; Pagni et al., 2003, 2005a, 2005b). DBS of pedunculopontine nucleus (PPN), a subcortical structure strongly connected with this loop is also reported to have a positive impact in PD (Mazzone et al., 2005; Plaha and Gill, 2005).

Within the motor loop, M1 would be the ideal target for HFS for PD symptomatic relief as stimulation of this region would be less invasive compared to subcortical structures. Indeed, a great deal of research has been undertaken in last decades to clarify the potential effect of cortical stimulation on advanced PD (see Arle and Shils, 2008 for review). In these studies, electrical stimulation has been applied either subdurally (stimulator located below the dura matter), extradurally (stimulator located at the surface of the dura matter, (Tsubokawa, et al., 1991; Canavero and Bonicalzi, 2007), or transcranially (stimulator located outside the cranium, Baker et al., 1994).

Extradural stimulation has been applied chronically at the frequency range of 20-60Hz at subthreshold intensity[25] (Canavero et al. 2000, 2002, 2003; Pagni et al., 2003, 2005a, 2005b), although, recent studies used 130Hz (Pagni et al., 2005a; Cilia et al., 2008; Fasano et al., 2008). The outcome of these studies was variable and sometimes contradictory. Some found clinical improvement, as measured using the Unified Parkinson's Disease Rating Scale (UPDRS) (Canavero et al. 2000, 2002, 2003; Pagni et al., 2003, 2005a, 2005b; Fasano et al., 2008), while others reported no significant effect (Kleiner-Fisman et al., 2003; Cilia et al., 2007).

---

[25] stimulation intensity which is 90% of the resting motor threshold for the right dorsal interosseous

Transcranial stimulation has been applied at much lower frequency range (0.2-25Hz) with different durations engaged by different studies (see Lefaucheur, 2006 for review). Many case studies of repetitive transcranial magnetic stimulation (rTMS) of M1 reported symptomatic improvement (as determined by UPDRS), in particular, in rigidity, and this effect was shown to last beyond the time of stimulation (Pascual-Leone *et al.,* 1994; Siebner *et al.,* 1999, 2000; Lefaucheur *et al.,* 2004; Khedr *et al.,* 2003, 2006).

The mechanisms underlying the beneficial effects of cortical stimulation are yet to be elucidated. As outlined in the chapter 1, PD is associated with exaggerated pathological beta oscillatory activity in the BG-thalamo-cortical loop and DBS of the STN reduces these pathological beta oscillations (Kühn *et al.,* 2006, 2008). In contrast, stimulation of STN at lower frequencies enhanced bradykinesia (Chen *et al.,* 2007) suggesting that the exaggerated beta activity is linked to symptoms of PD.

Recent reports indicate that stimulation of M1 can also reduce pathological oscillatory activity. Thus, TMS cortical stimulation appears to suppress STN beta activity in PD patients with apparent symptomatic improvement (Doyle Gaynor *et al.,* 2008) while extradural motor cortical stimulation alleviates PD symptoms (Drouot *et al.* 2004). In the latter study, HFS (at 130Hz) was applied to M1 of MPTP-treated primates while recording neuronal activity from STN and GPi. It was found that the activity of these two structures was initially synchronised but stimulation caused desynchronisation, an effect which corresponded with improvement in akinesia and bradykinesia. Interestingly, such a beneficial effect of extradural motor cortex stimulation is not only restricted to PD, but also for motor disorders associated with dystonia (Allam *et al.,* 2007) and stroke (Katayama *et al.,* 2001, 2002, 2003; Brown *et al.,* 2006).

We suspected that high frequency motor cortical stimulation modulates the pathological motor cortical beta oscillations, perhaps, reducing their power, allowing the functional cortical motor information to be transmitted to BG nuclei. Alternatively, stimulation may shift the pathological beta oscillation to gamma frequency band (thought to be the frequency band involving the motor information carrier; Brown *et al.,* 2001), which can then be transmitted to BG nuclei, specifically, striatum (via corticostriatal pathway) and STN (via hyper-direct pathway). Hence, the suppression

of beta activity, or re-patterning of their activity would disrupt abnormal beta synchronisation in the motor loop, perhaps restoring normal functionality.

In this chapter, we tested if HFS (125Hz) has an ability to modulate an *in vitro* model of beta oscillations. In addition we have also tested the effect of stimulation at beta frequency (20Hz, stimulation indicated to potentiate bradykinesia) and theta frequency (4Hz, frequency range commonly used for rTMS to reduce symptoms of PD).

5.2 THE EFFECT OF M1 LAYER I STIMULATION ON BETA OSCILLATION

Dual, simultaneous stimulation of layer I elicited oscillatory activity in layer II/III, which was subsequently mirrored by layer V (figure 5.1A and B). Two different responses, specifically, theta or gamma frequency oscillations, were evoked depending on stimulation paradigm applied. Gamma oscillations were always initially observed in layer II/III region, which were then transferred to layer V (figure 5.1A). Theta activity, in contrast, occurred concurrently in layer II/III and layer V (figure 5.1B). In this chapter, I will focus on influence of stimulation in layer V activity, in order to maintain consistency with chapters 3 and 4.
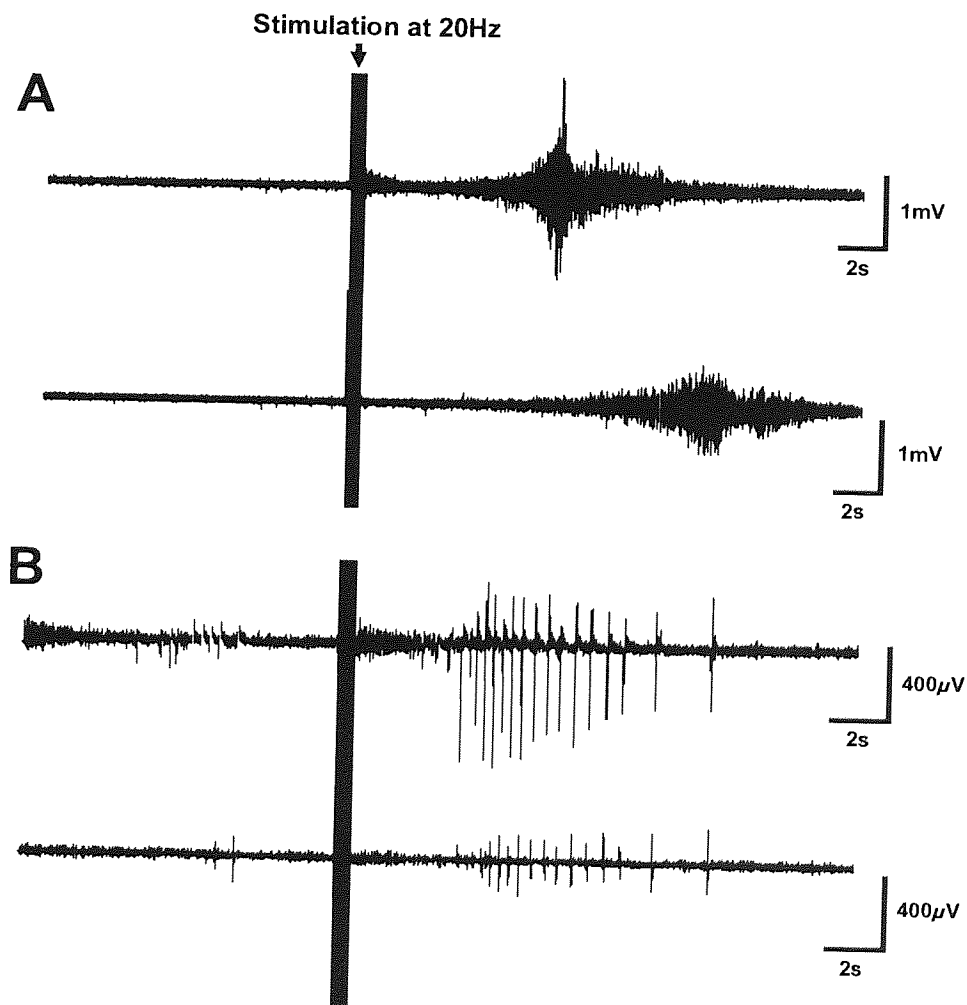
Figure 5.1 – Two different responses evoked by 20Hz stimulation of layer I (A) Representative traces of gamma activity evoked in layer II/III (top) and layer V (bottom). **(B)** Representative traces of theta activity evoked in layer II/III (top) and layer V (bottom). These responses are evoked in presence of pharmacologically-induced persistent beta oscillations.

5.2.1 Two-site stimulation of M1 layer I with HFS (125Hz)

In order to explore the mechanisms that may be associated with the therapeutic effect of the extradural HFS, two bipolar stimulating electrodes were placed in layer I, equidistant from the recording electrodes in order to activate a large area of M1 (see methods section 2.3 for schematic diagram), so as to replicate the activation of widely distributed neuronal populations by subdural / extradural stimulation (Drouot *et al.*, 2004; Canavero and Bonicalzi, 2007). A beta oscillation was pharmacologically induced before application of any stimulation (figure 5.2A, "pre" red box). 125 Hz stimulation (20 pulses at 0.5-1.5 mV) applied simultaneously to both electrodes constantly evoked gamma oscillatory activity, at average frequency of 56.1 ± 3.8 Hz with peak power of 4.74 ± 1.89 x10^{-11} V^2 (17 out of 18 slices, according to power spectrum analysis, figure 5.2A). These responses occurred after an average latency of 9.6 ± 2.9 seconds from the end of stimulation artefact (figure 5.2A). The average duration of evoked gamma oscillation was found to be 20.1 ± 2.7 seconds. Spectrogram analysis was also used to determine the effect of HFS on the persistent beta oscillation (figure 5.2B). This revealed that the power of beta oscillation gradually reduced as gamma oscillations appeared (figure 5.2B, red box). In addition, very fast oscillatory (VFO) components (>80Hz,) were observed which occurred concurrently with the early part of evoked gamma oscillation (figure 5.2B). In order to focus on population activity within beta frequency band, data were band-pass filtered at 20-35Hz. The resulting plot showed that beta oscillatory power was distributed evenly over time before stimulation (around 5μV/Hz in example shown in figure 5.2C) but during emerging gamma oscillation, this beta activity power was gradually reduced, though it never disappeared (around 2.5µV/Hz in example shown in figure 5.2C. Red box indicates suppressed beta). These data indicate that HFS generates transient gamma oscillations which may have a suppressive effect on persistent beta oscillations, or that beta and gamma oscillations depend to some extent on a similar population of neurones.

Figure 5.2 – Effect of 125Hz stimulation on persistent beta oscillations in M1. (A) Example trace of field activity. Arrow indicates where stimulation was applied. "Pre" indicates population activity before stimulation. "Post" indicates response evoked by 125Hz stimulation. **(B)** Spectrogram analysis of field activity at the location designated in (A). Hot colour indicates high activity intensity while cold colour indicates low activity. Image threshold $P<0.05$. The time scale for each spectrogram is 9 seconds. White line indicates the frequency of the persistent beta oscillations. **(C)** Data filtered at 20-35Hz showing nature of beta activity pre- and post-stimulation.

5.2.2 Two-site stimulation of M1 layer I with 4Hz

I next examined the effect of 4Hz (10 pulses at 0.5-1.5 mV) stimulation on on-going layer V beta oscillation. This frequency range was commonly used in rTMS clinical trials for PD patients (see Lefaucheur, 2006 for review). In contrast to HFS, 4Hz stimulation generated transient, large amplitude population spikes in the theta frequency range (13/21 slices, figure 5.3A and B). Indeed, power spectrum analysis revealed its average frequency to be 7.1 ± 0.4 Hz at an average power peak of 0.13 $\pm 0.06 \times 10^{-11} V^2$ (n=13). The latency and response duration was found to be 1.0 ± 0.1 seconds and 2.5 ± 0.7 seconds respectively. Subsequent spectrogram analysis revealed a detailed character of evoked theta activity (figure 5.3B). Thus, in addition to emergence of theta frequency activity (figure 5.3B, red box) increased beta and gamma oscillatory activity were evident (from ~4 to >100Hz in example figure 3B). Furthermore, this broadband enhancement of beta and gamma activity was modulated at theta frequency. Band-pass filtration of traces at 20-35Hz was then undertaken to focus solely on nature of beta oscillation activity. Before the stimulation, power of beta oscillatory activity was evenly distributed (around 2.5 µV/Hz as shown in figure 5.3C). However, after stimulation, beta oscillating power was substantially enhanced (figure 5.3C, red box) at theta frequency (figure 5.3C). These data indicate that 4Hz stimulation does not suppress but rather enhances beta activity, which is time-locked at theta frequency.
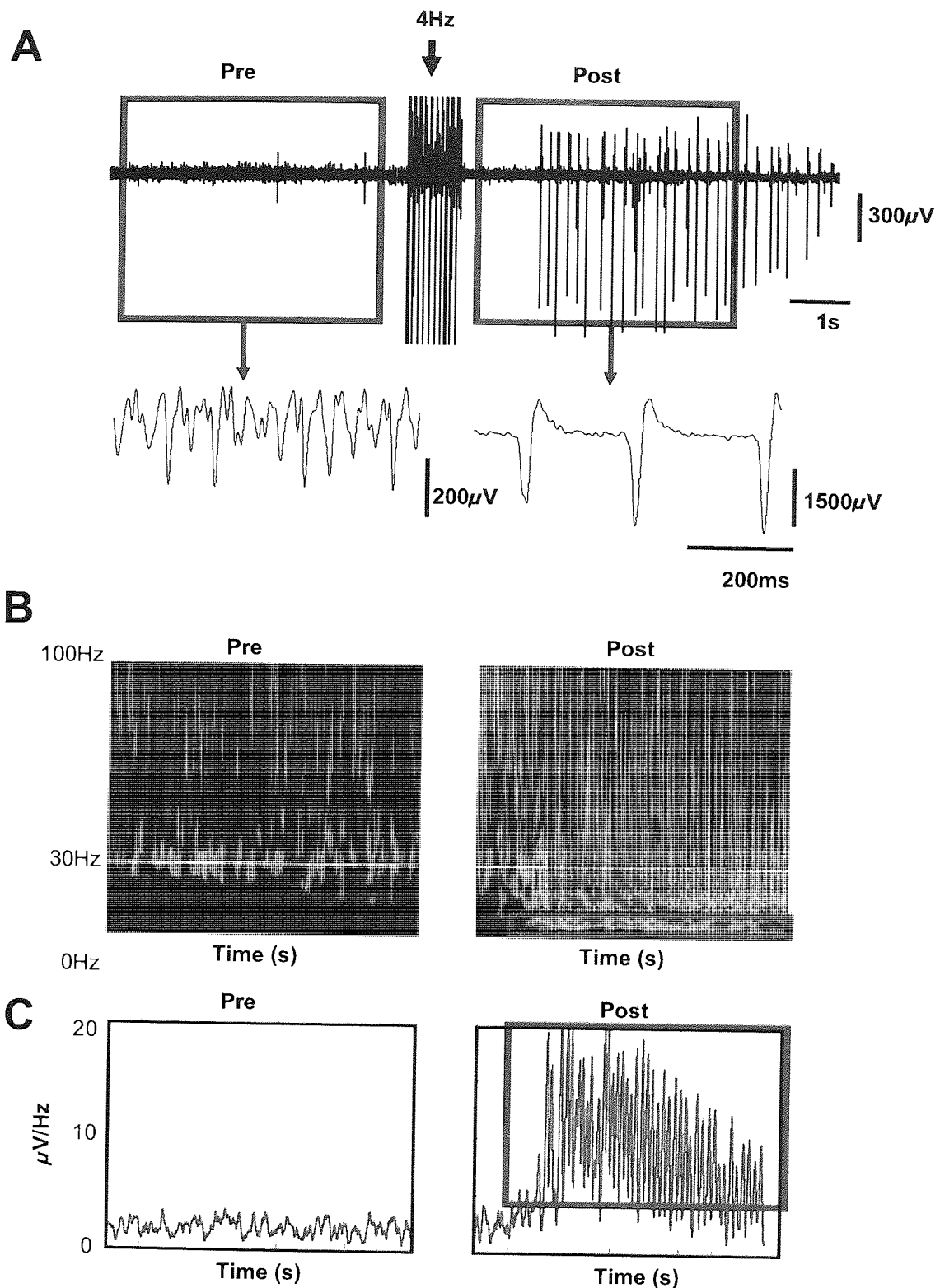
Figure 5.3 – Effect of 4Hz stimulation on persistent beta oscillations in M1. (A) Example trace of field activity. Arrow indicates where stimulation was applied. "Pre" indicates population activity before stimulation. "Post" indicates response evoked by 4Hz stimulation. Magnified traces from each location are also shown below each red box. **(B)** Spectrogram analysis of field activity at the location designated in (A). Hot colour indicates high activity intensity while cold colour indicates low activity. Image threshold $P<0.05$. Time scale for each spectrogram is 9 seconds. White line indicates the frequency of persistent beta oscillations. **(C)** Data filtered at 20-35Hz showing nature of beta activity pre- and post-stimulation.

5.2.3 Two-site stimulation of M1 layer I with 20Hz

I next, examined the effect of 20Hz stimulation (10 pulses at 0.5-1.5 mV) on the persistent beta oscillation in layer V. Beta frequency (20Hz) stimulation was found to exacerbate the symptoms on PD when applied to STN (Moro *et al.*, 2002; Chen *et al.* 2007; Eusebio *et al.*, 2008). Furthermore, when beta frequency stimulation was applied extradually, symptomatic relief of PD was shown to be less evident (Cilia *et al*, 2007). On the other hand, there have been reports of beta frequency stimulation producing positive effects in PD patients (see Lefaucheur, 2006 for review).

In our experiments, simultaneous stimulation of M1 layer I at beta frequency evoked two different responses. In 2 out of 9 slices, gamma oscillations with average frequency of 62.0 ± 5.2 Hz (power spectrum analysis) were generated (figure 5.4A). The peak power of this activity was found to be 6.7 ± 4.6 μV^2. When these traces were analysed using spectrogram, evoked responses were found to exhibit a similar distribution pattern of power as HFS-evoked response (figure 5.4B). In addition, a VFO component was also observed. Interestingly, however, on-going beta oscillatory activity was not affected by 20Hz stimulation. This was confirmed with band-pass filtration of trace at beta (20-35Hz) band, the data showing no notable change in beta power before, and after stimulation (around 5μV/Hz, see figure 5.4C).

In 4 out of 9 slices, theta (3.7 ± 0.4 Hz) oscillations were generated (figure 5.5A) with an average peak power of 2.6 ± 1.2 μV^2. Spectrogram analysis revealed the emergence of theta oscillations (figure 5.5B, red box) and enhancement of beta activity (figure 5.5B). Band-pass filtering of the trace at beta frequency (20-35Hz) revealed that before stimulation, power of beta oscillation was evenly distributed over time (around 5 μV/Hz, figure 5.5C). However, after stimulation beta activity was found to be enhanced at theta frequency (figure 5.5C, red box). These results indicate that 20Hz stimulation can enhance beta which can be modulated at theta frequency.
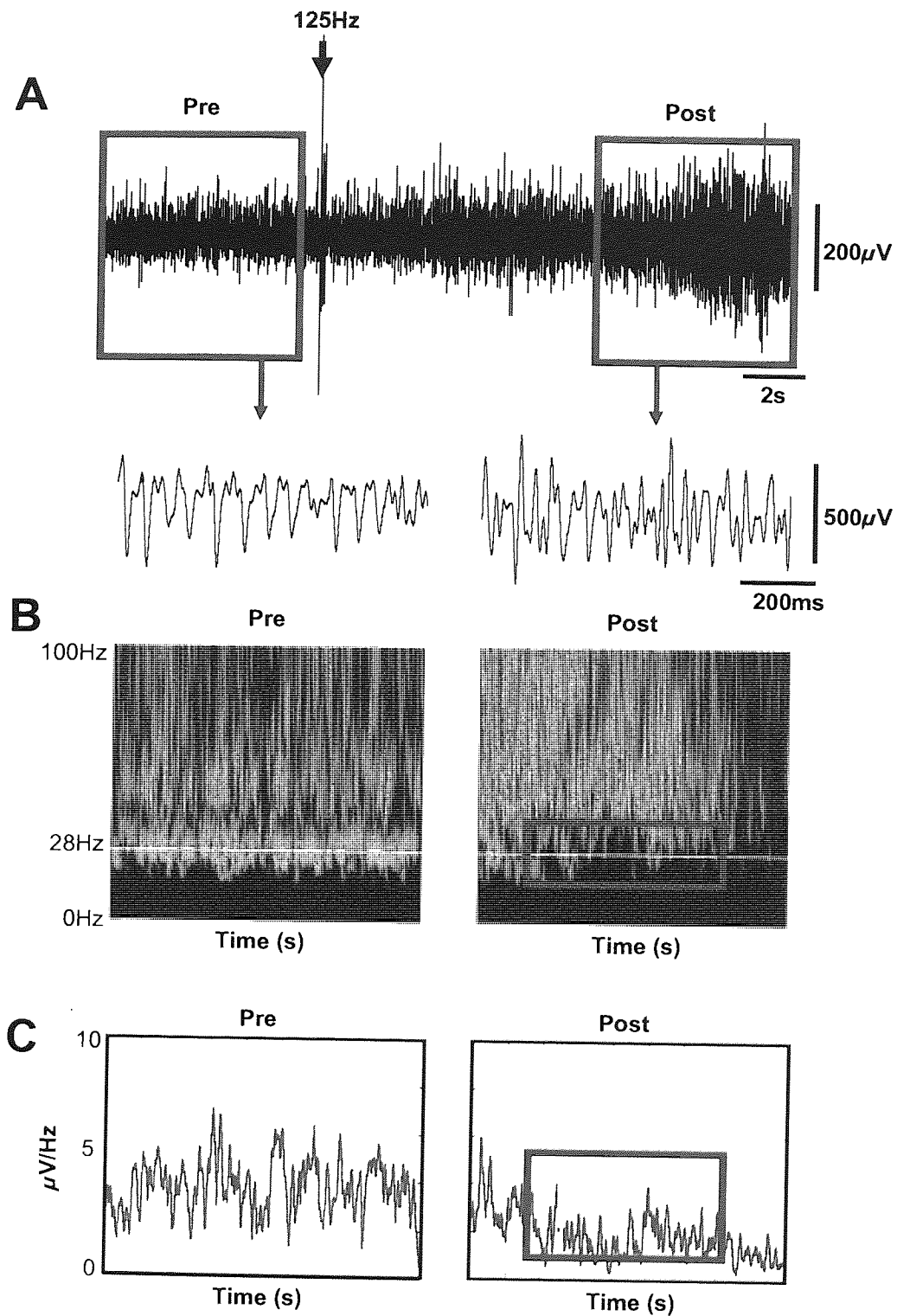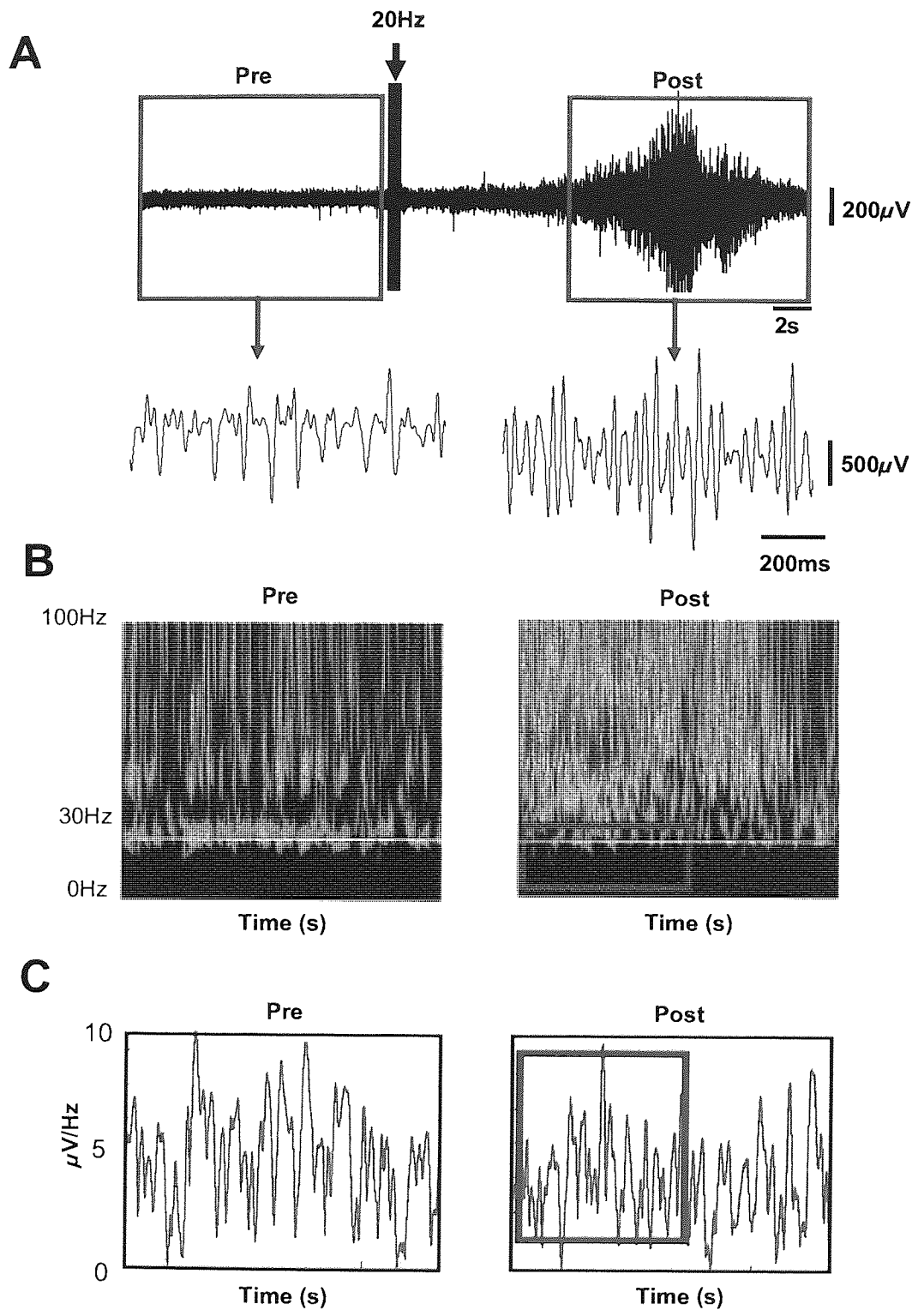
Figure 5.4 – Effect of 20Hz stimulation on persistent beta oscillations in M1. (A) Example trace of field activity. Arrow indicates where stimulation was applied. "Pre" indicates population activity before stimulation. "Post" indicates response evoked by 20Hz stimulation. Magnified traces from each location are also shown below each red box. (B) Spectrogram analysis of field activity at the location designated in (A). Hot colour indicates high activity while cold colour indicates low activity. Image threshold $P<0.05$. Time scale for each spectrogram is 9 seconds. White line indicates the frequency of persistent beta oscillations. (C) Data filtered at 20-35Hz showing nature of beta activity pre- and post-stimulation.

Figure 5.5 – Effect of 20Hz stimulation on persistent beta oscillation in M1. (A) Example trace of field activity. Arrow indicates where stimulation was applied. "Pre" indicates population activity before stimulation. "Post" indicates response evoked by 20Hz stimulation. Magnified traces from each location are also shown below each red box. **(B)** Spectrogram analysis of field activity at the location designated in (A). Hot colour indicates high activity while cold colour indicates low activity. Image threshold $P<0.05$. Time scale for each spectrogram is 9 seconds. White line indicates the frequency of persistent beta oscillations. **(C)** Data filtered at 20-35Hz showing nature of beta activity pre- and post-stimulation.

120

5.3 DISCUSSION

5.3.1 Summary

In this chapter, I have shown how cortical stimulation of M1 at different frequencies modulates the persistent pharmacologically induced beta oscillation and promotes additional oscillations which may modulate the ongoing beta activity. I have found that HFS (at 125Hz), a frequency range commonly used for clinical therapy, generated gamma frequency oscillations while apparently suppressing the ongoing beta oscillation. 4Hz stimulation, on the other hand, enhanced beta oscillatory activity, which was modulated at theta frequency. Finally, beta frequency stimulation (20Hz) generated mixed results, including gamma oscillations and beta bursts at theta frequency.

5.3.2 Is analysis of the post-stimulus response valid?

The relief of PD symptoms by DBS often correlates with ongoing stimulation, symptomatic relief ceasing almost immediately following the switching off of the stimulator. This may indicate the need to analyse ongoing activity during the stimulation paradigm itself. However, there is an obvious difficulty in separating the oscillatory activity from the stimulation artefacts (Kühn *et al.*, 2008) although, mathematically-constructed average stimulus artefact templates have been used to extract physiologically relevant oscillatory activity in some studies (Hashimoto *et al.*, 2003; Drouot *et al*, 2004; Li *et al.*, 2007).

Analysis of activity in a short post-stimulus time window has been carried in other studies (Temperli *et al.*, 2003; Wingeier *et al.*, 2006; Foffani *et al.*, 2006; Kühn *et al.*, 2008). This post-stimulus activity is often assumed to be similar to that evoked within the stimulation itself. The length of such a time window appears to be highly variable. Wingeier *et al.* (2006) reported that beta oscillatory activity remained suppressed for up to 15s after short HFS-DBS, while longer stimulation protocols prolonged the stimulus-induced effect. Furthermore, improved UPDRS scores after rTMS of M1

hand area of PD patients at 5Hz (for 30s x15, with inter-train interval of 10s) was reported to last for 1h (Siebner *et al.,* 2000). These studies provide support for the post stimulus modulation of oscillatory activity which is correlated with symptomatic relief and provides the rationale for post-stimulus analysis of evoked activity in our studies.

5.3.3 Use of two-site stimulation

Extradural cortical stimulation involves bipolar or quadripolar stimulating electrodes (Canavero and Paolotti, 2000; Cillia *et al.,* 2008) which are expected to activate extensive neuronal networks. Thus, in order to mimic this procedure *in vitro,* two-site stimulation was used. On a few occasions, I examined the effect of one-site stimulation, but no visible network activity in M1 was observed. This suggests that one-site was unable to provide the level of tonic depolarisation required. Previously, one-site tetanic stimulation was shown to be sufficient to evoke transient gamma oscillation in rat hippocampal CA1 *in vitro* (Whittington *et al.,* 1995, 1997a, 1997b). However, two-site stimulation was required for achieving coherent activity of distant neuronal populations (Traub *et al.,* 1996a, Whittington *et al.,* 1997a, 1997b).

Layer I was selected as the stimulation site to mimic clinical studies. This layer lacks pyramidal neurones but contains a large number of interneurones (Gabbott and Somogyi, 1986; DeFelipe and Jones, 1985; Chu *et al.,* 2003; Shlosberg *et al.,* 2003). Although pyramidal cell bodies are absent, dendrites of pyramidal cells from both deep and superficial layers are known to transverse layer I (Chu *et al.,* 2003; Molnár and Cheung, 2006). In addition, axon collaterals of layer II/III pyramidal cells also ramify through layer I (Chu *et al.,* 2003). In such an anatomical arrangement, focal stimulation of layer I would be expected to activate local interneurones, directly activate dendrites of pyramidal cells and also axon collaterals of layer II/III pyramidal cells.

5.3.4 Mechanistic thoughts – evoked gamma oscillations

From the data in chapter 3 and 4, I have suggested that FS cells are likely to be driving the network of neurones, at least, in layer V in M1. During 125Hz stimulation, gamma oscillations are generated while the ongoing beta oscillation was suppressed. This may indicate that beta and gamma oscillations are mutually destructive. However, stimulation at 20Hz evokes gamma without effect on beta.

These results may indicate:-

1) 125Hz stimulation activates a set of interneurones (such as RSNP) which entrain gamma oscillations, leaving FS cells to entrain beta oscillations.
2) Beta and gamma oscillations are driven by a different population of FS cells.
3) 125Hz stimulation of M1 evokes gamma oscillations by a different mechanism other than that involving interneurone-driven network.

In support of 3) distinct non-synaptic post-tetanic gamma and beta oscillations, caused by field effects, have been reported (Bracci *et al.,* 1999). However, these oscillations were evoked by high intensity stimulation with raised extracellular potassium concentration in hypo-osmotic conditions (i.e. non-physiological), which invariably promote epileptiform activity (Whittington *et al.,* 2001).

The suppression of persistent beta activity, during evoked gamma, will only occur when the populations described in 2) above, overlap. This mechanism could, in theory, reduce abnormally enhanced cortical beta power observed in PD (Sharott *et al.,* 2005a). Indeed, coherent cortical beta activity (10-35Hz) found in PD patients was reduced by HFS of STN or levodopa administration, which correlated with clinical improvement (Sliberstein *et al.,* 2005). These improvements coincided with the emergence of gamma oscillations in layer V and it is this which may disrupt pathological oscillatory firing patterns in the STN via the hyperdirect pathway (Nambu *et al.,* 2002).

5.3.5 Mechanistic thoughts – evoked theta oscillations

4Hz or 20Hz stimulation was found to evoke large amplitude theta oscillations. The beta and gamma oscillations were maintained and modulated at theta frequency. In contrast to STN, there are no subdural or extradural studies to date which have examined M1 stimulation in these frequency ranges. However, rTMS of M1 is commonly applied at this frequency range and this tends to produce positive effects on PD symptoms (Pascaul-Leone et al., 1994; Siebner et al., 1999, 2000; de Groot et al., 2001; Khedr et al., 2003; Kim et al., 2008). Mechanistic studies of these effects are limited to indirect assessment of change in cortical excitability or dopamine release (Shimamoto, et al., 2001; Ikeguchi et al., 2003; Lefaucheur et al., 2004; Ohnishi et al., 2004; Strafella et al., 2005; Khedr et al., 2007; Kim et al., 2008) and hence do not provide insight at the neuronal level.

4Hz stimulation in our studies promoted theta activity and enhanced beta and gamma oscillatory activity which were modulated at theta frequencies. The elevation of beta power during this period suggests an increase in the size of the population participating in beta frequency activity. Such an enhancement can be achieved via enhanced EPSPs at the perisomatic region of postsynaptic cells (Szabadics et al., 2001).

In vivo, theta oscillations (4-12Hz) have been observed in various cortical regions during rapid-eye-movement (REM) sleep and locomotion (see Buzsàki, 2002 for review). This activity was thought to be driven by the medial septum, as lesion of this area abolished cortical theta activity in vivo (Petsche et al., 1962). Persistent theta oscillations can also be induced by cholinergic activation in hippocampal slices, indicating the ability of local neuronal network for theta rhythmogenesis (Fisahn et al., 1998; Chapman and Lacaille, 1999). It has been shown that cholinergic activation also induces gamma oscillatory activity (30-80Hz) in hippocampus, nested on theta rhythm (Fisahn et al., 1998). It has been postulated that these different oscillating frequencies are generated by activity of distinct interneuronal populations. Indeed, during pharmacologically induced gamma oscillations in CA3 region, O-LM cells fire at theta frequency while other interneurones (basket, bistratified, and trilaminar) fire

at gamma frequency, indicative of their distinct role in promoting network oscillations (Gloveli *et al.,* 2005).

In this study all stimulations were applied at layer I (although as previously described, we cannot rule out the stimulation of other layers). Layer I contains neurogliaform cells, a type of LS neurone. This cell type was found to respond to weak depolarisations with slow depolarising ramps and single APs and regular spiking upon strong depolarisation (Kawaguchi 1995). These neurones project their axon to layer II/III pyramidal cell dendrites (Chu *et al.,* 2003) and also contact with dendritic tuft of layer V pyramidal neurones (Chu *et al.,* 2003; Zhu and Zhu, 2004). Furthermore, they receive extensive local and ascending excitatory drive.

The IPSPs promoted by these cells have a significantly slower kinetics compared to classic fast GABA$_A$ receptor-mediated currents mediated by FS cells (Overstreet and Westbrook, 2003; Szabadics *et al.,* 2007). This observation was attributed to spillover, low probability of GABA release and low affinity of GABA$_A$ receptors (Szabadics *et al.,* 2007). Thus, enhancing GABA transient by blocking active reuptake increased the amplitude of the slow GABA$_A$ current, but not fast GABA$_A$ current mediated by FS cells (Szabadics *et al.,* 2007). These cells can also generate IPSPs mediated by GABA$_B$ receptors (Tamás *et al.,* 2004). Taking these data together, I would propose that 4Hz stimulation preferentially activates LS cells, which entrain temporarily dynamic neuronal populations which express beta activity, at theta frequency (figure 5.6). As these cells innervate the dendrite of layer II/III and layer V they could mediate concurrent activation of oscillations in these regions. The latency observed between the end of stimulation and theta activity may reflect the slow depolarisation of LS cells. Alternatively, it may reflect the time period for pyramidal dendrites to recover from summated slow GABA$_A$ and GABA$_B$ currents. Rebound APs may be then be produced after the IPSP induced de-inactivation of I$_h$ and subsequent activation of T-type Ca^{2+} channels (de la and Geijo-Barrientos, 1996; Magistretti and de Curtis, 1998).
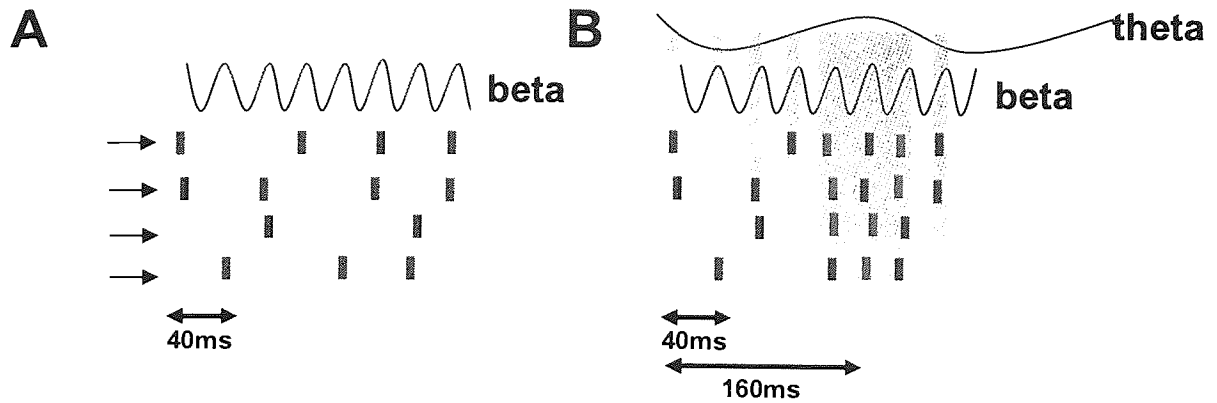
Figure 5.6 – Possible mechanism of co-existence of beta and evoked theta oscillation in M1. (A)
Relationship of pyramidal cell firing and field beta oscillations. Each arrow indicates the firing pattern (black vertical line) of an individual pyramidal cell during beta oscillatory activity. This firing pattern collectively generates beta field oscillations. **(B)** Possible firing pattern that may be occurring during beta oscillation and theta population spikes. Red line indicates new spike produced by same/different pyramidal cells in (A) by, for example, the activation of T-type calcium currents after profound, slow dendritic IPSPs.

The possible involvement of LS, LTS, or RSNP cells in other layers cannot, however, be ruled out. Indeed, orthodromic/antidromic stimulation of pyramidal cells between two layers may provide simultaneous, recurrent excitation to these interneurones thereby allowing theta/gamma long range synchrony.

CHAPTER 6:
GENERAL DISCUSSION
AND FUTURE
EXPERIMENTS

What mechanisms underly network oscillatory activity in M1 and how can oscillations be modulated by stimulation protocols and by pharmacological interventions? In order to address this question, I first investigated the underlying mechanisms of synchronous network oscillations in primary motor cortex (M1) in vitro. Application of KA and CCh generated persistent synchronous beta frequency network activity in M1, a frequency range consistent with in vivo observations (Murthy and Fetz, 1992). The significance of $GABA_A$ receptors and gap junctions became evident through pharmacological dissection of beta oscillatory activity (chapter 3). Recording of individual cell activity during beta oscillations indicated that FS cells entrain the beta network activity by generating the APs at beta frequency, which in turn, provide rhythmic $GABA_A$ receptor-mediated IPSPs to postsynaptic cells (chapter 4). Other cell types (i.e. RS and IB pyramidal cells) also fired APs phase-locked to field beta oscillation, but not at every beta cycle. Here, identification of the morphological profile of electrophysiologically characterised cell type using biocytin would have distinguished the cell types more precisely. Nevertheless, these findings suggested that beta oscillations in M1 engage similar mechanism to pharmacologically-induced persistent gamma oscillations observed in other cortical structures in vitro (Fisahn et al., 1998). However, there was one critical difference. M1 beta oscillatory activity did not require AMPA receptor-mediated currents, whereas previous studies of gamma oscillations in vitro and computer simulations have indicated a necessity for AMPA receptor activity, in particular, from pyramidal cells to interneurones in order to maintain precise spike timing and hence, synchrony of distant network activity (Traub et al., 2001, 2004). Thus, AMPA receptor activity is not required in M1 oscillatory activity and individual pyramidal cells do not follow the beta oscillation precisely. These data indicate the relatively loose regulation of pyramidal neuronal activity by FS cells in M1. In this way, dynamic neuronal pools within a given beta oscillating network could be modulated by newly arriving motor information which shifts oscillatory frequency from beta to gamma oscillations allowing motor function (Brown et al., 2001).

In support of this notion, muscle contraction intensity is characterised by a dynamic shift of coherent activity between motor cortex (measured by MEG) and muscle (measured by EMG) from beta to gamma frequency (Brown et al., 1998). Indeed, Brown et al. (1998) has shown that during weak muscle contraction, coherence

between these two areas exhibited a peak at beta frequency. However, as intensity of muscle contraction increases, a second peak emerged at gamma frequency, which coincided with a decrease in level of beta coherent activity. During maximum contraction, coherence is solely characterised by gamma frequency. In addition, during movement, activity of motor cortex and muscles is also found to be strongly correlated at gamma frequency (Brown et al., 1998). Moreover, in human studies involving the subdural EEG recordings from the sensorimotor region, cortical network activity can be characterised by event-related desynchronisation (ERD) of alpha and beta activity (Crone et al., 1998a) and event-related synchronisation (ERS) of gamma activity (Crone et al., 1998a, 1998b).

Interestingly, two distinct types of gamma oscillations have been observed during movement (Crone et al., 1998b). These were termed "low gamma" (35-50Hz) and "high gamma" (75-100Hz). Low gamma oscillatory activity appears to persist through the course of movement, while high gamma activity occurs sporadically. In addition, it has been reported that arm and leg are characterised by differences in the coherence of gamma activity with cortico-muscle activity. No such distinction has been made with reference to beta oscillations in vivo (Brown et al., 1998). These data indicate the specificity of gamma frequency activity with regards to motor control and the association of gamma frequency with dynamic movements while beta oscillation reflects more passive events such a setting a resting muscle tone and maintenance of posture.

How dopamine depletion, as seen in PD, could cause the enhanced beta oscillation is still remains unanswered. Expression of both D1-like and D2-like receptors, as well as anatomical evidence of dopaminergic projections to M1, indicate loss of motor functioning may be directly related to altered activity within M1 circuits (Descarries et al., 1987; Berger et al., 1988). In the present study, application of dopamine to M1 was found to have no significant effect on beta oscillatory power although oscillatory frequency was reduced. Although the complex effect of dopamine makes it hard to predict its action (as discussed in chapter 3) this seemingly contradictory observation may be explained by (1) the beta oscillation generated in current study is mechanistically different to excegerrated beta oscillation found in DA-depleted state. Roopun et al. (2006) has recently described beta oscillations which are intrinsically

generated by IB cells. Such a mechanism may be more susceptible to extracellular DA levels than the oscillatory activcity which is dependent upon synaptic mechanism described in this thesis. (2) DA-depletion may be affecting the synaptic inputs to M1 from other cortical/subcortical areas rather than affecting M1 itself.

The stimulation experiments presented in this thesis relate specifically to DBS and the possibility of replacing DBS with cortical stimulation paradigms. The data presented also sheds light on the mechanisms of oscillatory activity and the changes in frequency associated with beneficial effects in movement disorders. Alternatively, one may consider stimulation of the primary somatosensory cortex (S1). A recent study has shown that the whisker motor cortex is strongly guided by sensory input in rat (Ferezou *et al.*, 2007). Furthermore, inactivation of S1 disrupted chewing (Lin *et al.*, 1993; Hiraba *et al.*, 2000), fine motor coordination, sustained muscle contraction and appropriate grip force (Rothwell *et al.*, 1982; Johansson and Westling, 1984; Hikosaka *et al.*, 1985). Therefore, stimulation of S1 may be well suited for modulating the M1 activity.

Anatomical studies indicate that sensory input to motor cortex originates from somatosensory cortex and thalamus (Zin-Ka-Ieu, 1998; Miyachi *et al.*, 2005). In addition, Rocco *et al.* (2007) has recently reported the optimum plane of dissection in order to conserve the reciprocal connectivity of S1 and M1. Once appropriate stimulation frequency and intensity have been determined, simultaneous recording of population and single-cell activity from S1/M1 could be performed with pharmacological dissection to characterise the physiologically relevant gamma tuning (i.e. ERS of gamma) and beta suppression (or, ERD of beta) in the slice.

The results presented in chapter 5 have indicated how M1 cortical stimulation may alleviate the symptoms of PD. Although pharmacology and intracellular recording would be required for confirmation, it is likely that HFS of M1 alleviates the symptoms of PD by changing beta firing FS cell activity to gamma firing, and by doing so, reducing the beta oscillatory activity. Such a mutually destructive relationship of beta and gamma oscillation is inevitable if they are governed by a common interneuronal type as suggested.

However, to mimic PD more closely, one could record from slices obtained from dopamine-depleted animals. The beta oscillations observed in control animals may be mechanistically different from those which exhibit enhanced pathological beta oscillations. One hypothesis is that the power of the beta is so enhanced that the emergence of gamma oscillatory activity is difficult or even impossible.

Although exaggerated beta oscillatory activity has been shown in rodent STN and M1, surprisingly, it has yet to be shown in human M1. This may be related to the ethical issues and the inability to record from M1 PD patients undergoing DBS. The MEG is an ideal tool to address this question. In addition, using Pharmaco-MEG, the effects of levodopa and zolpidem administration on oscillatory activity could be determined and these effects directly related to clinical outcomes. As levodopa and zolpidem work by different mechanisms they may affect different oscillatory frequencies and clinically one may hypothesise that there actions are synergistic.

REFERENCES

Axon Guide. Sunnyvale, CA: MDS Analytical Technologies.

Abbruzzese G, Berardelli A (2003) Sensorimotor integration in movement disorders. Mov Disord 18:231-240.

Adjamian P, Barnes GR, Hillebrand A, Holliday IE, Singh KD, Furlong PL, Harrington E, Barclay CW, Route PJ (2004) Co-registration of magnetoencephalography with magnetic resonance imaging using bite-bar-based fiducials and surface-matching. Clin Neurophysiol 115:691-698.

Albin RL, Young AB, Penney JB (1989) The functional anatomy of basal ganglia disorders. Trends Neurosci 12:366-375.

Ali AB (2003) Involvement of post-synaptic kainate receptors during synaptic transmission between unitary connections in rat neocortex. Eur J Neurosci 17:2344-2350.

Allam N, Brasil-Neto JP, Brandao P, Weiler F, Barros FJ, Tomaz C (2007) Relief of primary cervical dystonia symptoms by low frequency transcranial magnetic stimulation of the premotor cortex: case report. Arq Neuropsiquiatr 65:697-699.

Amtage F, Henschel K, Schelter B, Vesper J, Timmer J, Lucking CH, Hellwig B (2008) Tremor-correlated neuronal activity in the subthalamic nucleus of Parkinsonian patients. Neurosci Lett 442:195-199.

Andersen P, Silfvenius H, Sundberg SH, Sveen O, Wigstrom H (1978) Functional characteristics of unmyelinated fibres in the hippocampal cortex. Brain Res 144:11-18.

Arle JE, Apetauerova D, Zani J, Deletis DV, Penney DL, Hoit D, Gould C, Shils JL (2008) Motor cortex stimulation in patients with Parkinson disease: 12-month follow-up in 4 patients. J Neurosurg 109:133-139.

Asanuma H, Ward JE (1971) Patterns of contraction of distal forelimb muscles produced by intracortical stimulation in cats. Brain Res 27:97-109.

Aziz TZ, Peggs D, Sambrook MA, Crossman AR (1991) Lesion of the subthalamic nucleus for the alleviation of 1-methyl-4-phenyl-1,2,3,6-tetrahydropyridine (MPTP)-induced parkinsonism in the primate. Mov Disord 6:288-292.

Bacci A, Rudolph U, Huguenard JR, Prince DA (2003a) Major differences in inhibitory synaptic transmission onto two neocortical interneuron subclasses. J Neurosci 23:9664-9674.

Bacci A, Huguenard JR, Prince DA (2003b) Functional autaptic neurotransmission in fast-spiking interneurons: a novel form of feedback inhibition in the neocortex. J Neurosci 23:859-866.

Bacci A, Huguenard JR (2006) Enhancement of spike-timing precision by autaptic transmission in neocortical inhibitory interneurons. Neuron 49:119-130.

Baker SN, Olivier E, Lemon RN (1994) Recording an identified pyramidal volley evoked by transcranial magnetic stimulation in a conscious macaque monkey. Exp Brain Res 99:529-532.

Baker SN, Olivier E, Lemon RN (1997) Coherent oscillations in monkey motor cortex and hand muscle EMG show task-dependent modulation. J Physiol 501 (Pt 1):225-241.

Baker SN, Kilner JM, Pinches EM, Lemon RN (1999) The role of synchrony and oscillations in the motor output. Exp Brain Res 128:109-117.

Baroni A, Benvenuti F, Fantini L, Pantaleo T, Urbani F (1984) Human ballistic arm abduction movements: effects of L-dopa treatment in Parkinson's disease. Neurology 34:868-876.

Basso MR, Carona FD, Lowery N, Axelrod BN (2002) Practice effects on the WAIS-III across 3- and 6-month intervals. Clin Neuropsychol 16:57-63.

Bear MF, Carnes KM, Ebner FF (1985) An investigation of cholinergic circuitry in cat striate cortex using acetylcholinesterase histochemistry. J Comp Neurol 234:411-430.

Beaulieu C, Kisvarday Z, Somogyi P, Cynader M, Cowey A (1992) Quantitative distribution of GABA-immunopositive and -immunonegative neurons and synapses in the monkey striate cortex (area 17). Cereb Cortex 2:295-309.

Beierlein M, Gibson JR, Connors BW (2000) A network of electrically coupled interneurons drives synchronized inhibition in neocortex. Nat Neurosci 3:904-910.

Benabid AL, Pollak P, Gervason C, Hoffmann D, Gao DM, Hommel M, Perret JE, de RJ (1991) Long-term suppression of tremor by chronic stimulation of the ventral intermediate thalamic nucleus. Lancet 337:403-406.

Benabid AL, Pollak P, Gao D, Hoffmann D, Limousin P, Gay E, Payen I, Benazzouz A (1996) Chronic electrical stimulation of the ventralis intermedius nucleus of the thalamus as a treatment of movement disorders. J Neurosurg 84:203-214.

Benazzouz A, Piallat B, Pollak P, Benabid AL (1995) Responses of substantia nigra pars reticulata and globus pallidus complex to high frequency stimulation of the subthalamic nucleus in rats: electrophysiological data. Neurosci Lett 189:77-80.

Benazzouz A, Gao DM, Ni ZG, Piallat B, Bouali-Benazzouz R, Benabid AL (2000) Effect of high-frequency stimulation of the subthalamic nucleus on the neuronal activities of the substantia nigra pars reticulata and ventrolateral nucleus of the thalamus in the rat. Neuroscience 99:289-295.

Berardelli A, Sabra AF, Hallett M, Berenberg W, Simon SR (1983) Stretch reflexes of triceps surae in patients with upper motor neuron syndromes. J Neurol Neurosurg Psychiatry 46:54-60.

Berger B, Trottier S, Verney C, Gaspar P, Alvarez C (1988) Regional and laminar distribution of the dopamine and serotonin innervation in the macaque cerebral cortex: a radioautographic study. J Comp Neurol 273:99-119.

Berger B, Gaspar P, Verney C (1991) Dopaminergic innervation of the cerebral cortex: unexpected differences between rodents and primates. Trends Neurosci 14:21-27.

Bergman H, Wichmann T, DeLong MR (1990) Reversal of experimental parkinsonism by lesions of the subthalamic nucleus. Science 249:1436-1438.

Bergman H, Wichmann T, Karmon B, DeLong MR (1994) The primate subthalamic nucleus. II. Neuronal activity in the MPTP model of parkinsonism. J Neurophysiol 72:507-520.

Bernheimer H, Birkmayer W, Hornykiewicz O, Jellinger K, Seitelberger F (1973) Brain dopamine and the syndromes of Parkinson and Huntington. Clinical, morphological and neurochemical correlations. J Neurol Sci 20:415-455.

Bibbig A, Faulkner HJ, Whittington MA, Traub RD (2001) Self-organized synaptic plasticity contributes to the shaping of gamma and beta oscillations in vitro. J Neurosci 21:9053-9067.

Bolam JP, Smith Y (1992) The striatum and the globus pallidus send convergent synaptic inputs onto single cells in the entopeduncular nucleus of the rat: a double anterograde labelling study combined with postembedding immunocytochemistry for GABA. J Comp Neurol 321:456-476.

Boraud T, Bezard E, Guehl D, Bioulac B, Gross C (1998) Effects of L-DOPA on neuronal activity of the globus pallidus externalis (GPe) and globus pallidus internalis (GPi) in the MPTP-treated monkey. Brain Res 787:157-160.

Bracci E, Vreugdenhil M, Hack SP, Jefferys JG (1999) On the synchronizing mechanisms of tetanically induced hippocampal oscillations. J Neurosci 19:8104-8113.

Bragin A, Jando G, Nadasdy Z, Hetke J, Wise K, Buzsaki G (1995) Gamma (40-100 Hz) oscillation in the hippocampus of the behaving rat. J Neurosci 15:47-60.

Brecht M, Krauss A, Muhammad S, Sinai-Esfahani L, Bellanca S, Margrie TW (2004) Organization of rat vibrissa motor cortex and adjacent areas according to cytoarchitectonics, microstimulation, and intracellular stimulation of identified cells. J Comp Neurol 479:360-373.

Breese GR, Duncan GE, Napier TC, Bondy SC, Iorio LC, Mueller RA (1987) 6-hydroxydopamine treatments enhance behavioral responses to intracerebral microinjection of D1- and D2-dopamine agonists into nucleus accumbens and striatum without changing dopamine antagonist binding. J Pharmacol Exp Ther 240:167-176.

Brown JA, Lutsep HL, Weinand M, Cramer SC (2006) Motor cortex stimulation for the enhancement of recovery from stroke: a prospective, multicenter safety study. Neurosurgery 58:464-473.

Brown P, Salenius S, Rothwell JC, Hari R (1998) Cortical correlate of the Piper rhythm in humans. J Neurophysiol 80:2911-2917.

Brown P, Oliviero A, Mazzone P, Insola A, Tonali P, Di L, V (2001) Dopamine dependency of oscillations between subthalamic nucleus and pallidum in Parkinson's disease. J Neurosci 21:1033-1038.

Brown P (2003) Oscillatory nature of human basal ganglia activity: relationship to the pathophysiology of Parkinson's disease. Mov Disord 18:357-363.

Buhl EH, Tamas G, Fisahn A (1998) Cholinergic activation and tonic excitation induce persistent gamma oscillations in mouse somatosensory cortex in vitro. J Physiol 513 (Pt 1):117-126.

Buzsaki G (2002) Theta oscillations in the hippocampus. Neuron 33:325-340.

Calne DB, Sandler M (1970) L-Dopa and Parkinsonism. Nature 226:21-24.

Campbell SL, Mathew SS, Hablitz JJ (2007) Pre- and postsynaptic effects of kainate on layer II/III pyramidal cells in rat neocortex. Neuropharmacology 53:37-47.

Canavero S, Paolotti R (2000) Extradural motor cortex stimulation for advanced Parkinson's disease: case report. Mov Disord 15:169-171.

Canavero S, Paolotti R, Bonicalzi V, Castellano G, Greco-Crasto S, Rizzo L, Davini O, Zenga F, Ragazzi P (2002) Extradural motor cortex stimulation for advanced Parkinson disease. Report of two cases. J Neurosurg 97:1208-1211.

Canavero S, Bonicalzi V, Paolotti R, Castellano G, Greco-Crasto S, Rizzo L, Davini O, Maina R (2003) Therapeutic extradural cortical stimulation for movement disorders: a review. Neurol Res 25:118-122.

Canavero S, Bonicalzi V (2007) Extradural cortical stimulation for central pain. Acta Neurochir Suppl 97:27-36.

Canive JM, Lewine JD, Edgar JC, Davis JT, Torres F, Roberts B, Graeber D, Orrison WW, Jr., Tuason VB (1996) Magnetoencephalographic assessment of spontaneous brain activity in schizophrenia. Psychopharmacol Bull 32:741-750.

Cauli B, Audinat E, Lambolez B, Angulo MC, Ropert N, Tsuzuki K, Hestrin S, Rossier J (1997) Molecular and physiological diversity of cortical nonpyramidal cells. J Neurosci 17:3894-3906.

Cauller LJ, Connors BW (1994) Synaptic physiology of horizontal afferents to layer I in slices of rat SI neocortex. J Neurosci 14:751-762.

Chan CS, Shigemoto R, Mercer JN, Surmeier DJ (2004) HCN2 and HCN1 channels govern the regularity of autonomous pacemaking and synaptic resetting in globus pallidus neurons. J Neurosci 24:9921-9932.

136

Chapman CA, Lacaille JC (1999) Intrinsic theta-frequency membrane potential oscillations in hippocampal CA1 interneurons of stratum lacunosum-moleculare. J Neurophysiol 81:1296-1307.

Chen CC, Litvak V, Gilbertson T, Kuhn A, Lu CS, Lee ST, Tsai CH, Tisch S, Limousin P, Hariz M, Brown P (2007) Excessive synchronization of basal ganglia neurons at 20 Hz slows movement in Parkinson's disease. Exp Neurol 205:214-221.

Chen W, Zhang JJ, Hu GY, Wu CP (1996) Electrophysiological and morphological properties of pyramidal and nonpyramidal neurons in the cat motor cortex in vitro. Neuroscience 73:39-55.

Chu Z, Galarreta M, Hestrin S (2003) Synaptic interactions of late-spiking neocortical neurons in layer 1. J Neurosci 23:96-102.

Cilia R, Landi A, Vergani F, Sganzerla E, Pezzoli G, Antonini A (2007) Extradural motor cortex stimulation in Parkinson's disease. Mov Disord 22:111-114.

Cilia R, Marotta G, Landi A, Isaias IU, Vergani F, Benti R, Sganzerla E, Gerundini P, Pezzoli G, Antonini A (2008) Cerebral activity modulation by extradural motor cortex stimulation in Parkinson's disease: a perfusion SPECT study. Eur J Neurol 15:22-28.

Clauss R, Nel W (2006) Drug induced arousal from the permanent vegetative state. NeuroRehabilitation 21:23-28.

Cobb SR, Buhl EH, Halasy K, Paulsen O, Somogyi P (1995) Synchronization of neuronal activity in hippocampus by individual GABAergic interneurons. Nature 378:75-78.

Cohen D (1968) Magnetoencephalography: evidence of magnetic fields produced by alpha-rhythm currents. Science 161:784-786.

Cohen L, Chaaban B, Habert MO (2004) Transient improvement of aphasia with zolpidem. N Engl J Med 350:949-950.

Condorelli DF, Belluardo N, Trovato-Salinaro A, Mudo G (2000) Expression of Cx36 in mammalian neurons. Brain Res Brain Res Rev 32:72-85.

Connors BW, Gutnick MJ, Prince DA (1982) Electrophysiological properties of neocortical neurons in vitro. J Neurophysiol 48:1302-1320.

Conway BA, Halliday DM, Farmer SF, Shahani U, Maas P, Weir AI, Rosenberg JR (1995) Synchronization between motor cortex and spinal motoneuronal pool during the performance of a maintained motor task in man. J Physiol 489 (Pt 3):917-924.

Cossart R, Esclapez M, Hirsch JC, Bernard C, Ben-Ari Y (1998) GluR5 kainate receptor activation in interneurons increases tonic inhibition of pyramidal cells. Nat Neurosci 1:470-478.

Cossart R, Tyzio R, Dinocourt C, Esclapez M, Hirsch JC, Ben-Ari Y, Bernard C (2001) Presynaptic kainate receptors that enhance the release of GABA on CA1 hippocampal interneurons. Neuron 29:497-508.

Courtemanche R, Fujii N, Graybiel AM (2003) Synchronous, focally modulated beta-band oscillations characterize local field potential activity in the striatum of awake behaving monkeys. J Neurosci 23:11741-11752.

Crestani F, Martin JR, Mohler H, Rudolph U (2000) Mechanism of action of the hypnotic zolpidem in vivo. Br J Pharmacol 131:1251-1254.

Crone NE, Miglioretti DL, Gordon B, Lesser RP (1998a) Functional mapping of human sensorimotor cortex with electrocorticographic spectral analysis. II. Event-related synchronization in the gamma band. Brain 121 (Pt 12):2301-2315.

Crone NE, Miglioretti DL, Gordon B, Sieracki JM, Wilson MT, Uematsu S, Lesser RP (1998b) Functional mapping of human sensorimotor cortex with electrocorticographic spectral analysis. I. Alpha and beta event-related desynchronization. Brain 121 (Pt 12):2271-2299.

Csicsvari J, Hirase H, Czurko A, Mamiya A, Buzsaki G (1999a) Fast network oscillations in the hippocampal CA1 region of the behaving rat. J Neurosci 19:RC20.

Csicsvari J, Hirase H, Czurko A, Mamiya A, Buzsaki G (1999b) Oscillatory coupling of hippocampal pyramidal cells and interneurons in the behaving Rat. J Neurosci 19:274-287.

Cunningham MO, Davies CH, Buhl EH, Kopell N, Whittington MA (2003) Gamma oscillations induced by kainate receptor activation in the entorhinal cortex in vitro. J Neurosci 23:9761-9769.

Cunningham MO, Whittington MA, Bibbig A, Roopun A, Lebeau FE, Vogt A, Monyer H, Buhl EH, Traub RD (2004) A role for fast rhythmic bursting neurons in cortical gamma oscillations in vitro. Proc Natl Acad Sci U S A 101:7152-7157.

Dauer W, Przedborski S (2003) Parkinson's disease: mechanisms and models. Neuron 39:889-909.

de la PE, Geijo-Barrientos E (1996) Laminar localization, morphology, and physiological properties of pyramidal neurons that have the low-threshold calcium current in the guinea-pig medial frontal cortex. J Neurosci 16:5301-5311.

de GM, Hermann W, Steffen J, Wagner A, Grahmann F (2001) [Contralateral and ipsilateral repetitive transcranial magnetic stimulation in Parkinson patients]. Nervenarzt 72:932-938.

Deans MR, Gibson JR, Sellitto C, Connors BW, Paul DL (2001) Synchronous activity of inhibitory networks in neocortex requires electrical synapses containing connexin36. Neuron 31:477-485.

DeFelipe J, Jones EG (1985) Vertical organization of gamma-aminobutyric acid-accumulating intrinsic neuronal systems in monkey cerebral cortex. J Neurosci 5:3246-3260.

DeFelipe J, Farinas I (1992) The pyramidal neuron of the cerebral cortex: morphological and chemical characteristics of the synaptic inputs. Prog Neurobiol 39:563-607.

DeLong MR (1990) Primate models of movement disorders of basal ganglia origin. Trends Neurosci 13:281-285.

Descarries L, Lemay B, Doucet G, Berger B (1987) Regional and laminar density of the dopamine innervation in adult rat cerebral cortex. Neuroscience 21:807-824.

Descarries L, Lemay B, Doucet G, Berger B (1987) Regional and laminar density of the dopamine innervation in adult rat cerebral cortex. Neuroscience 21:807-824.

Destexhe A, Pare D (1999) Impact of network activity on the integrative properties of neocortical pyramidal neurons in vivo. J Neurophysiol 81:1531-1547.

Deuschl G, et al. (2006) A randomized trial of deep-brain stimulation for Parkinson's disease. N Engl J Med 355:896-908.

Dickinson R, Awaiz S, Whittington MA, Lieb WR, Franks NP (2003) The effects of general anaesthetics on carbachol-evoked gamma oscillations in the rat hippocampus in vitro. Neuropharmacology 44:864-872.

Donoghue JP, Kerman KL, Ebner FF (1979) Evidence for two organizational plans within the somatic sensory-motor cortex of the rat. J Comp Neurol 183:647-663.

Donoghue JP, Herkenham M (1986) Neostriatal projections from individual cortical fields conform to histochemically distinct striatal compartments in the rat. Brain Res 365:397-403.

Donoghue JP, Leibovic S, Sanes JN (1992) Organization of the forelimb area in squirrel monkey motor cortex: representation of digit, wrist, and elbow muscles. Exp Brain Res 89:1-19.

Donoghue JP, Sanes JN, Hatsopoulos NG, Gaal G (1998) Neural discharge and local field potential oscillations in primate motor cortex during voluntary movements. J Neurophysiol 79:159-173.

Dooley M, Plosker GL (2000) Zaleplon: a review of its use in the treatment of insomnia. Drugs 60:413-445.

Douglas R, Martin K (2003) Neocortex. In: The Synaptic Organization of the Brain (Shepherd GM, ed), pp 459. New York: Oxford University Inc.

Doyle Gaynor LM, Kuhn AA, Dileone M, Litvak V, Eusebio A, Pogosyan A, Androulidakis AG, Tisch S, Limousin P, Insola A, Mazzone P, Di L, V, Brown P (2008) Suppression of beta oscillations in the subthalamic nucleus following cortical stimulation in humans. Eur J Neurosci.

Draguhn A, Traub RD, Schmitz D, Jefferys JG (1998) Electrical coupling underlies high-frequency oscillations in the hippocampus in vitro. Nature 394:189-192.

Drouot X, Oshino S, Jarraya B, Besret L, Kishima H, Remy P, Dauguet J, Lefaucheur JP, Dolle F, Conde F, Bottlaender M, Peschanski M, Keravel Y, Hantraye P, Palfi S (2004) Functional recovery in a primate model of Parkinson's disease following motor cortex stimulation. Neuron 44:769-778.

Ebrahimi A, Pochet R, Roger M (1992) Topographical organization of the projections from physiologically identified areas of the motor cortex to the striatum in the rat. Neurosci Res 14:39-60.

Edin BB, Johansson N (1995) Skin strain patterns provide kinaesthetic information to the human central nervous system. J Physiol 487 (Pt 1):243-251.

Emson PC, Lindvall O (1979) Distribution of putative neurotransmitters in the neocortex. Neuroscience 4:1-30.

Engel AK, Konig P, Kreiter AK, Singer W (1991) Interhemispheric synchronization of oscillatory neuronal responses in cat visual cortex. Science 252:1177-1179.

Erisir A, Lau D, Rudy B, Leonard CS (1999) Function of specific K(+) channels in sustained high-frequency firing of fast-spiking neocortical interneurons. J Neurophysiol 82:2476-2489.

Eusebio A, Chen CC, Lu CS, Lee ST, Tsai CH, Limousin P, Hariz M, Brown P (2008) Effects of low-frequency stimulation of the subthalamic nucleus on movement in Parkinson's disease. Exp Neurol 209:125-130.

Farver DK, Khan MH (2001) Zolpidem for antipsychotic-induced parkinsonism. Ann Pharmacother 35:435-437.

Fasano A, Piano C, De SC, Cioni B, Di GD, Zinno M, Daniele A, Meglio M, Giordano A, Bentivoglio AR (2008) High frequency extradural motor cortex stimulation transiently improves axial symptoms in a patient with Parkinson's disease. Mov Disord.

Ferezou I, Haiss F, Gentet LJ, Aronoff R, Weber B, Petersen CC (2007) Spatiotemporal dynamics of cortical sensorimotor integration in behaving mice. Neuron 56:907-923.

Filali M, Hutchison WD, Palter VN, Lozano AM, Dostrovsky JO (2004) Stimulation-induced inhibition of neuronal firing in human subthalamic nucleus. Exp Brain Res 156:274-281.

Filion M, Tremblay L (1991) Abnormal spontaneous activity of globus pallidus neurons in monkeys with MPTP-induced parkinsonism. Brain Res 547:142-151.

Fink-Jensen A, Mikkelsen JD (1989) The striato-entopeduncular pathway in the rat. A retrograde transport study with wheatgerm-agglutinin-horseradish peroxidase. Brain Res 476:194-198.

Fisahn A, Pike FG, Buhl EH, Paulsen O (1998) Cholinergic induction of network oscillations at 40 Hz in the hippocampus in vitro. Nature 394:186-189.

Flowers KA (1976) Visual "closed-loop" and "open-loop" characteristics of voluntary movement in patients with Parkinsonism and intention tremor. Brain 99:269-310.

Foffani G, Ardolino G, Egidi M, Caputo E, Bossi B, Priori A (2006) Subthalamic oscillatory activities at beta or higher frequency do not change after high-frequency DBS in Parkinson's disease. Brain Res Bull 69:123-130.

Freeman WJ (1968) Patterns of variation in waveform of averaged evoked potentials from prepyriform cortex of cats. J Neurophysiol 31:1-13.

Frerking M, Malenka RC, Nicoll RA (1998) Synaptic activation of kainate receptors on hippocampal interneurons. Nat Neurosci 1:479-486.

Freund TF, Katona I (2007) Perisomatic inhibition. Neuron 56:33-42.

Fuhrmann G, Markram H, Tsodyks M (2002) Spike frequency adaptation and neocortical rhythms. J Neurophysiol 88:761-770.

Funk AP, Epstein CM (2004) Natural rhythm: evidence for occult 40 Hz gamma oscillation in resting motor cortex. Neurosci Lett 371:181-184.

Gabbott PL, Somogyi P (1986) Quantitative distribution of GABA-immunoreactive neurons in the visual cortex (area 17) of the cat. Exp Brain Res 61:323-331.

Galarreta M, Hestrin S (1999) A network of fast-spiking cells in the neocortex connected by electrical synapses. Nature 402:72-75.

Galarreta M, Hestrin S (2002) Electrical and chemical synapses among parvalbumin fast-spiking GABAergic interneurons in adult mouse neocortex. Proc Natl Acad Sci U S A 99:12438-12443.

Galvan A, Wichmann T (2008) Pathophysiology of parkinsonism. Clin Neurophysiol 119:1459-1474.

Gandia JA, Gimenez-Amaya JM (1991) A neuroanatomical analysis of the rostral striatopallidal pathway in the rat. J Hirnforsch 32:79-88.

Gao WJ, Wang Y, Goldman-Rakic PS (2003) Dopamine modulation of perisomatic and peridendritic inhibition in prefrontal cortex. J Neurosci 23:1622-1630.

Gao WJ, Zheng ZH (2004) Target-specific differences in somatodendritic morphology of layer V pyramidal neurons in rat motor cortex. J Comp Neurol 476:174-185.

Gauthier J, Parent M, Levesque M, Parent A (1999) The axonal arborization of single nigrostriatal neurons in rats. Brain Res 834:228-232.

Gerlach M, Gsell W, Kornhuber J, Jellinger K, Krieger V, Pantucek F, Vock R, Riederer P (1996) A post mortem study on neurochemical markers of dopaminergic, GABA-ergic and glutamatergic neurons in basal ganglia-thalamocortical circuits in Parkinson syndrome. Brain Res 741:142-152.

Ghione I, Di FA, Saladino F, Del BR, Bresolin N, Comi GP, Rango M (2007) Parkin polymorphisms and environmental exposure: decrease in age at onset of Parkinson's disease. Neurotoxicology 28:698-701.

Gibson JR, Beierlein M, Connors BW (1999) Two networks of electrically coupled inhibitory neurons in neocortex. Nature 402:75-79.

Glaze DG (1990) Drug Effects. In: Current Practice in Electroencephalography (Daly DD, Pedley TA, eds), pp 489. New York: Raven Press.

Gloveli T, Dugladze T, Saha S, Monyer H, Heinemann U, Traub RD, Whittington MA, Buhl EH (2005) Differential involvement of oriens/pyramidale interneurones in hippocampal network oscillations in vitro. J Physiol 562:131-147.

Gonzalez-Islas C, Hablitz JJ (2003) Dopamine enhances EPSCs in layer II-III pyramidal neurons in rat prefrontal cortex. J Neurosci 23:867-875.

Gorelova N, Seamans JK, Yang CR (2002) Mechanisms of dopamine activation of fast-spiking interneurons that exert inhibition in rat prefrontal cortex. J Neurophysiol 88:3150-3166.

Gray CM, Singer W (1989) Stimulus-specific neuronal oscillations in orientation columns of cat visual cortex. Proc Natl Acad Sci U S A 86:1698-1702.

Gray CM, Konig P, Engel AK, Singer W (1989) Oscillatory responses in cat visual cortex exhibit inter-columnar synchronization which reflects global stimulus properties. Nature 338:334-337.

Gruner JE, Hirsch JC, Sotelo C (1974) Ultrastructural features of the isolated suprasylvian gyrus in the cat. J Comp Neurol 154:1-27.

Gulledge AT, Jaffe DB (1998) Dopamine decreases the excitability of layer V pyramidal cells in the rat prefrontal cortex. J Neurosci 18:9139-9151.

Halabisky B, Shen F, Huguenard JR, Prince DA (2006) Electrophysiological classification of somatostatin-positive interneurons in mouse sensorimotor cortex. J Neurophysiol 96:834-845.

Halasy K, Buhl EH, Lorinczi Z, Tamas G, Somogyi P (1996) Synaptic target selectivity and input of GABAergic basket and bistratified interneurons in the CA1 area of the rat hippocampus. Hippocampus 6:306-329.

Hall SD, Holliday IE, Hillebrand A, Singh KD, Furlong PL, Hadjipapas A, Barnes GR (2005) The missing link: analogous human and primate cortical gamma oscillations. Neuroimage 26:13-17.

Hamada I, DeLong MR (1992) Excitotoxic acid lesions of the primate subthalamic nucleus result in transient dyskinesias of the contralateral limbs. J Neurophysiol 68:1850-1858.

Hamdy S, Rothwell JC, Aziz Q, Singh KD, Thompson DG (1998) Long-term reorganization of human motor cortex driven by short-term sensory stimulation. Nat Neurosci 1:64-68.

Hampson EC, Vaney DI, Weiler R (1992) Dopaminergic modulation of gap junction permeability between amacrine cells in mammalian retina. J Neurosci 12:4911-4922.

Hashimoto T, Elder CM, Okun MS, Patrick SK, Vitek JL (2003) Stimulation of the subthalamic nucleus changes the firing pattern of pallidal neurons. J Neurosci 23:1916-1923.

HASSLER R, RIECHERT T, MUNDINGER F, UMBACH W, GANGLBERGER JA (1960) Physiological observations in stereotaxic operations in extrapyramidal motor disturbances. Brain 83:337-350.

Henze DA, Gonzalez-Burgos GR, Urban NN, Lewis DA, Barrionuevo G (2000) Dopamine increases excitability of pyramidal neurons in primate prefrontal cortex. J Neurophysiol 84:2799-2809.

Herkenham M (1980) Laminar organization of thalamic projections to the rat neocortex. Science 207:532-535.

Hikosaka O, Wurtz RH (1985) Modification of saccadic eye movements by GABA-related substances. II. Effects of muscimol in monkey substantia nigra pars reticulata. J Neurophysiol 53:292-308.

Hille B (1992) Ion Channels of Excitable Membranes. Sunderland, MA: Sinauer Associates, Inc.

Hillebrand A, Barnes GR (2002) A quantitative assessment of the sensitivity of whole-head MEG to activity in the adult human cortex. Neuroimage 16:638-650.

Hillebrand A, Singh KD, Holliday IE, Furlong PL, Barnes GR (2005) A new approach to neuroimaging with magnetoencephalography. Hum Brain Mapp 25:199-211.

Hiraba H, Yamaguchi Y, Satoh H, Ishibashi Y, Iwamura Y (2000) Deficits of masticatory movements caused by lesions in the orofacial somatosensory cortex of the awake cat. Somatosens Mot Res 17:361-372.

Ho N, Destexhe A (2000) Synaptic background activity enhances the responsiveness of neocortical pyramidal neurons. J Neurophysiol 84:1488-1496.

Holm KJ, Goa KL (2000) Zolpidem: an update of its pharmacology, therapeutic efficacy and tolerability in the treatment of insomnia. Drugs 59:865-889.

Hormuzdi SG, Pais I, Lebeau FE, Towers SK, Rozov A, Buhl EH, Whittington MA, Monyer H (2001) Impaired electrical signaling disrupts gamma frequency oscillations in connexin 36-deficient mice. Neuron 31:487-495.

Huffman KJ, Krubitzer L (2001) Area 3a: topographic organization and cortical connections in marmoset monkeys. Cereb Cortex 11:849-867.

Hutchison WD, Lozano AM, Tasker RR, Lang AE, Dostrovsky JO (1997) Identification and characterization of neurons with tremor-frequency activity in human globus pallidus. Exp Brain Res 113:557-563.

Hutchison WD, Lang AE, Dostrovsky JO, Lozano AM (2003) Pallidal neuronal activity: implications for models of dystonia. Ann Neurol 53:480-488.

Ikeguchi M, Touge T, Nishiyama Y, Takeuchi H, Kuriyama S, Ohkawa M (2003) Effects of successive repetitive transcranial magnetic stimulation on motor performances and brain perfusion in idiopathic Parkinson's disease. J Neurol Sci 209:41-46.

Ingham CA, Hood SH, Arbuthnott GW (1989) Spine density on neostriatal neurones changes with 6-hydroxydopamine lesions and with age. Brain Res 503:334-338.

Jarry C, Fontenas JP, Jonville-Bera AP, utret-Leca E (2002) Beneficial effect of zolpidem for dementia. Ann Pharmacother 36:1808.

Jenner P (2008) Molecular mechanisms of L-DOPA-induced dyskinesia. Nat Rev Neurosci 9:665-677.

Jensen O, Goel P, Kopell N, Pohja M, Hari R, Ermentrout B (2005) On the human sensorimotor-cortex beta rhythm: sources and modeling. Neuroimage 26:347-355.

Johansson K, Lindgren I, Widner H, Wiklund I, Johansson BB (1993) Can sensory stimulation improve the functional outcome in stroke patients? Neurology 43:2189-2192.

Johansson RS, Westling G (1984) Roles of glabrous skin receptors and sensorimotor memory in automatic control of precision grip when lifting rougher or more slippery objects. Exp Brain Res 56:550-564.

Jones EG, Leavitt RY (1974) Retrograde axonal transport and the demonstration of non-specific projections to the cerebral cortex and striatum from thalamic intralaminar nuclei in the rat, cat and monkey. J Comp Neurol 154:349-377.

Jones EG (1983) The nature of the afferent pathways conveying short-latency inputs to primate motor cortex. Adv Neurol 39:263-285.

Juergens E, Guettler A, Eckhorn R (1999) Visual stimulation elicits locked and induced gamma oscillations in monkey intracortical- and EEG-potentials, but not in human EEG. Exp Brain Res 129:247-259.

Jurkiewicz MT, Gaetz WC, Bostan AC, Cheyne D (2006) Post-movement beta rebound is generated in motor cortex: evidence from neuromagnetic recordings. Neuroimage 32:1281-1289.

Kabbani N, Levenson R (2007) A proteomic approach to receptor signaling: molecular mechanisms and therapeutic implications derived from discovery of the dopamine D2 receptor signalplex. Eur J Pharmacol 572:83-93.

Kaelin-Lang A, Luft AR, Sawaki L, Burstein AH, Sohn YH, Cohen LG (2002) Modulation of human corticomotor excitability by somatosensory input. J Physiol 540:623-633.

Kalinichenko SG, Pushchin II, Dyuizen IV (2006) Neurochemical diversity of neurogliaform cells in the human primary motor cortex. J Chem Neuroanat 31:304-310.

Kaneko T, Cho R, Li Y, Nomura S, Mizuno N (2000) Predominant information transfer from layer III pyramidal neurons to corticospinal neurons. J Comp Neurol 423:52-65.

Karayannis T, Huerta-Ocampo I, Capogna M (2006) GABAergic and Pyramidal Neurons of Deep Cortical Layers Directly Receive and Differently Integrate Callosal Input. Cereb Cortex.

Katayama Y, Yamamoto T, Kobayashi K, Kasai M, Oshima H, Fukaya C (2001) Motor cortex stimulation for post-stroke pain: comparison of spinal cord and thalamic stimulation. Stereotact Funct Neurosurg 77:183-186.

Katayama Y, Oshima H, Fukaya C, Kawamata T, Yamamaoto T (2002) Control of post-stroke movement disorders using chronic motor cortex stimulation. Acta Neurochir Suppl 79:89-92.

Katayama Y, Yamamoto T, Kobayashi K, Oshima H, Fukaya C (2003) Deep brain and motor cortex stimulation for post-stroke movement disorders and post-stroke pain. Acta Neurochir Suppl 87:121-123.

Kawaguchi Y (1995) Physiological subgroups of nonpyramidal cells with specific morphological characteristics in layer II/III of rat frontal cortex. J Neurosci 15:2638-2655.

Kawaguchi Y, Kubota Y (1997) GABAergic cell subtypes and their synaptic connections in rat frontal cortex. Cereb Cortex 7:476-486.

Kha HT, Finkelstein DI, Pow DV, Lawrence AJ, Horne MK (2000) Study of projections from the entopeduncular nucleus to the thalamus of the rat. J Comp Neurol 426:366-377.

Khedr EM, Farweez HM, Islam H (2003) Therapeutic effect of repetitive transcranial magnetic stimulation on motor function in Parkinson's disease patients. Eur J Neurol 10:567-572.

Khedr EM, Rothwell JC, Shawky OA, Ahmed MA, Hamdy A (2006) Effect of daily repetitive transcranial magnetic stimulation on motor performance in Parkinson's disease. Mov Disord 21:2201-2205.

Khedr EM, Rothwell JC, Shawky OA, Ahmed MA, Foly N, Hamdy A (2007) Dopamine levels after repetitive transcranial magnetic stimulation of motor cortex in patients with Parkinson's disease: preliminary results. Mov Disord 22:1046-1050.

Kim JY, Chung EJ, Lee WY, Shin HY, Lee GH, Choe YS, Choi Y, Kim BJ (2008) Therapeutic effect of repetitive transcranial magnetic stimulation in Parkinson's disease: analysis of [11C] raclopride PET study. Mov Disord 23:207-211.

Kita H, Chang HT, Kitai ST (1983) Pallidal inputs to subthalamus: intracellular analysis. Brain Res 264:255-265.

Kita H, Kitai ST (1994) The morphology of globus pallidus projection neurons in the rat: an intracellular staining study. Brain Res 636:308-319.

Klausberger T, Magill PJ, Marton LF, Roberts JD, Cobden PM, Buzsaki G, Somogyi P (2003) Brain-state- and cell-type-specific firing of hippocampal interneurons in vivo. Nature 421:844-848.

Klausberger T, Marton LF, Baude A, Roberts JD, Magill PJ, Somogyi P (2004) Spike timing of dendrite-targeting bistratified cells during hippocampal network oscillations in vivo. Nat Neurosci 7:41-47.

Kleiner-Fisman G, Fisman DN, Kahn FI, Sime E, Lozano AM, Lang AE (2003) Motor cortical stimulation for parkinsonism in multiple system atrophy. Arch Neurol 60:1554-1558.

Kosar E, Waters RS, Tsukahara N, Asanuma H (1985) Anatomical and physiological properties of the projection from the sensory cortex to the motor cortex in normal cats: the difference between corticocortical and thalamocortical projections. Brain Res 345:68-78.

Krack P, Benazzouz A, Pollak P, Limousin P, Piallat B, Hoffmann D, Xie J, Benabid AL (1998) Treatment of tremor in Parkinson's disease by subthalamic nucleus stimulation. Mov Disord 13:907-914.

Krack P, Fraix V, Mendes A, Benabid AL, Pollak P (2002) Postoperative management of subthalamic nucleus stimulation for Parkinson's disease. Mov Disord 17 Suppl 3:S188-S197.

Kuhn AA, Kupsch A, Schneider GH, Brown P (2006) Reduction in subthalamic 8-35 Hz oscillatory activity correlates with clinical improvement in Parkinson's disease. Eur J Neurosci 23:1956-1960.

Kuhn AA, Kempf F, Brucke C, Gaynor DL, Martinez-Torres I, Pogosyan A, Trottenberg T, Kupsch A, Schneider GH, Hariz MI, Vandenberghe W, Nuttin B, Brown P (2008) High-frequency stimulation of the subthalamic nucleus suppresses oscillatory beta activity in patients with Parkinson's disease in parallel with improvement in motor performance. J Neurosci 28:6165-6173.

Kwan HC, MacKay WA, Murphy JT, Wong YC (1978) An intracortical microstimulation study of output organization in precentral cortex of awake primates. J Physiol (Paris) 74:231-233.

Lebeau FE, Traub RD, Monyer H, Whittington MA, Buhl EH (2003) The role of electrical signaling via gap junctions in the generation of fast network oscillations. Brain Res Bull 62:3-13.

Lee FJ, Liu F (2008) Genetic factors involved in the pathogenesis of Parkinson's disease. Brain Res Rev 58:354-364.

Lefaucheur JP, Drouot X, Von RF, Menard-Lefaucheur I, Cesaro P, Nguyen JP (2004) Improvement of motor performance and modulation of cortical excitability by repetitive transcranial magnetic stimulation of the motor cortex in Parkinson's disease. Clin Neurophysiol 115:2530-2541.

Lefaucheur JP (2006) Repetitive transcranial magnetic stimulation (rTMS): insights into the treatment of Parkinson's disease by cortical stimulation. Neurophysiol Clin 36:125-133.

Lei W, Jiao Y, Del MN, Reiner A (2004) Evidence for differential cortical input to direct pathway versus indirect pathway striatal projection neurons in rats. J Neurosci 24:8289-8299.

Li S, Arbuthnott GW, Jutras MJ, Goldberg JA, Jaeger D (2007) Resonant antidromic cortical circuit activation as a consequence of high-frequency subthalamic deep-brain stimulation. J Neurophysiol 98:3525-3537.

Limousin P, Pollak P, Benazzouz A, Hoffmann D, Le Bas JF, Broussolle E, Perret JE, Benabid AL (1995) Effect of parkinsonian signs and symptoms of bilateral subthalamic nucleus stimulation. Lancet 345:91-95.

Lin LD, Murray GM, Sessle BJ (1993) The effect of bilateral cold block of the primate face primary somatosensory cortex on the performance of trained tongue-protrusion task and biting tasks. J Neurophysiol 70:985-996.

Lindvall O, Bjorklund A (1979) Dopaminergic innervation of the globus pallidus by collaterals from the nigrostriatal pathway. Brain Res 172:169-173.

Lisman JE, Idiart MA (1995) Storage of 7 +/- 2 short-term memories in oscillatory subcycles. Science 267:1512-1515.

Llinas R, Ribary U, Contreras D, Pedroarena C (1998) The neuronal basis for consciousness. Philos Trans R Soc Lond B Biol Sci 353:1841-1849.

Llinas RR (1988) The intrinsic electrophysiological properties of mammalian neurons: insights into central nervous system function. Science 242:1654-1664.

Llinas RR, Grace AA, Yarom Y (1991) In vitro neurons in mammalian cortical layer 4 exhibit intrinsic oscillatory activity in the 10- to 50-Hz frequency range. Proc Natl Acad Sci U S A 88:897-901.

Logothetis NK, Pauls J, Augath M, Trinath T, Oeltermann A (2001) Neurophysiological investigation of the basis of the fMRI signal. Nature 412:150-157.

Logothetis NK (2003) MR imaging in the non-human primate: studies of function and of dynamic connectivity. Curr Opin Neurobiol 13:630-642.

Lucas-Meunier E, Fossier P, Baux G, Amar M (2003) Cholinergic modulation of the cortical neuronal network. Pflugers Arch 446:17-29.

Lysakowski A, Wainer BH, Rye DB, Bruce G, Hersh LB (1986) Cholinergic innervation displays strikingly different laminar preferences in several cortical areas. Neurosci Lett 64:102-108.

147

Magee JC, Cook EP (2000) Somatic EPSP amplitude is independent of synapse location in hippocampal pyramidal neurons. Nat Neurosci 3:895-903.

Magill PJ, Bolam JP, Bevan MD (2001) Dopamine regulates the impact of the cerebral cortex on the subthalamic nucleus-globus pallidus network. Neuroscience 106:313-330.

Magill PJ, Sharott A, Harnack D, Kupsch A, Meissner W, Brown P (2005) Coherent spike-wave oscillations in the cortex and subthalamic nucleus of the freely moving rat. Neuroscience 132:659-664.

Magistretti J, de CM (1998) Low-voltage activated T-type calcium currents are differently expressed in superficial and deep layers of guinea pig piriform cortex. J Neurophysiol 79:808-816.

Mann EO, Radcliffe CA, Paulsen O (2005) Hippocampal gamma-frequency oscillations: from interneurones to pyramidal cells, and back. J Physiol 562:55-63.

Marchese R, Trompetto C, Buccolieri A, Abbruzzese G (2000) Abnormalities of motor cortical excitability are not correlated with clinical features in atypical parkinsonism. Mov Disord 15:1210-1214.

Marsden CD, Obeso JA (1994) The functions of the basal ganglia and the paradox of stereotaxic surgery in Parkinson's disease. Brain 117 (Pt 4):877-897.

Marsden JF, Werhahn KJ, Ashby P, Rothwell J, Noachtar S, Brown P (2000) Organization of cortical activities related to movement in humans. J Neurosci 20:2307-2314.

Mazzone P, Lozano A, Stanzione P, Galati S, Scarnati E, Peppe A, Stefani A (2005) Implantation of human pedunculopontine nucleus: a safe and clinically relevant target in Parkinson's disease. Neuroreport 16:1877-1881.

McCormick DA, Connors BW, Lighthall JW, Prince DA (1985) Comparative electrophysiology of pyramidal and sparsely spiny stellate neurons of the neocortex. J Neurophysiol 54:782-806.

McCormick DA, Prince DA (1986) Mechanisms of action of acetylcholine in the guinea-pig cerebral cortex in vitro. J Physiol 375:169-194.

McCormick DA, Bal T (1994) Sensory gating mechanisms of the thalamus. Curr Opin Neurobiol 4:550-556.

McGeorge AJ, Faull RL (1989) The organization of the projection from the cerebral cortex to the striatum in the rat. Neuroscience 29:503-537.

McIntosh GC, Brown SH, Rice RR, Thaut MH (1997) Rhythmic auditory-motor facilitation of gait patterns in patients with Parkinson's disease. J Neurol Neurosurg Psychiatry 62:22-26.

Meissner W, Leblois A, Hansel D, Bioulac B, Gross CE, Benazzouz A, Boraud T (2005) Subthalamic high frequency stimulation resets subthalamic firing and reduces abnormal oscillations. Brain 128:2372-2382.

Miles R (1990) Variation in strength of inhibitory synapses in the CA3 region of guinea-pig hippocampus in vitro. J Physiol 431:659-676.

Miles R, Toth K, Gulyas AI, Hajos N, Freund TF (1996) Differences between somatic and dendritic inhibition in the hippocampus. Neuron 16:815-823.

Miller WC, DeLong MR (1988) Parkinsonian symptomatology. An anatomical and physiological analysis. Ann N Y Acad Sci 515:287-302.

Missale C, Nash SR, Robinson SW, Jaber M, Caron MG (1998) Dopamine receptors: from structure to function. Physiol Rev 78:189-225.

Mitzdorf U (1987) Properties of the evoked potential generators: current source-density analysis of visually evoked potentials in the cat cortex. Int J Neurosci 33:33-59.

Miyachi S, Lu X, Inoue S, Iwasaki T, Koike S, Nambu A, Takada M (2005) Organization of multisynaptic inputs from prefrontal cortex to primary motor cortex as revealed by retrograde transneuronal transport of rabies virus. J Neurosci 25:2547-2556.

Molnar Z, Cheung AF (2006) Towards the classification of subpopulations of layer V pyramidal projection neurons. Neurosci Res 55:105-115.

Moro E, Esselink RJ, Xie J, Hommel M, Benabid AL, Pollak P (2002) The impact on Parkinson's disease of electrical parameter settings in STN stimulation. Neurology 59:706-713.

Morris ME, Matyas TA, Iansek R, Summers JJ (1996) Temporal stability of gait in Parkinson's disease. Phys Ther 76:763-777.

Muller W, Misgeld U (1986) Slow cholinergic excitation of guinea pig hippocampal neurons is mediated by two muscarinic receptor subtypes. Neurosci Lett 67:107-112.

Murakoshi T, Guo JZ, Ichinose T (1993) Electrophysiological identification of horizontal synaptic connections in rat visual cortex in vitro. Neurosci Lett 163:211-214.

Murthy VN, Fetz EE (1992) Coherent 25- to 35-Hz oscillations in the sensorimotor cortex of awake behaving monkeys. Proc Natl Acad Sci U S A 89:5670-5674.

Murthy VN, Fetz EE (1996a) Oscillatory activity in sensorimotor cortex of awake monkeys: synchronization of local field potentials and relation to behavior. J Neurophysiol 76:3949-3967.

Murthy VN, Fetz EE (1996b) Synchronization of neurons during local field potential oscillations in sensorimotor cortex of awake monkeys. J Neurophysiol 76:3968-3982.

Nambu A, Tokuno H, Takada M (2002) Functional significance of the cortico-subthalamo-pallidal 'hyperdirect' pathway. Neurosci Res 43:111-117.

Nini A, Feingold A, Slovin H, Bergman H (1995) Neurons in the globus pallidus do not show correlated activity in the normal monkey, but phase-locked oscillations appear in the MPTP model of parkinsonism. J Neurophysiol 74:1800-1805.

Nuwer MR, Hovda DA, Schrader LM, Vespa PM (2005) Routine and quantitative EEG in mild traumatic brain injury. Clin Neurophysiol 116:2001-2025.

Obadiah J, vidor-Reiss T, Fishburn CS, Carmon S, Bayewitch M, Vogel Z, Fuchs S, Levavi-Sivan B (1999) Adenylyl cyclase interaction with the D2 dopamine receptor family; differential coupling to Gi, Gz, and Gs. Cell Mol Neurobiol 19:653-664.

Ohnishi T, Hayashi T, Okabe S, Nonaka I, Matsuda H, Iida H, Imabayashi E, Watabe H, Miyake Y, Ogawa M, Teramoto N, Ohta Y, Ejima N, Sawada T, Ugawa Y (2004) Endogenous dopamine release induced by repetitive transcranial magnetic stimulation over the primary motor cortex: an [11C]raclopride positron emission tomography study in anesthetized macaque monkeys. Biol Psychiatry 55:484-489.

Okada Y, Lauritzen M, Nicholson C (1987) MEG source models and physiology. Phys Med Biol 32:43-51.

Oliveira RM, Gurd JM, Nixon P, Marshall JC, Passingham RE (1997) Micrographia in Parkinson's disease: the effect of providing external cues. J Neurol Neurosurg Psychiatry 63:429-433.

Overstreet LS, Westbrook GL (2003) Synapse density regulates independence at unitary inhibitory synapses. J Neurosci 23:2618-2626.

Page RD, Sambrook MA, Crossman AR (1993) Thalamotomy for the alleviation of levodopa-induced dyskinesia: experimental studies in the 1-methyl-4-phenyl-1,2,3,6-tetrahydropyridine-treated parkinsonian monkey. Neuroscience 55:147-165.

Pagni CA, Zeme S, Zenga F (2003) Further experience with extradural motor cortex stimulation for treatment of advanced Parkinson's disease. Report of 3 new cases. J Neurosurg Sci 47:189-193.

Pagni CA, Zeme S, Zenga F, Maina R (2005) Extradural motor cortex stimulation in advanced Parkinson's disease: the Turin experience: technical case report. Neurosurgery 57:E402.

Pagni CA, Altibrandi MG, Bentivoglio A, Caruso G, Cioni B, Fiorella C, Insola A, Lavano A, Maina R, Mazzone P, Signorelli CD, Sturiale C, Valzania F, Zeme S, Zenga F (2005) Extradural motor cortex stimulation (EMCS) for Parkinson's disease. History and first results by the study group of the Italian neurosurgical society. Acta Neurochir Suppl 93:113-119.

Pagni CA, Zeme S, Zenga F, Maina R (2005) Extradural motor cortex stimulation in advanced Parkinson's disease: the Turin experience: technical case report. Neurosurgery 57:E402.

Pakhotin PI, Pakhotina ID, Andreev AA (1997) Functional stability of hippocampal slices after treatment with cyclooxygenase inhibitors. Neuroreport 8:1755-1759.

Palhalmi J, Paulsen O, Freund TF, Hajos N (2004) Distinct properties of carbachol- and DHPG-induced network oscillations in hippocampal slices. Neuropharmacology 47:381-389.

Papadopoulos GC, Parnavelas JG, Buijs R (1987) Monoaminergic fibers form conventional synapses in the cerebral cortex. Neurosci Lett 76:275-279.

Parent A, Hazrati LN (1995) Functional anatomy of the basal ganglia. II. The place of subthalamic nucleus and external pallidum in basal ganglia circuitry. Brain Res Brain Res Rev 20:128-154.

Pascual-Leone A, Valls-Sole J, Brasil-Neto JP, Cammarota A, Grafman J, Hallett M (1994) Akinesia in Parkinson's disease. II. Effects of subthreshold repetitive transcranial motor cortex stimulation. Neurology 44:892-898.

Passler MA, Riggs RV (2001) Positive outcomes in traumatic brain injury-vegetative state: patients treated with bromocriptine. Arch Phys Med Rehabil 82:311-315.

PENFIELD W, Rasmussen T (1950) Cerebral cortex in man. New York: The Macmillan Company.

PENFIELD W (1954) Mechanisms of voluntary movement. Brain 77:1-17.

Penny GR, Itoh K, Diamond IT (1982) Cells of different sizes in the ventral nuclei project to different layers of the somatic cortex in the cat. Brain Res 242:55-65.

PETSCHE H, STUMPF C (1962) [The origin of theta-rhytm in the rabbit hippocampus.]. Wien Klin Wochenschr 74:696-700.

Pfurtscheller G (2001) Functional brain imaging based on ERD/ERS. Vision Res 41:1257-1260.

Plaha P, Gill SS (2005) Bilateral deep brain stimulation of the pedunculopontine nucleus for Parkinson's disease. Neuroreport 16:1883-1887.

Porter LL, Sakamoto K (1988) Organization and synaptic relationships of the projection from the primary sensory to the primary motor cortex in the cat. J Comp Neurol 271:387-396.

Porter LL (1991) Patterns of connectivity in the cat sensory-motor cortex: a light and electron microscope analysis of the projection arising from area 3a. J Comp Neurol 312:404-414.

Porter LL (1992) Patterns of projections from area 2 of the sensory cortex to area 3a and to the motor cortex in cats. Exp Brain Res 91:85-93.

Porter LL (1996) Somatosensory input onto pyramidal tract neurons in rodent motor cortex. Neuroreport 7:2309-2315.

Poza J, Hornero R, Abasolo D, Fernandez A, Garcia M (2007) Extraction of spectral based measures from MEG background oscillations in Alzheimer's disease. Med Eng Phys 29:1073-1083.

151

Priori A, Ardolino G, Marceglia S, Mrakic-Sposta S, Locatelli M, Tamma F, Rossi L, Foffani G (2006) Low-frequency subthalamic oscillations increase after deep brain stimulation in Parkinson's disease. Brain Res Bull 71:149-154.

Rasch MJ, Gretton A, Murayama Y, Maass W, Logothetis NK (2008) Inferring spike trains from local field potentials. J Neurophysiol 99:1461-1476.

Rausell E, Avendano C (1985) Thalamocortical neurons projecting to superficial and to deep layers in parietal, frontal and prefrontal regions in the cat. Brain Res 347:159-165.

Raz A, Vaadia E, Bergman H (2000) Firing patterns and correlations of spontaneous discharge of pallidal neurons in the normal and the tremulous 1-methyl-4-phenyl-1,2,3,6-tetrahydropyridine vervet model of parkinsonism. J Neurosci 20:8559-8571.

Rioult-Pedotti MS, Friedman D, Hess G, Donoghue JP (1998) Strengthening of horizontal cortical connections following skill learning. Nat Neurosci 1:230-234.

Rocco MM, Brumberg JC (2007) The sensorimotor slice. J Neurosci Methods 162:139-147.

Roopun AK, Middleton SJ, Cunningham MO, Lebeau FE, Bibbig A, Whittington MA, Traub RD (2006) A beta2-frequency (20-30 Hz) oscillation in nonsynaptic networks of somatosensory cortex. Proc Natl Acad Sci U S A 103:15646-15650.

Roopun AK, Kramer MA, Carracedo LM, Kaiser M, Davies CH, Traub RD, Kopell NJ, Whittington MA (2008) Period Concatenation Underlies Interactions between Gamma and Beta Rhythms in Neocortex. Front Cell Neurosci 2:1.

Rothwell JC, Traub MM, Day BL, Obeso JA, Thomas PK, Marsden CD (1982) Manual motor performance in a deafferented man. Brain 105 (Pt 3):515-542.

Rothwell JC, Obeso JA, Traub MM, Marsden CD (1983) The behaviour of the long-latency stretch reflex in patients with Parkinson's disease. J Neurol Neurosurg Psychiatry 46:35-44.

Salin PA, Prince DA (1996) Electrophysiological mapping of GABAA receptor-mediated inhibition in adult rat somatosensory cortex. J Neurophysiol 75:1589-1600.

Salmelin R, Hamalainen M, Kajola M, Hari R (1995) Functional segregation of movement-related rhythmic activity in the human brain. Neuroimage 2:237-243.

Sanchez-Vives MV, McCormick DA (2000) Cellular and network mechanisms of rhythmic recurrent activity in neocortex. Nat Neurosci 3:1027-1034.

Sanes JN, Donoghue JP (1993) Oscillations in local field potentials of the primate motor cortex during voluntary movement. Proc Natl Acad Sci U S A 90:4470-4474.

Sanes JN, Donoghue JP (2000) Plasticity and primary motor cortex. Annu Rev Neurosci 23:393-415.

Schapira AH (2008) Progress in Parkinson's disease. Eur J Neurol 15:1.

Schieber MH, Hibbard LS (1993) How somatotopic is the motor cortex hand area? Science 261:489-492.

Schmitz D, Gloveli T, Behr J, Dugladze T, Heinemann U (1998) Subthreshold membrane potential oscillations in neurons of deep layers of the entorhinal cortex. Neuroscience 85:999-1004.

Schmitz D, Schuchmann S, Fisahn A, Draguhn A, Buhl EH, Petrasch-Parwez E, Dermietzel R, Heinemann U, Traub RD (2001) Axo-axonal coupling. a novel mechanism for ultrafast neuronal communication. Neuron 31:831-840.

Seijo FJ, varez-Vega MA, Gutierrez JC, Fdez-Glez F, Lozano B (2007) Complications in subthalamic nucleus stimulation surgery for treatment of Parkinson's disease. Review of 272 procedures. Acta Neurochir (Wien) 149:867-875.

Semyanov A, Kullmann DM (2001) Kainate receptor-dependent axonal depolarization and action potential initiation in interneurons. Nat Neurosci 4:718-723.

Shames JL, Ring H (2008) Transient reversal of anoxic brain injury-related minimally conscious state after zolpidem administration: a case report. Arch Phys Med Rehabil 89:386-388.

Sharott A, Magill PJ, Harnack D, Kupsch A, Meissner W, Brown P (2005a) Dopamine depletion increases the power and coherence of beta-oscillations in the cerebral cortex and subthalamic nucleus of the awake rat. Eur J Neurosci 21:1413-1422.

Sharott A, Magill PJ, Bolam JP, Brown P (2005b) Directional analysis of coherent oscillatory field potentials in the cerebral cortex and basal ganglia of the rat. J Physiol 562:951-963.

Shi WX, Smith PL, Pun CL, Millet B, Bunney BS (1997) D1-D2 interaction in feedback control of midbrain dopamine neurons. J Neurosci 17:7988-7994.

Shimamoto H, Takasaki K, Shigemori M, Imaizumi T, Ayabe M, Shoji H (2001) Therapeutic effect and mechanism of repetitive transcranial magnetic stimulation in Parkinson's disease. J Neurol 248 Suppl 3:III48-III52.

Shipp S (2005) The importance of being agranular: a comparative account of visual and motor cortex. Philos Trans R Soc Lond B Biol Sci 360:797-814.

Shlosberg D, Patrick SL, Buskila Y, Amitai Y (2003) Inhibitory effect of mouse neocortex layer I on the underlying cellular network. Eur J Neurosci 18:2751-2759.

Sidhu A, Niznik HB (2000) Coupling of dopamine receptor subtypes to multiple and diverse G proteins. Int J Dev Neurosci 18:669-677.

Siebner HR, Mentschel C, Auer C, Conrad B (1999) Repetitive transcranial magnetic stimulation has a beneficial effect on bradykinesia in Parkinson's disease. Neuroreport 10:589-594.

Siebner HR, Rossmeier C, Mentschel C, Peinemann A, Conrad B (2000) Short-term motor improvement after sub-threshold 5-Hz repetitive transcranial magnetic

stimulation of the primary motor hand area in Parkinson's disease. J Neurol Sci 178:91-94.

Silberberg G, Markram H (2007) Disynaptic inhibition between neocortical pyramidal cells mediated by Martinotti cells. Neuron 53:735-746.

Silberstein P, Pogosyan A, Kuhn AA, Hotton G, Tisch S, Kupsch A, Dowsey-Limousin P, Hariz MI, Brown P (2005) Cortico-cortical coupling in Parkinson's disease and its modulation by therapy. Brain 128:1277-1291.

Singer W (1993) Synchronization of cortical activity and its putative role in information processing and learning. Annu Rev Physiol 55:349-374.

Singh KD, Barnes GR, Hillebrand A, Forde EM, Williams AL (2002) Task-related changes in cortical synchronization are spatially coincident with the hemodynamic response. Neuroimage 16:103-114.

Sinha R, Racette B, Perlmutter JS, Parsian A (2005) Prevalence of parkin gene mutations and variations in idiopathic Parkinson's disease. Parkinsonism Relat Disord 11:341-347.

Sloper JJ, Hiorns RW, Powell TP (1979) A qualitative and quantitative electron microscopic study of the neurons in the primate motor and somatic sensory cortices. Philos Trans R Soc Lond B Biol Sci 285:141-171.

Smeyne RJ, Jackson-Lewis V (2005) The MPTP model of Parkinson's disease. Brain Res Mol Brain Res 134:57-66.

Smith Y, Bolam JP (1989) Neurons of the substantia nigra reticulata receive a dense GABA-containing input from the globus pallidus in the rat. Brain Res 493:160-167.

Smith Y, Bolam JP (1991) Convergence of synaptic inputs from the striatum and the globus pallidus onto identified nigrocollicular cells in the rat: a double anterograde labelling study. Neuroscience 44:45-73.

Somogyi P, Klausberger T (2005) Defined types of cortical interneurone structure space and spike timing in the hippocampus. J Physiol 562:9-26.

Steriade M (2006) Grouping of brain rhythms in corticothalamic systems. Neuroscience 137:1087-1106.

Stoney SD, Jr., Thompson WD, Asanuma H (1968) Excitation of pyramidal tract cells by intracortical microstimulation: effective extent of stimulating current. J Neurophysiol 31:659-669.

Strafella AP, Ko JH, Grant J, Fraraccio M, Monchi O (2005) Corticostriatal functional interactions in Parkinson's disease: a rTMS/[11C]raclopride PET study. Eur J Neurosci 22:2946-2952.

Szabadics J, Lorincz A, Tamas G (2001) Beta and gamma frequency synchronization by dendritic gabaergic synapses and gap junctions in a network of cortical interneurons. J Neurosci 21:5824-5831.

Szabadics J, Tamas G, Soltesz I (2007) Different transmitter transients underlie presynaptic cell type specificity of GABAA,slow and GABAA,fast. Proc Natl Acad Sci U S A 104:14831-14836.

SZENTAGOTHAI J (1965) THE USE OF DEGENERATION METHODS IN THE INVESTIGATION OF SHORT NEURONAL CONNEXIONS. Prog Brain Res 14:1-32.

Tamas G, Buhl EH, Somogyi P (1997) Fast IPSPs elicited via multiple synaptic release sites by different types of GABAergic neurone in the cat visual cortex. J Physiol 500 (Pt 3):715-738.

Tamas G, Buhl EH, Lorincz A, Somogyi P (2000) Proximally targeted GABAergic synapses and gap junctions synchronize cortical interneurons. Nat Neurosci 3:366-371.

Tamas G, Lorincz A, Simon A, Szabadics J (2003) Identified sources and targets of slow inhibition in the neocortex. Science 299:1902-1905.

Tamas G, Szabadics J, Lorincz A, Somogyi P (2004) Input and frequency-specific entrainment of postsynaptic firing by IPSPs of perisomatic or dendritic origin. Eur J Neurosci 20:2681-2690.

Taniguchi M, Kato A, Fujita N, Hirata M, Tanaka H, Kihara T, Ninomiya H, Hirabuki N, Nakamura H, Robinson SE, Cheyne D, Yoshimine T (2000) Movement-related desynchronization of the cerebral cortex studied with spatially filtered magnetoencephalography. Neuroimage 12:298-306.

Tanji J (1994) The supplementary motor area in the cerebral cortex. Neurosci Res 19:251-268.

Tateno T, Harsch A, Robinson HP (2004) Threshold firing frequency-current relationships of neurons in rat somatosensory cortex: type 1 and type 2 dynamics. J Neurophysiol 92:2283-2294.

Tecchio F, Zappasodi F, Pasqualetti P, Tombini M, Caulo M, Ercolani M, Rossini PM (2006) Long-term effects of stroke on neuronal rest activity in rolandic cortical areas. J Neurosci Res 83:1077-1087.

Temperli P, Ghika J, Villemure JG, Burkhard PR, Bogousslavsky J, Vingerhoets FJ (2003) How do parkinsonian signs return after discontinuation of subthalamic DBS? Neurology 60:78-81.

Thomson AM, Bannister AP, Hughes DI, Pawelzik H (2000) Differential sensitivity to Zolpidem of IPSPs activated by morphologically identified CA1 interneurons in slices of rat hippocampus. Eur J Neurosci 12:425-436.

Towers SK, Lebeau FE, Gloveli T, Traub RD, Whittington MA, Buhl EH (2002) Fast network oscillations in the rat dentate gyrus in vitro. J Neurophysiol 87:1165-1168.

Towers SK, Hestrin S (2008) D1-like dopamine receptor activation modulates GABAergic inhibition but not electrical coupling between neocortical fast-spiking interneurons. J Neurosci 28:2633-2641.

Traub RD, Whittington MA, Stanford IM, Jefferys JG (1996a) A mechanism for generation of long-range synchronous fast oscillations in the cortex. Nature 383:621-624.

Traub RD, Whittington MA, Colling SB, Buzsaki G, Jefferys JG (1996b) Analysis of gamma rhythms in the rat hippocampus in vitro and in vivo. J Physiol 493 (Pt 2):471-484.

Traub RD, Whittington MA, Buhl EH, Jefferys JG, Faulkner HJ (1999a) On the mechanism of the gamma --> beta frequency shift in neuronal oscillations induced in rat hippocampal slices by tetanic stimulation. J Neurosci 19:1088-1105.

Traub RD, Jefferys JG, Whittington MA (1999b) Fast Oscillations in Cortical Circuits (Computational Neuroscience). Cambridge, Massattusets: Bradford Book.

Traub RD, Bibbig A, Fisahn A, Lebeau FE, Whittington MA, Buhl EH (2000) A model of gamma-frequency network oscillations induced in the rat CA3 region by carbachol in vitro. Eur J Neurosci 12:4093-4106.

Traub RD, Kopell N, Bibbig A, Buhl EH, Lebeau FE, Whittington MA (2001) Gap junctions between interneuron dendrites can enhance synchrony of gamma oscillations in distributed networks. J Neurosci 21:9478-9486.

Traub RD, Pais I, Bibbig A, Lebeau FE, Buhl EH, Hormuzdi SG, Monyer H, Whittington MA (2003) Contrasting roles of axonal (pyramidal cell) and dendritic (interneuron) electrical coupling in the generation of neuronal network oscillations. Proc Natl Acad Sci U S A 100:1370-1374.

Traub RD, Bibbig A, Lebeau FE, Buhl EH, Whittington MA (2004) Cellular mechanisms of neuronal population oscillations in the hippocampus in vitro. Annu Rev Neurosci 27:247-278.

Traub RD, Bibbig A, Lebeau FE, Cunningham MO, Whittington MA (2005) Persistent gamma oscillations in superficial layers of rat auditory neocortex: experiment and model. J Physiol 562:3-8.

Trudel E, Bourque CW (2003) A rat brain slice preserving synaptic connections between neurons of the suprachiasmatic nucleus, organum vasculosum lamina terminalis and supraoptic nucleus. J Neurosci Methods 128:67-77.

Tsubokawa T, Katayama Y, Yamamoto T, Hirayama T, Koyama S (1991) Treatment of thalamic pain by chronic motor cortex stimulation. Pacing Clin Electrophysiol 14:131-134.

Tukker JJ, Fuentealba P, Hartwich K, Somogyi P, Klausberger T (2007) Cell type-specific tuning of hippocampal interneuron firing during gamma oscillations in vivo. J Neurosci 27:8184-8189.

Urschel S, Hoher T, Schubert T, Alev C, Sohl G, Worsdorfer P, Asahara T, Dermietzel R, Weiler R, Willecke K (2006) Protein kinase A-mediated phosphorylation of connexin36 in mouse retina results in decreased gap junctional communication between All amacrine cells. J Biol Chem 281:33163-33171.

van Brederode JF, Snyder GL (1992) A comparison of the electrophysiological properties of morphologically identified cells in layers 5B and 6 of the rat neocortex. Neuroscience 50:315-337.

Vignes M, Collingridge GL (1997) The synaptic activation of kainate receptors. Nature 388:179-182.

von KM, Smith Y, Bolam JP, Smith AD (1992) Synaptic organization of GABAergic inputs from the striatum and the globus pallidus onto neurons in the substantia nigra and retrorubral field which project to the medullary reticular formation. Neuroscience 50:531-549.

Vrba J, Robinson SE (2001) Signal processing in magnetoencephalography. Methods 25:249-271.

Weaver FM, Stern MB, Follett K (2006) Deep-brain stimulation in Parkinson's disease. Lancet Neurol 5:900-901.

Weintraub D, Comella CL, Horn S (2008) Parkinson's disease--Part 1: Pathophysiology, symptoms, burden, diagnosis, and assessment. Am J Manag Care 14:S40-S48.

Weiss T, Veh RW, Heinemann U (2003) Dopamine depresses cholinergic oscillatory network activity in rat hippocampus. Eur J Neurosci 18:2573-2580.

Whittington MA, Traub RD, Jefferys JG (1995) Synchronized oscillations in interneuron networks driven by metabotropic glutamate receptor activation. Nature 373:612-615.

Whittington MA, Stanford IM, Colling SB, Jefferys JG, Traub RD (1997a) Spatiotemporal patterns of gamma frequency oscillations tetanically induced in the rat hippocampal slice. J Physiol 502 (Pt 3):591-607.

Whittington MA, Traub RD, Faulkner HJ, Stanford IM, Jefferys JG (1997b) Recurrent excitatory postsynaptic potentials induced by synchronized fast cortical oscillations. Proc Natl Acad Sci U S A 94:12198-12203.

Whittington MA, Traub RD, Kopell N, Ermentrout B, Buhl EH (2000) Inhibition-based rhythms: experimental and mathematical observations on network dynamics. Int J Psychophysiol 38:315-336.

Whittington MA, Doheny HC, Traub RD, Lebeau FE, Buhl EH (2001) Differential expression of synaptic and nonsynaptic mechanisms underlying stimulus-induced gamma oscillations in vitro. J Neurosci 21:1727-1738.

Wichmann T, DeLong MR (2006) Basal ganglia discharge abnormalities in Parkinson's disease. J Neural Transm Suppl21-25.

Williams JH, Kauer JA (1997) Properties of carbachol-induced oscillatory activity in rat hippocampus. J Neurophysiol 78:2631-2640.

Wilson JM, Levey AI, Rajput A, Ang L, Guttman M, Shannak K, Niznik HB, Hornykiewicz O, Pifl C, Kish SJ (1996) Differential changes in neurochemical

markers of striatal dopamine nerve terminals in idiopathic Parkinson's disease. Neurology 47:718-726.

Windels F, Bruet N, Poupard A, Urbain N, Chouvet G, Feuerstein C, Savasta M (2000) Effects of high frequency stimulation of subthalamic nucleus on extracellular glutamate and GABA in substantia nigra and globus pallidus in the normal rat. Eur J Neurosci 12:4141-4146.

Wingeier B, Tcheng T, Koop MM, Hill BC, Heit G, Bronte-Stewart HM (2006) Intra-operative STN DBS attenuates the prominent beta rhythm in the STN in Parkinson's disease. Exp Neurol 197:244-251.

Wise SP, Jones EG (1977) Cells of origin and terminal distribution of descending projections of the rat somatic sensory cortex. J Comp Neurol 175:129-157.

Wu J, Hablitz JJ (2005) Cooperative activation of D1 and D2 dopamine receptors enhances a hyperpolarization-activated inward current in layer I interneurons. J Neurosci 25:6322-6328.

Wu Y, Richard S, Parent A (2000) The organization of the striatal output system: a single-cell juxtacellular labeling study in the rat. Neurosci Res 38:49-62.

Yamamoto T, Katayama Y, Oshima H, Fukaya C, Kawamata T, Tsubokawa T (2002) Deep brain stimulation therapy for a persistent vegetative state. Acta Neurochir Suppl 79:79-82.

Yang CR, Seamans JK (1996) Dopamine D1 receptor actions in layers V-VI rat prefrontal cortex neurons in vitro: modulation of dendritic-somatic signal integration. J Neurosci 16:1922-1935.
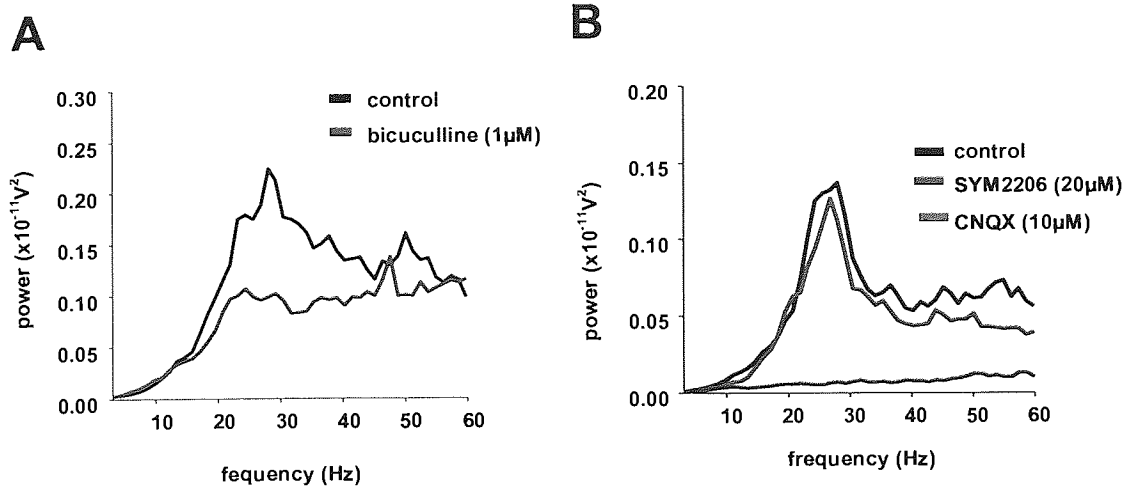
Zhou FM, Hablitz JJ (1999) Dopamine modulation of membrane and synaptic properties of interneurons in rat cerebral cortex. J Neurophysiol 81:967-976.

Zhu Y, Zhu JJ (2004) Rapid arrival and integration of ascending sensory information in layer 1 nonpyramidal neurons and tuft dendrites of layer 5 pyramidal neurons of the neocortex. J Neurosci 24:1272-1279.

Zin-Ka-Ieu S, Roger M, Arnault P (1998) Direct contacts between fibers from the ventrolateral thalamic nucleus and frontal cortical neurons projecting to the striatum: a light-microscopy study in the rat. Anat Embryol (Berl) 197:77-87.

http://www.staff.ncl.ac.uk/oliver.hinton/eee305/Chapter6.pdf. "EEE305", "EEE801 Part A": Digital Signal Processing. Chapter 6: Describing Random Sequence

APPENDIX

A

power (x10^{-11}V^2)

0.30
0.25
0.20
0.15
0.10
0.05
0.00

■ control
▬ bicuculline (1µM)

10 20 30 40 50 60

fequency (Hz)

B

power (x10^{-11}V^2)

0.20
0.15
0.10
0.05
0.00

■ control
▬ SYM2206 (20µM)
▬ CNQX (10µM)

10 20 30 40 50 60

frequency (Hz)

C

n=4	control	bicuculline
Power (x10^{-11}V^2)	0.25 ± 0.11	0.12 ± 0.02
Frequency (Hz)	24.7 ± 1.2	27.7 ± 1.4

D

n=2	control	SYM2206 (20µM)	CNQX (10µM)
Peak power (x10^{-11}V^2)	0.14 ± 0.05	0.12 ± 0.04	abolished
Frequency (Hz)	26.8 ± 1.2	27.4 ± 0.6	abolished

Appendix I – Role of GABAA receptors and AMPA/Kainate receptors on KA-induced beta oscillations in layer V. (A) Averaged power spectrum (n=4) showing addition of GABA$_A$ antagonist receptor bicuculline (1µM) reduced beta oscillatory activity. **(B)** Average power spectrum (n=2) showing addition of CNQX (10µM) but not SYM2206 (20µM) abolished beta oscillatory activity. **(C and D)** Averaged values for (A) and (B). These data indicate KA-induced and KA+CCh-induced beta oscillatory activity in layer V are mechanistically similar.

A

control

PTX (50µM)

0.7µV

100ms

B

C

control

SYM2206 (10µM)

1.5µV

100ms

D
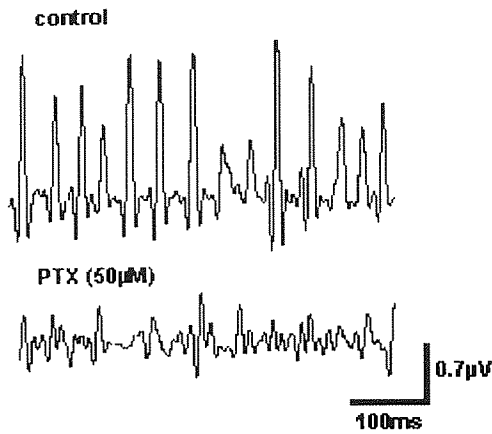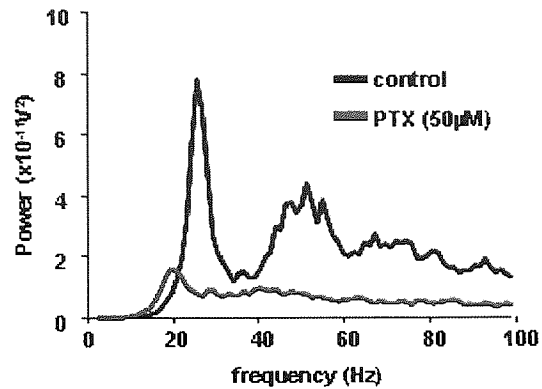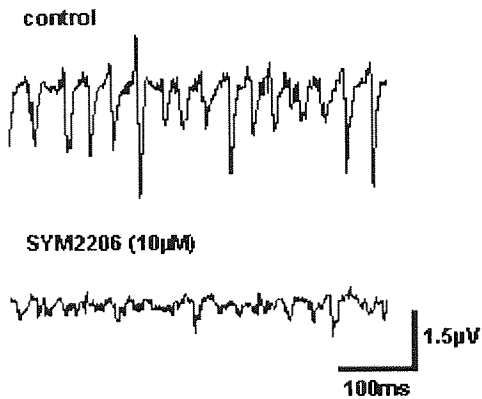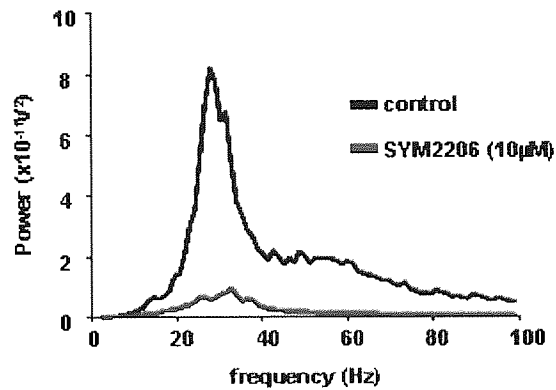
n=2	control	PTX (50µM)
Power (x10^{-11}V^2)	7.82 ± 7.77	1.62 ± 01.61
Frequency (Hz)	31.1 ± 5.5	25.6 ± 6.1

n=3	control	SYM2206 (10µM)
Power (x10^{-11}V^2)	8.34 ± 7.43	0.97 ± 0.91
Frequency (Hz)	28.5 ± 1.1	29.7 ± 1.1

Appendix II – Gamma oscillations in hippocampal CA3. (A) Representative traces of CA3 gamma oscillation before (top) and after (bottom) addition of picrotoxin (PTX, 50µM). **(B)** Average power spectrum (n=2) showing that PTX reduced gamma oscillations in CA3.**(C)** Representative traces of gamma oscillation before (top) and after (bottom) addition of SYM2206. **(D)** Average power spectrum (n=3) showing that SYM2206 reduced gamma oscillations. All data consistent with Fisahn *et al.*, 1998.

A control

B

C +zolpidem (100nM)

D
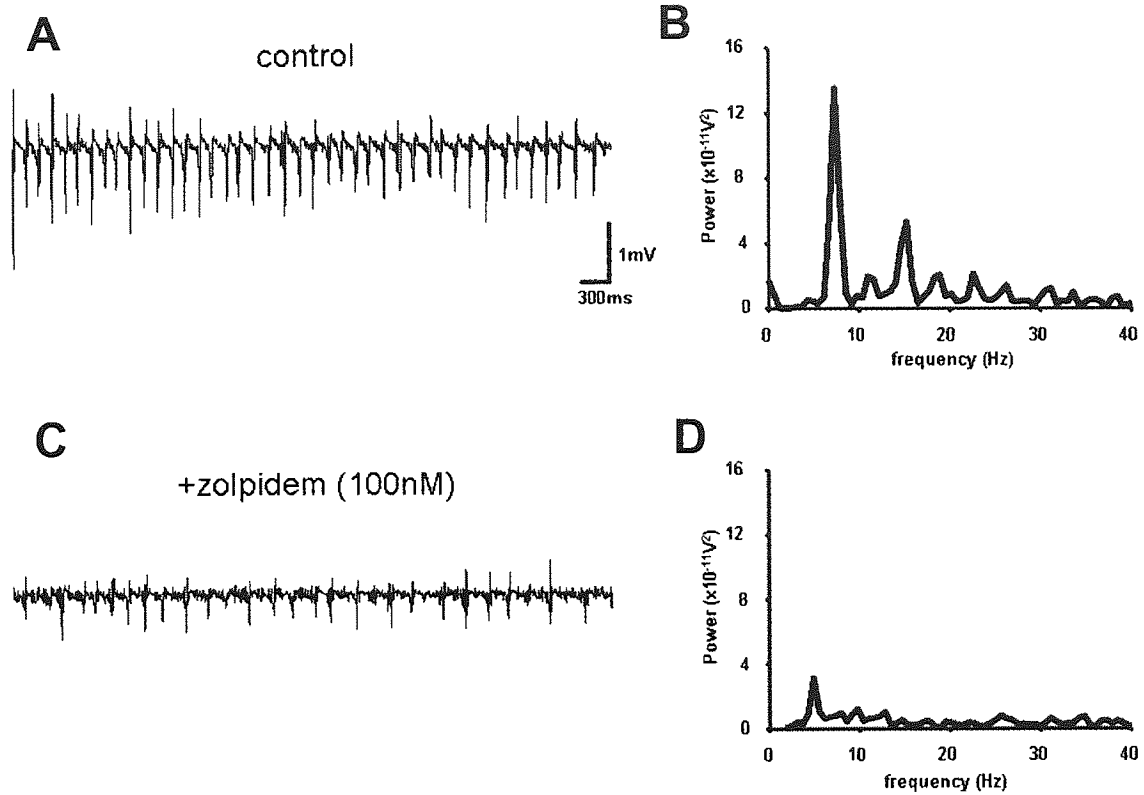
Appendix III – Evoked theta oscillation – A model for pathological slow-wave oscillation? (A) Representative trace of 4Hz stimulation-evoked theta oscillations. **(B)** Power spectrum of trace shown in (A). **(C)** After addition of zolpidem (100nM, n=2). **(D)** Power spectrum of (C) showing slow-wave oscillatory activity was reduced by 100nM zolpidem.

Appendix IV:
EFFECT OF ZOLPIDEM ON PATHOLOGICAL OSCILLATORY ACTIVITY IN M1

INTRODUCTION

The family of 'z drugs' which includes zolpidem, zopiclone and zaleplon are non-benzodiazepine sedative/hypnotic agents usually prescribed (10-30mg) for insomnia (Dooley and Plosker, 2000; Holm and Gao, 2000) taking advantage of their fast absorption, short half-life and resultant limited duration of action. However, over recent years there have been an increasing number of reports that have highlighted the paradoxical ability of sub-sedative doses (2-5mg) of zolpidem to improve cognitive and motor ability for patients in persistent vegetative state (Clauss and Nel, 2006), brain injury (Cohen *et al.*, 2004; Shames and Ring, 2008), idiopathic PD (Brown *et al.*, 2001), drug-induced Parkinsonism (Farver and Khan, 2001), and dementia (Jarry *et al.*, 2002).

Previous single-photon emission computed tomography (SPECT) studies have suggested that there is reduced regional blood perfusion in the affected brain area, with respect to the contralateral hemisphere, suggestive of diminished neuronal activity. Following administration of low-dose zolpidem, SPECT studies in a brain injured patient showed increased perfusion, implying recovery of cortical activity (Cohen *et al.*, 2004).

These observations coupled with the results from our *in vitro* studies led us to hypothesise that the beneficial effect of sub-sedative doses of zolpidem on motor disorders are related to the desynchronisation of pathological beta oscillations.

In order to test this hypothesis, we recruited patient JP, who presented with specific sensorimotor deficits, specifically, unilateral somatosensory diminution and abnormal motor gait. In addition, JP reported no sensation on his right side while his motor ability of the same side remained intact. This was characterised by uncontrolled grip strength, presumably due to an absence of sensory feedback to regulate the degree of force. JP also displayed cognitive deficits, characterized by difficulties comprehending specific words (a specific auditory-verbal deficit) with word finding difficulties and semantic paraphasias. These deficits showed marked improvement following a single daily dose (5mg) of zolpidem.

METHODS

Single Photon Emission Computed Tomography (SPECT)

SPECT is an imaging method which uses nuclear isomers (in this case ^{99m}Tc), attached to molecules (in this case hexamethylpropylene amine oxime (HMPAO)), to visualise various structures or processes. Here the ^{99m}Tc-HMPAO is taken up by brain tissue at a rate roughly proportional to blood flow. The nuclear isomer emits gamma rays, which are then detected by a series of gamma cameras. Reconstruction of the signals detected by the cameras provides a 3-D image of the pattern of blood flow. Here the patient JP underwent SPECT analysis before and after zolpidem administration. The comparison of these two conditions provides information about change in blood flow as a consequence of zolpidem administration.

Previous ^{99m}Tc-HMPAO SPECT imaging of JP identified a reduced cerebrovascular perfusion in the region of the posterior left temporal lobe with respect to normalised control data which was observed to improve following zolpidem administration (5mg, Clauss and Nel, 2004).

Magnetic Resonance Imaging (MRI)

MRI is an imaging tool which uses a series of large, specific, magnetic fields to obtain information about the anatomical structure. A primary magnetic field causes the alignment of the protons that are abundantly contained in water molecules. A secondary magnetic field is used to temporarily interrupt the alignment of the protons along a perpendicular plane. When this field in removed protons return to their primary alignment (relaxation), during which time they emit a detectable radio-frequency signal. This signal is detected by a receiver tuned to this frequency range and computational processing reconstructs a detailed anatomical image of the structure of the brain tissues. The relaxation process involves the recovery of proton spin along both the longitudinal and transverse planes, both of which generate measureable signal components (T1 and T2 respectively), which vary dependent upon the profiles of the magnetic pulses used. Here, a T1 acquisition was used to

obtain a high resolution image of the brain. Additionally, a specific T2 acquisition was used to obtain information about the grey and white matter distribution within regions of interest to determine the specific nature of tissue observed.

In order to obtain a structural image of JP's brain and identify the extent of any lesion, we employed a variety of MRI approaches. A 3-Tesla MRI scanner (Siemens Trio: Erlangen, Germany) was used to acquire a detailed T1 weighted image for subsequent neuro-imaging reconstruction and co-registration and a series of T2-weighted images to provide detailed information regarding the grey and white matter structure of the lesioned area.

Proton Magnetic Resonance Spectroscopy (1H MRS)

MRS employs the same principles discussed previously for MRI, with the exception that it uses specific magnetic pulses to interrupt the spins of protons within a predetermined tissue voxel (here within the brain). This magnetic pulse interrupts the protons with all molecules (not just water), resulting in a radiofrequency signal from a broad range of brain chemicals. This signal spans a range of frequencies (the spectrum); within which each frequency reflects the chemical composition and concentration of the tissue voxel.

1H MRS was used to obtain chemical information reflecting structural integrity of the central lesion, lesion periphery and contralateral control region. In summary, this method generates a spectrum that reflects the presence or absence of typical metabolic substrates, which form markers of viable brain tissue. These substrates, including N-acetyl-aspartate (NAA), creatine (Cr), choline (Ch) and *myo*-inositol (mI) are reflected in robust ratios in healthy brain tissue. A variation in this ratio or the presence of other abnormal metabolites, such as a lactate (Lac) peak, is a reflection of altered neuronal tissue viability or altered metabolism, indicative of pathological conditions; these data were processed using LCModel software.

Pharmaco-MEG

The Pharmaco-MEG technique (Hall *et al.,* in submission) was used to determine the oscillatory power change in JP's cortex induced by a drug over time. Synthetic aperture magnetometry (SAM) was used to identify the spatial distribution of oscillatory power changes in the theta (4-10Hz), alpha (7-14Hz), beta (15-30Hz) and gamma (30-80Hz) frequency bands between two time periods of the MEG trace. The localisation of task-related changes were determined by comparing pre-task 'passive' and during task 'active' periods. Localisation of drug action was performed by comparing the first 7.5 minutes (considered to be 'drug inactive') with each of the subsequent five periods (considered to be 'drug active'). At the regions of interest identified from the SAM analysis we placed virtual electrodes (Hall *et al.,* 2005) which were band pass filtered to the frequency band of interest. This enabled the reconstruction of oscillatory power change over the entire period of drug uptake. Data obtained from comparative locations in the intact contralateral hemisphere were used a controls.

Aston University

Illustration removed for copyright restrictions

Figure A1 – Phamaco-MEG. SAM localise the brain area where significant activity change has been induced by drug relative to other area. Virtual electrode can then be inserted into that area so that change in oscillatory activity at specific frequency band over time can be extracted/defined via spectrogram. Hall *et al.* in submission.

Our study consisted of a double blind MEG investigation of three different drug states, carried out over three days. On the morning of each day our patient (JP), was instructed to consume breakfast, without caffeine, two hours prior to recording. At the same time on each day (10.30am) JP was comfortably situated in a 275 channel MEG system (CTF Systems, Canada) in a supine position whilst a continuous data acquisition was made for a period of 60 minutes at a sampling rate of 600Hz. At the beginning of this period JP was administered either zolpidem (5mg), zopiclone (3.5mg) or placebo. Head position with respect to the sensors was determined continuously with the use of three localization electrodes and a 3-dimensional digitization of the participant's scalp. This afforded the ability to control for head movement and co-register the measured MEG signal with the participant's anatomical MRI (Adjamian *et al.,* 2004).

During each session the 60 minute acquisition was divided into six identical 10 minute sessions. During these 10 minute sessions JP was required to perform five 30 second tasks: eye closure, isometric contraction of the left then right hands, covert letter fluency and category naming tasks. These tasks were spread throughout the 10 minute period, being interleaved bwith 7.5 minutes passive periods. This served the purpose of spatially localising right and left motor cortex (Taniguchi *et al.,* 2000) and regions involved in letter fluency (Singh *et al.,* 2002) and category naming paradigms and maintaining attention across the 60 minute acquisition period.

RESULTS

Initial SPECT results reported by Clauss and Nel, 2004 are included (figure A2A and B). T1-weighted MRI confirmed left lateralised lesion (figure A2C) T2-weighted scan of JP in the horizontal plane revealed the extent of the left temporal lobe lesion, impinging on language and motor areas (figure A2D). T2-weighted scan was also used within the lesion to identify the intact contralateral hemisphere and lesion penumbra (indicated by A, B and C respectively). Subsequently, these loci were investigated using MRS and MEG. MRS analysis of the lesion site revealed an absence of typical metabolic markers NAA, Cr, Ch and ml, although a Lac peak was seen in cerebrospinal fluid (CSF) (figure A2E). Investigation of the contralateral hemisphere revealed a typical chemical spectral profile, with normal ratios of NAA, Cr, Cho and ml (Figure A2F). However, whilst the lesion penumbra location also showed relatively normal ratios of these metabolites, the spectrum was dominated by an abnormally high Lac peak (figure A2G), suggesting a degree of ongoing metabolic stress within neuronal populations close to the original lesion.

MEG virtual electrode analysis, derived from the Synthetic Aperture Magnetometry (SAM) beamforming method (Vrba and Robinson, 2001) was used to derive power spectra from the voxels used in MRS analysis (1-60Hz). A MEG signal was not detectable in the lesion voxel (figure A2H), whereas the contralateral voxel was typified by a normal amplitude spectrum with moderate power across the low-frequency range (figure A2I). Analysis of the penumbral voxel revealed strikingly high power in the theta frequency range (peak 8Hz) superimposed on a high degree of broadband low-frequency oscillatory activity (figure A2J). This pattern of slow wave activity was evident across all virtual electrode placements ipsilateral to the lesion, including the dorsolateral prefrontal cortex (DLPFC), parietal lobe, superior temporal lobe and sensorimotor cortex (figure A3C and E), and was not evident in contralateral electrode (figure A3D and F).
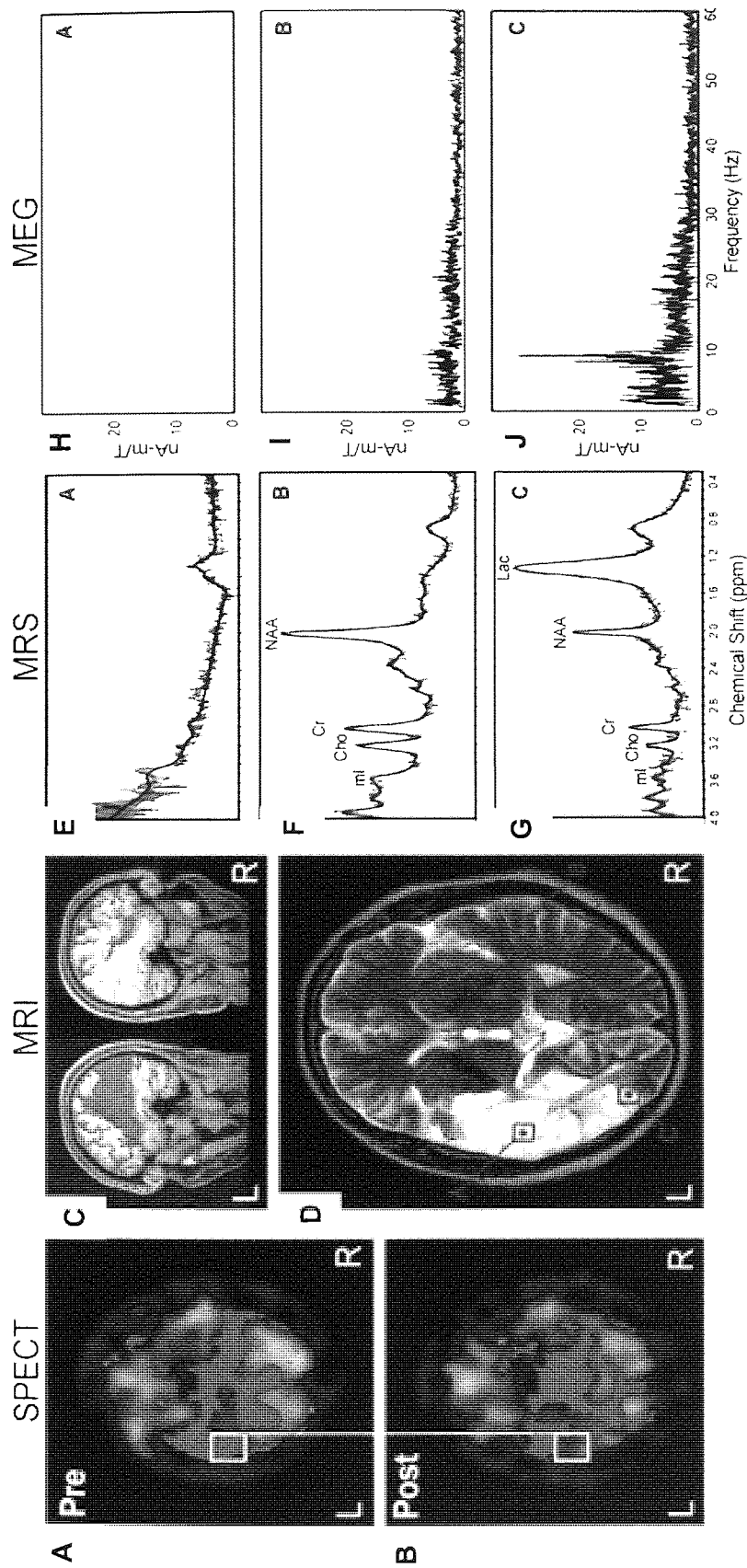
Figure A2 – Characterisation of pathology. SPECT analysis showing cerebral blood perfusion **(A)** before and **(B)** after zolpidem; white boxes indicate left temporal region where perfusion is increased. MRI images showing the extent of the lesion in the left hemisphere in **(C)** a T1 weighted sagittal section and **(D)** T2-weighted horizontal section; red boxes (A, B and C) indicate lesion, contralateral control and lesion penumbra voxels used for subsequent MRS and MEG analyses. MRS analysis of voxels identified from MRI (**E**, **F** and **G** derived from A, B and C respectively); abbreviated annotations indicate chemical markers observed. MEG analysis of voxels A, B and C (**H**, **I** and **J** respectively), showing power spectral analyses (0-60Hz).

170

Double blind, placebo controlled pharmaco-MEG analyses of a 60 minute period following drug administration, used SAM techniques (Vrba and Robinson, 2001; Hillebrand et al., 2005) to identify the spatial distribution of power change in delta (1-3Hz), theta (4-10Hz), alpha (7-14Hz), beta (15-30Hz) and gamma (30-80Hz) frequency bands. This approach revealed a powerful desynchronising effect of zolpidem on the enhanced theta and beta activity seen within ipsilateral cortex, in both language-associated (figure A3A and C) and sensorimotor areas (figure A3B and E). By contrast, we observed no effects of zolpidem on baseline low-frequency activity in electrodes placed contralateral to the lesion (figure A3D and F). When we repeated these experiments using a placebo we observed no effects on MEG activity. Conversely, following zopiclone administration at sub-sedative dose (3.5 mg), we noted a striking, bilateral, broadband increase (figure A3G to L) in oscillatory activity in the beta frequency range (15-30 Hz), consistent with previous MEG observations using a similarly non-specific $GABA_A$ receptor modulator (Jensen et al., 2005). These data indicate that 12 years following initial insult, neuronal tissue surrounding the original lesion continues to exhibit pathological behaviour in the form of slow wave oscillations and also that zolpidem has a unique, desynchronising effect that is specific to such activity.

We next investigated how focal desynchronisation was related to cognitive and sensorimotor function in JP through MEG measures of language and motor function. The use of independent isometric contraction of the left and right hands allowed us to localise the respective contralateral sensorimotor cortex through desynchronisation of beta activity (figure A4A) consistent with previous observations (Taniguchi et al., 2000). Similarly, category naming and covert letter fluency tasks were employed to localize language related areas through peak desynchronisation (figure A4J and K), consistent with previous observations in the DLPFC (Singh et al., 2002). These latter activations were important since these tasks typify the language difficulty that JP exhibited under drug-free conditions. We found a strong spatial and frequency domain correspondence between the zolpidem-induced (figure A4A and B) and functional desynchronisation events (figure A4I to K), suggesting that zolpidem administration had direct functional consequences within modalities in which JP is compromised.

With the aim of identifying the temporal profile of oscillatory changes that underlie the improvements in cognitive and sensorimotor performance, we implemented a virtual electrode reconstruction of discrete neuronal activity at the peaks of desynchronisation in both the passively and functionally identified loci. This method is a measure of discrete neuronal activity (Hall *et al.,* 2005) resembling those made at the local field potential level (Logothetis *et al.,* 2001). We reconstructed the envelope of oscillatory power over the entire 60 minute duration following drug administration. This approach revealed that the abnormally high sensorimotor beta oscillations observed prior to drug uptake were persistent, and were chronically suppressed following zolpidem administration (figure A4C and F). Similarly, abnormally high and persistent theta oscillations observed in language performance areas such as DLPFC were also suppressed by zolpidem (figure A4D, E, G and H).
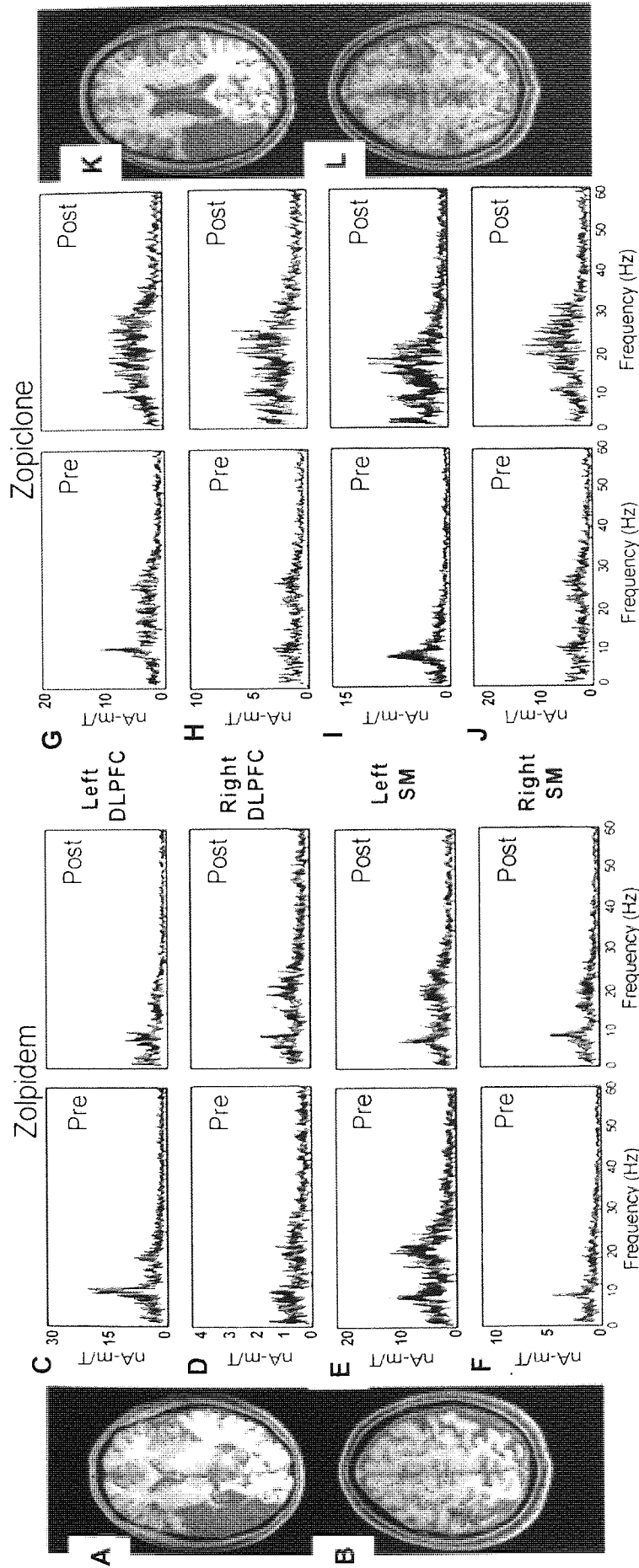
Figure A3 – Drug induced oscillatory modulation. Results of SAM analyses indicating the spatial distribution of oscillatory power change as a consequence of zolpidem (A and B) and zopiclone (K and L) administration; blue indicates a reduction and orange an increase in oscillatory power. **(A)** Theta desynchronisation and **(B)** beta desynchronisation following zolpidem administration. **(C and D)** Power spectral change in left and right DLPFC and **(E and F)** left and right sensorimotor (SM) cortex pre- and post-zolpidem administration. **(K)** Beta synchronisation bilaterally in frontal cortex and **(L)** sensorimotor (SM) cortex, pre- and post-zopiclone administration. **(G and H)** Power spectral change bilaterally in DLPFC and **(I and J)** SM cortex, pre- and post-zopiclone administration.
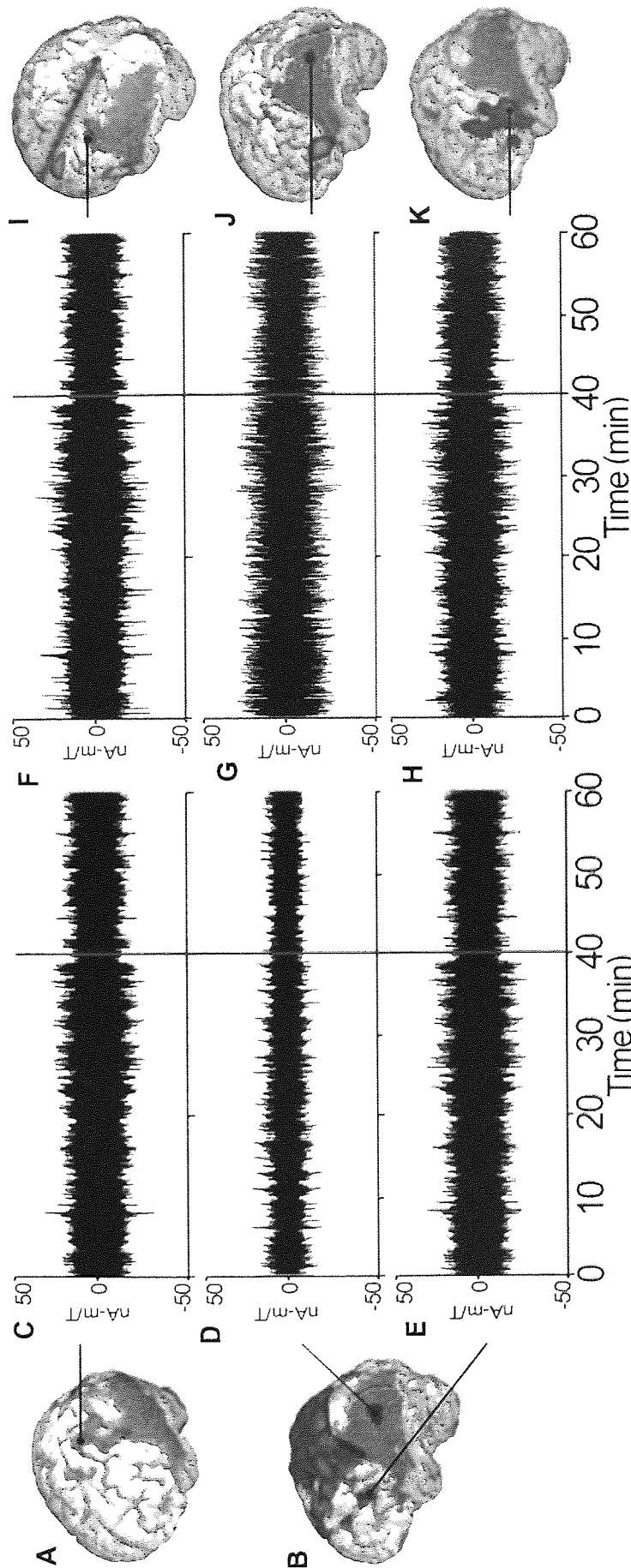
173

Figure A4 – Pharmacodynamic profile of zolpidem induced desynchronisation. SAM and images co-registered with the 3-dimensional MRI and band-pass filtered virtual electrode traces recorded for 60 minutes post zolpidem administration. Distribution and time-course of desynchronisation in the beta (**A** and **C**) and theta (**B**, **D** and **E**) frequencies. Event-related desynchronisation (ERD) in the beta range in response to contraction of the right hand (**I**) and in the theta range in response to category naming (**J**) and covert letter fluency tasks (**K**). Virtual Electrode analysis indicated the electrical activity at these peak ERD loci over the 60 minutes duration, band-pass filtered to beta (**F**) and theta (**G and H**). Red lines denote onset of zolpidem-induced cognitive and motor improvements.

The onset of these reductions in synchronous power occurred at 35-45 minutes post-drug administration, consistent with both JP's self-reported improvements on language-related tasks and the pharmacokinetic profile of zolpidem. Neither the therapeutic benefit nor the associated desynchronisation was observed following administration of zopiclone or placebo. Psychometric evaluation of JP used the WAIS-III to evaluate drug-enhanced cognitive performance, firstly with zolpidem and then 6 months later without zolpidem. Test-retest gains in performance across WAIS-III Index and IQ scores due to practice effects are well documented (Basso *et al.*, 2002). Therefore, the order of administration was chosen to underestimate rather than overestimate gains due to zolpidem. JP achieved highest scores on the Perceptual Organization Index, with scores falling in the top 12-18% of his age group. In the absence of zolpidem results revealed deterioration in performance across all Index and IQ scores with the exception of the Working Memory Index, which remained within the bottom 1% of the population across both test occasions. The greatest change was evident in the Verbal Comprehension Index and JP's standardized score dropped by 27 percentile points, moving from the 'average' to the 'low average' range (Figure A5); these observations were consistent with clinical presentation.
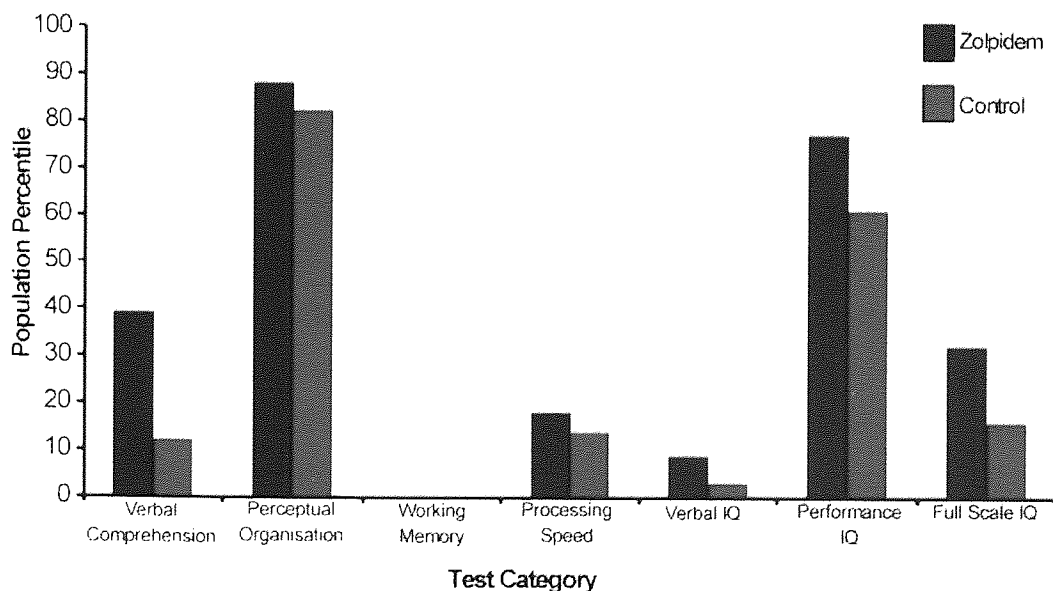

Figure A5 – Psychometric analysis of zolpidem mediated improvement. Bar chart reflecting the results of JP's WAIS-III assessments carried out with zolpidem (blue) and without zolpidem (red). Scores are age-standardised and displayed as percentiles.

DISCUSSION

In summary, in JP, a left temporal lesion resulted in an increase in pathological theta and beta frequency oscillatory power compared to the undamaged contralateral hemisphere. In sub-sedative doses, zolpidem was capable of suppressing pathological slow wave activity to a level that allowed functionality to return. It seems reasonable to infer that the action of zolpidem in brain injury is related to its unique dose-dependent selectivity for $GABA_A$ receptors containing the α-1 subunit. The desynchronising effect of zolpidem may reflect the differential distribution of α-1 subunit containing $GABA_A$ receptors between specific interneuronal subtypes sub-serving oscillatory activity (Thomson et al., 2000). Consistent with this interpretation, non-selective $GABA_A$ receptor modulators such as lorazepam (Jensen et al., 2005) and zopiclone do not desynchronise neuronal network activity, indeed, oscillatory power is enhanced.

Synchronisation across extensive neuronal populations can result in a marked reduction in information transfer. Specifically, a broad elevation in the mutual information between cortical regions will reduce the capacity for computational processing. In this scenario, the consequent reduction in the complexity of information encoding would provide an explanation for the cognitive decline observed under pathological conditions. Exaggerated slow wave activity is a feature common to a diverse array of neuropathologies, including traumatic brain injury (Nuwer et al., 2005), stroke (Tecchio et al., 2006), Alzheimer's disease (Poza et al., 2007) and schizophrenia (Canive et al., 1996) and therefore may represent a biomarker for impaired CNS functionality. Desynchronisation of pathological oscillatory activity appears to improve CNS function. For example, in Parkinson's disease, dopamine replacement therapy has been demonstrated to reverse enhanced beta activity, which correlates with symptomatic relief (Brown et al., 2001). Similarly, administration of dopamine agonists is efficacious in the treatment of brain injury (Passler and Riggs, 2001). Furthermore, following DBS positive functional outcomes linked to a desynchronisation of EEG oscillatory activity have been observed in persistent vegetative state (Yamamoto et al., 2002).

It is widely accepted that event-related desynchronisation (ERD) is a central phenomenon in normal brain activity (Pfurtscheller, 2001) and ERD has been

established as a feature of sensorimotor (Taniguchi *et al.*, 2000) and cognitive processing (Singh *et al.*, 2002). In JP, the high power and persistent nature of pathological oscillations appears to represent an obstacle to adequate ERD; this inability to desynchronise may represent a barrier to effective computation in neuronal networks. Here we show that drug induced suppression of this functional barrier affords a return of cognitive performance, typically associated with ERD. An alternative explanation is that the observed reduction in synchronous power is an epiphenomenon of increased neural activation, similar to that observed in ERD. However, this argument only emphasises the interpretation that normalisation of the MEG signal permits regular processing; albeit by a different mechanism.

At present my *in vitro* results where zolpidem appears to enhance beta oscillatory power appear at odds with the desynchronising effects observed in MEG studies. However, very recently I have shown that the theta oscillation evoked by 4Hz stimulation (see chapter 5) is sensitive to 100nM zolpidem (see appendix III). Plans are now in place to use this *in vitro* model to assess different concentrations of both zolpidem and zopiclone, in order to correlate data with that obtained from MEG studies.